Ferdowsi University of Mashhad
ISSN 2008-9147
Numbers: 7

JCMR

Journal of Cell and Molecular Research

Volume4 , Number 1, Summer 2012

JCMR

بسم الله الرحمن الرحیم

Issuance License No. 124/902-27.05.2008 from Ministry of Culture and Islamic Guidance
Scientific Research Issuance License No. 161675 from the Ministry of Science, Research and Technology, Iran

Journal of Cell and Molecular Research (JCMR)

Volume 4, Number 1, Summer 2012

Copyright and Publisher
Ferdowsi University of Mashhad

This Journal is indexed in the Islamic World Science Citation Center (ISC)

Head Office: Department of Biology, Faculty of Sciences, Ferdowsi University of Mashhad, Mashhad, Iran.
Postal Code: 9177948953
P.O. Box: 917751436
Tel./Fax: +98-511-8795162
E-mail: fuijbs@um.ac.ir
Online Submission: http://jm.um.ac.ir/index.php/biology

Journal Manager

Morteza Behnam Rassouli, Ph.D., (Professor of Physiology), Department of Biology, Faculty of Sciences, Ferdowsi University of Mashhad, Mashhad, Iran
E-mail: behnam@um.ac.ir

Editor-in-Chief

Ahmad Reza Bahrami, Ph.D., (Associate Professor of Molecular Biology and Biotechnology), Ferdowsi University of Mashhad, Mashhad, Iran
E-mail: ar-bahrami@um.ac.ir

Editorial Board

Table of Contents

Journal of Cell and Molecular Research (2012) 4 (1), 1-10

Cloning and expression analysis of *Arabidopsis TRR14* gene under salt and drought stress

Mahnaz Aghdasi*, Fariba Fazli and Mohammad Bagher Bagherieh

Department of Biology, Faculty of Science, Golestan University, Gorgan, Iran

Received 1 May 2012 Accepted 12 July 2012

Abstract

TRR14 is a novel protein important in trehalose (α-D-glucosyl-[1,1]-α-D-glucopyranoside) signaling in *Arabidopsis*. In this research, we provided evidences to demonstrate that *TRR14* plays role in *Arabidopsis* responses to salt and drought stress. Transgenic *Arabidopsis* plants over-expressing *TRR14* under the control of CaMV 35S promoter were generated. The transformed lines showed higher transcript levels of *TRR14* than that of the Wild Type (WT) *Arabidopsis* plants. The RT-PCR results showed that *TRR14* transcript level increased markedly by salt and drought stress both in WT and transformed lines. Further experiments indicated that the *TRR14* transformed lines had unchanged seed germination, root length and chlorophyll content under stress conditions. In addition, the activity of oxidative enzymes like peroxidase and catalase were significantly induced in transformed lines under salt and drought treatments. Thus, the present data indicate that a novel protein, TRR14, is involved in plant salt and drought tolerance.

Keywords**:** *TRR14*, over-expression, *Arabidopsis,* salt, drought

Introduction

Abiotic stresses, especially salinity and drought, influence plant growth and limit agricultural crop production throughout the word. Plants have biochemical and physiological mechanisms to adapt and survive against these kinds of stresses (Zhu, 2001). One of these adaptive mechanisms is the synthesis or accumulation of osmolytes such as proline (Kishore et al., 2004), fructan (Pilson-Smits et al., 1995), glycinebetaine (Holmstrom et al., 2000), sorbitol (Gao et al., 2001), and or trehalose (Garg et al., 2002).

The TRR14 protein is an unknown protein that is encoded by At4g10300. It was first identified as a component of *Arabidopsis* responses to trehalose treatment (Aghdasi et al., 2012). Phylogenetic analyses revealed that TRR14 is a member of a small and divergent gene-family in *Arabidopsis* with a single Cupin domain. In plants, proteins containing a single Cupin domain and of similar size as TRR14, about 150 amino acids (aa), include diverse functions including: phosphomanose isomerase, polyketide synthase, dioxygenase, oxalate oxidase (germins), auxin binding protein and the somewhat larger 185 aa epimerase (Dunwell, 1998; Dunwell et al., 2001). TRR14 has six homologues in *Arbidopsis*. Its closest homologues are found in plants and cyanobacteria. TRR14 is located in chloroplastd and its expression is ubiquitous (Aghdasi et al., 2012).

Our previous work showed that TRR14 may involve in plant salt and drought tolerance. We isolated two *trr14* T-DNA insertion mutants from SALK collection. Characterization of *trr14* mutants revealed that *trr14* mutants have reduced seed germination, root length, survival rate and chlorophyll content under stress conditions. Furthermore the activity of oxidative enzyme, such as peroxidase, catalase and polyphenol oxidase, was decreased under salt and drought treatments.

In current research, we indicated that over-expression of *AtTRR14* in *Arabidopsis* leads to improvement of plant salt and drought tolerance. These results confirm the previous results that TRR14 involves in stress tolerance.

Materials and Methods

Plant materials and growth conditions

The *Arabidopsis thaliana* wild type (WT) plants accession Columbia-0 (COL-0) was used in this study. Seeds were surface sterilized for 5 min with 70% (v/v) ethanol followed by 10 min in 20% commercial bleach (4% (w/v) chlorine) and washed 5 times in sterile milli-Q water. Sterilized seeds were planted on half strength MS medium (Murashige and Skoog, 1962) supplemented with either 100 mM trehalose or sorbitol and solidified

*Corresponding author E-mail: m.aghdsi@gu.ac.ir

with 0.8% (w/v) agar. Seeds were stratified in darkness at 4oC for 2 days before the plates were transferred to a growth chamber at 25°C under a 16-h-light/8-h-dark photoperiod.

DNA extraction and PCR analysis

Three small leaves of seedlings were frozen in liquid nitrogen, pulverized with glass beads for 2 minutes at 2800 rpm in a dismembranator (Braun, Melsungen, Germany), and then genomic DNA was extracted using the Pure Gene DNA isolation kit (Amersham Pharmaciabiotec, England) following the manufacturer's instructions. PCR was performed with specific primers: 5'-acccaactcggtgttcgtag-3' (forward) and 5'-tgatagcagccattcactcg-3' (Reverse). After denaturation for 2 minutes at 94 ºC, DNA amplification was performed with 35 cycles (30 sec 94ºC, 30 sec 56ºC and 2 min 72ºC) followed by a final step at 72ºC for 5 minutes.

Plasmid construction of the gene, its plant transformation

For over-expression cDNA was first amplified by PCR, and ligated into pGEM-T easy vector (Promega). Briefly the CaMV35S expression cassette was isolated by digestion with *Eco*RV from pUC-18 vector: Amp resistant. The cassette was filled with Klenow and dNTPs and subsequently ligated into the pBin19 (*Hin*dIII/*Eco*RI) vector to yield pBin-35S. Purified fragments were cloned into the pBin-35S expression cassette using restriction enzymes, resulting in pBin35S/cDNA/NOS. The construct was introduced by electroporation into *Agrobacterium tumefaciens*, containing pGV2260 plasmid. The floral dip method (Clough and Bent, 1998) was used for transformation of the plant material, Col-0 WT bolting plants with *Agrobacterium tumefaciens.* Re-transformed seedlings were selected on ½ MS media containing 50 mg/L Kanamycin.

Sequence analysis

Sequences obtained from analysis with forward and reverse primers (T7: tatttaggtgacactatag and SP6: taatacgactcactataggg) were aligned and the PCR fragment structure was reconstructed by BLAST (Basic Local Alignement Search Tool) searches in TAIR (http://www.arabidopsis.org/Blast/).

RNA Isolation, RT-PCR and Real-Time PCR

Total RNA from Re-transformed lines and WT were isolated with RNeasy plant mini kit (QIAGEN USA, Valencia, CA). RNA concentration and purity were determined by measuring absorbtion at 260 nm. 10 ng RNA was treated with 2 U DNAse I (DNA- free, Ambion, Austin, USA) to remove genomic DNA. Absence of DNA was analyzed by performing a PCR reaction (40 cycles, similar to the real–time PCR program) on the DNaseI- treated RNA using Taq-DNA polymerase. RT-PCR experiments were performed using 1 ng of total RNA extracted and used for first-strand cDNA synthesis with 60 units M-MLV Reverse Transcriptase (promega, Madison, WI), 0.5 µg of odT16v (custom oligo from invitrogen, Carlsbad, CA) and 0.5 µg random hexamer (invitrogen). The gene specific primers used were: 5'-aacttgatcgggatatggagtg-3' (forward) and 5'-aacttgatcgggatatggagtg-3' (Reverse) for *TRR14* and 5'- gacccaaagacggagactctt-3' and 5'-gccaagtgattgtggagactc-3' for *AtACTIN2* as reference gene.

Stress treatments

The *Arabidopsis thaliana* accession Columbia-0 (COL-0) and re-transformed lines, seeds were sterilized 5 minutes with 70% ethanol followed by 10 minutes in 20 % commercial bleach (4% w/v chlorine) and washed 5 times in sterile Milli-Q water. The seeds were grown on MS medium solidified with 0.8% agar. Seeds were stratified in darkness at 4ºC for 2 days before the plates were transferred to a growth chamber at 22ºC under a 16-h-light /8-h-dark photoperiod. For determining the salt effect on germination, MS medium was supplemented with 0, 75, 100 or 150 mM NaCl. To determine the effect of dehydration on germination, medium was supplemented with 200 or 300 mM manitol. Germination assays were carried out with three replicates of 50 seeds. Germination rates was determined by measuring the time of radical emergence and germinating seeds were selected in the same period to measure root length.

For survival test, WT and re-transformed lines, seeds were fully germinated on MS medium and 3 days old seedlings were transferred to solid MS medium, supplemented with different levels of NaCl or manitol concentrations, and seedlings, growth was monitored for 14 days.

To measure root length under stress condition, the seedlings were grown on vertically positioned plates for 14-days. Then photographs were taken and root length measured with the Image J program (Wayne Rasband, NIH Maryland, USA).

Chlorophyll measurements

Chlorophyll levels were measured spectrophotometrically as described by Jeffery and Humphrey, (1975). In brief, 14 day old seedlings

were ground in liquid nitrogen and extracted with 80% (V/ V) acetone. Absorbance was determined at 647, 652 and 664 nm and the data were used to calculate chlorophyll content.

Oxidative enzymes activity assay

For preparation of crude enzyme extract, 0.05 g of fresh leaves were ground in 2 mM of 0.1 M cool phosphate buffer (pH 6.8) on ice bath as described by Kar and Mishra (1976). Homogenates were centrifuged at 15000 rpm for 15 min at 4ºC. The supernatants were used for catalase, peroxidase and polyphenoloxidase activity assays. The protein concentration of the supernatant was measured according to Lowery et al. (1951).

Catalase activity was determined by the consumption of H_2O_2 (Chensy and Mehler 1955). The reaction mixture (3 ml total volume) contained 50 mM phosphate buffer (pH 6.8), 100 µL enzyme extract and 15 mM H_2O_2. Absorbance decline in 240 nm was scanned automatically with spectrophotometer (Shimadzu UV-160) in kinetic mode. Peroxide reaction mixture (3 ml) contained 20 mM guaiacol, 25 mM phosphate buffer (pH: 6.8), 40 mM and 10 µL enzymes extract. Guaiacol peroxidase activity was scanned in 470 nm. Polyphenol oxidase assay mixture (3 mL) contained 10 mM pirogalol, 25 mM phosphate buffer (pH 6.8) and 200 µL enzymes extract. Enzyme activity was determined at 420 nm.

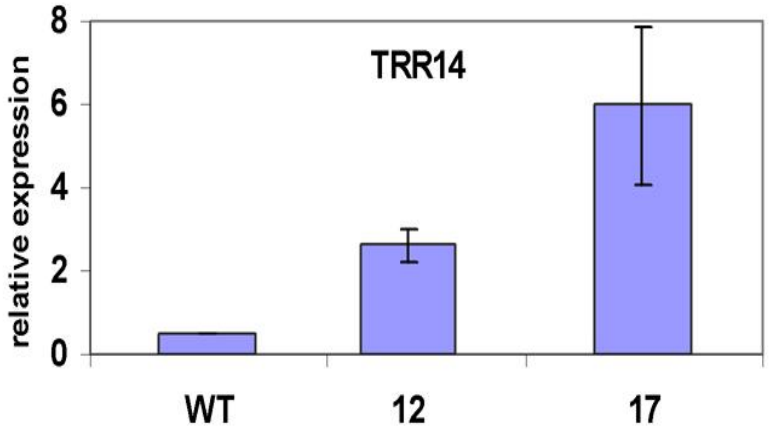

Figure 1. Q-PCR analysis of *TRR14* gene expression in WT and transformed lines (12 and 17).

Statistical analysis

The data presented in the figures and tables are the mean of three independent experiments with calculated standard deviations. A Duncan test has been done to identify statistical differences between pairs of means at a confidence level of 95% for each set of data.

Results

Transformation of cDNA constructs into WT

To analyze the function of *TRR14* in response to salt and drought stress, cDNA was constructed into binary vector pBin19 under the control of CaMV 35S promoter and were then transformed into the WT seedlings. Transformations with the full length cDNAs of *TRR14* yielded 20 independent lines per construct with resistance to the selection marker. The transformed lines did not show different phenotype compared to WT, on soil and under long-day conditions. The transformed lines remained unaltered with respect to flowering time and were fully fertile. Transformation yielded plants with higher expression levels of the *TRR14* gene. The mRNA level of *TRR14* was more than 2 times higher in the transformed lines compared to the WT (figure 1).

TRR14 expression under salt and drought stress

To investigate the effect of salt and drought stresses on the transcript level of *TRR14* gene, WT and transformed lines were subjected to the salt and dehydration stress. *TRR14* expression level was very low in unstressed control plants. After treatment with 100 mM NaCl, transcript level increased in control plants (figure 2A). Drought stress also sharply induced the expression of the *TRR14* gene in WT plants. The expression level of *TRR14* gene in manitol treatment was much higher than that in NaCl treatment (figure 2B). Similarly, *TRR14* expression was also induced by NaCl and manitol treatment in the transformed plants.

Salt response of Re-transformed lines

Physiological characteristics including seed

germination rate, root length, survival rate, chlorophyll content and oxidative enzyme activity were investigated in the transformed lines (lines 12 and 17) and WT plants under salt treatment.

To investigate the function of TRR14 under salt stress, the transformed lines and WT seeds were grown on MS medium supplemented with various levels of NaCl for 14 days. There was no difference in seed germination between the WT and transformed lines on MS medium. The germination rate of WT seeds was largely decreased under salt stress (figure 3, 4a). When the seeds were imbibed in 100 mM NaCl, about 23% of WT seeds were germinated, but the germination rate of the transformed lines was 75% (T12) and 80% (T17). While seed germination of the WT was retarded by 150 mM NaCl treatment, 10% and 8% of the transformed seeds were germinated (figure 4a).

To determine the effect of *TRR14* over-expression on plant growth under salt stress, the root length was measured in 14-day-old seedlings growing on MS medium containing various levels of NaCl. The root length of WT seedlings was significantly reduced in response to salt stress. There was no significant difference between root lengths of transformed lines growing on MS medium containing various NaCl concentrtion (figure 4b).

We also examined whether TRR14 affected *Arabidopsis* plant survival under salt stress. Seeds of WT and transformed lines were allowed to germinate on MS medium for 3 days, and then transferred to medium containing 75, 100 and 150 mM NaCl. The whole WT seedlings died after 100 mM NaCl treatment. In contrast about 25% of seedlings from the transformed lines survived at the same concentration of NaCl. All transformed lines seedlings died after 150 mM NaCl treatment (figure 4c).

There was no difference in chlorophyll a, chlorophyll b and the total chlorophyll contents of the transformed lines and WT seedlings on MS medium. When NaCl concentration increased to 100 mM, these three parameters decreased in WT seedlings. In contrast transformed seedlings were still green and the Chl a level significantly increased in response to 100 mM NaCl treatment (figure 3 and table 1). Chl a/b ratio was decreased in WT seedlings in response to 75 mM NaCl treatment. Whereas by adding 100 mM NaCl to the MS medium, this ratio was increased in WT seedlings (table 1).

Catalase, peroxidase and polyphenol oxidase activities were assayed as an indicator of oxidative stress. There was no significant difference in catalase, peroxidase and polyphenol oxidase activities between the WT and transformed lines on MS medium (table 1). When WT seedlings were grown in the presence of NaCl, catalase, peroxidaxe and polyphenol oxidase activities were significantly reduced compared with plants grown under normal condition. For transformed lines, the oxidative enzymes activity was induced by increasing NaCl concentration. The highest enzyme activity observed at 100 mM NaCl treatment (table 1).

Dehydration response of the Re-transformed lines

We further investigated the effect of TRR14 on seed germination under dehydration stress. The transformed lines (12 and 17) and WT seeds were grown on MS medium containing 200 or 300 mM mannitol for 14 days. Upon 200 mM manitol treatment, the seed germination of the transformed lines was bout 65%, whereas only 48% of the WT seeds were germinated by the 14th day. Seed germination was more decreased at 300 mM mannitol (figure 5a).

To test the possible role of *TRR14* overexpression on *Arabidopsis* growth under dehydration stress, root length was measured in 14-day-old seedlings growing on 200 or 300 mM mannitol. The root length of the WT seedlings significantly reduced in response of manitol stress. While no difference in root length was observed in the transformed lines when grown on different concentration of manitol (figure 5b)

In the next experiment, when 3-day-old WT and transformed seedlings were treated to 300 mM mannitol, most (87%) of the WT seedlings died. While about 49% of the transformed lines seedlings subjected to the same dehydration treatment survived (figure 5c)

Upon manitol stress, chlorophyll a and total chlorophyll contents were decreased and the Chl a/b ratio and Chl b content was increased in WT seedlings. While Chl a and total chlorophyll was increased in the transformed seedling, growing on 200 or 300 mM mannitol. Surprisingly the Chl a level was unchanged, but Chl a/b ratio was decreased in the transformed seedlings under manitol treatment (table 2).

While catalse and peroxidase activities were significantly decreased in WT seedlings, growing in 200 or 300 mM mannitol, they were significantly increased in the transformed lines. Significant difference was not observed in polyphenol oxidase activity in WT seedlings under different concentrations of mannitol. Polyphenol oxidase activity was significantly increased sharply in the transformed seedlings after 300 mM manitol treatment (table 2).

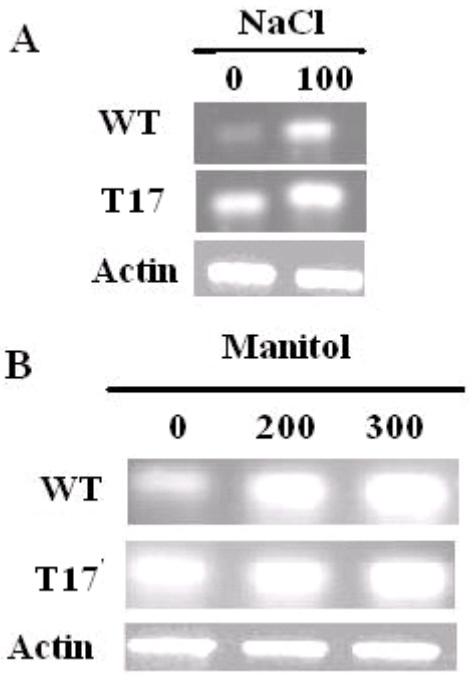

Figure 2. Expression analysis of *TRR14* in (**A**) salt stress condition (100 mM) and (**B**) drought stress condition (200 and 300 mM) from 14-days WT and Re-transformed line17 (T17) by RT-PCR. *AtACTIN2* expression levels are shown as control.

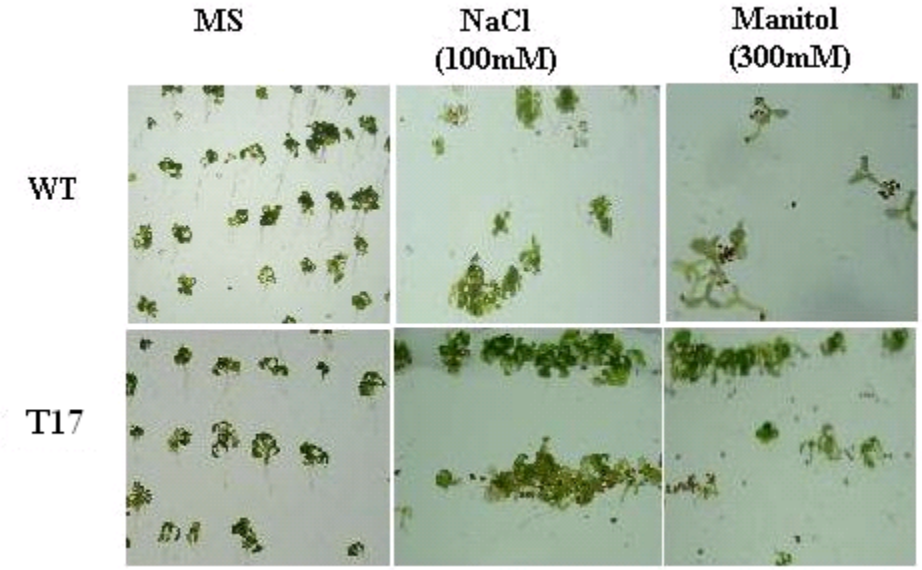

Figure 3. Effect of salt or drought stress on germination and seedling growth of WT and Re-transformed line 17.

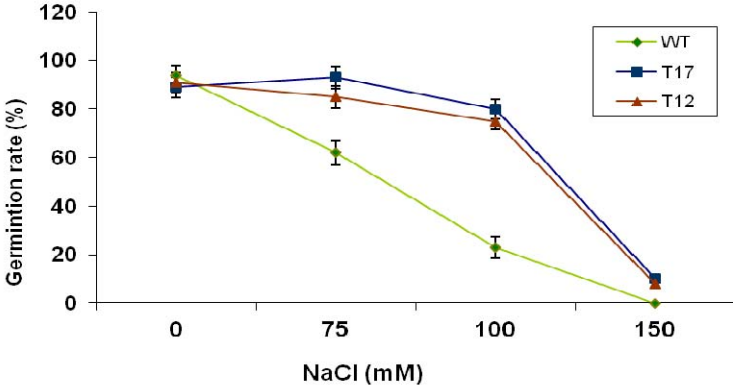

a)

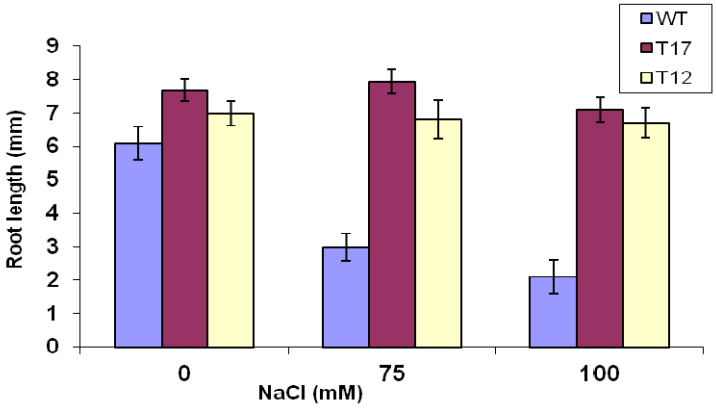

b)

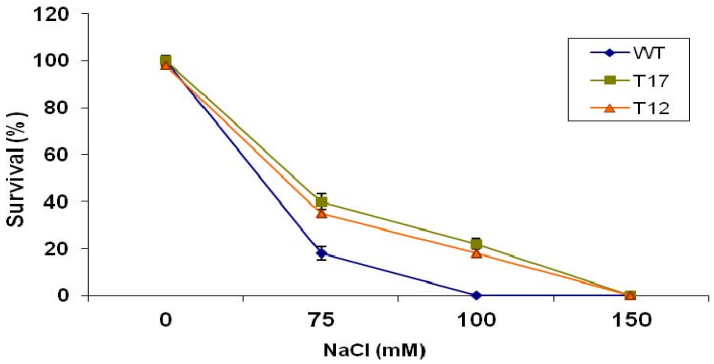

c)

Figure 4. Effect of salt stress on germination and seedling growth in WT and Re-transformed lines (T). Germination rate (a) and root length (b) of WT and transformed seeds grown on MS medium supplemented with 0, 75, 100 and 150 mM mannitol for 14 days. (c) The seeds of WT and Re-transformed lines were grown on MS medium, the 3-day-old seedlings were transferred to medium containing different concentrations of NaCl and the survival rate of the seedlings were measured after 14 days. The data were obtained from three independent experiments. Data are means ± SE. WT wild type, T12 and T17 Re-transformed lines.

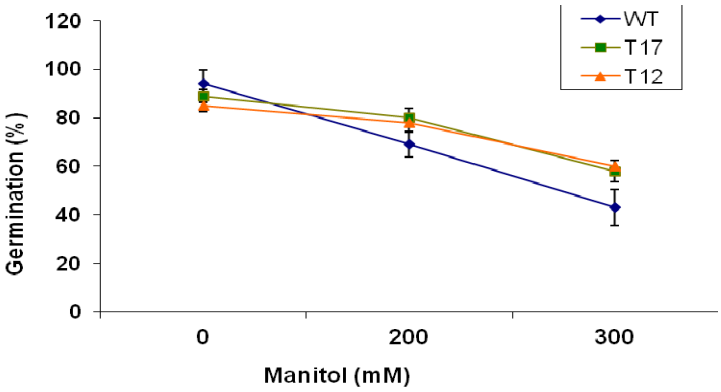

a)

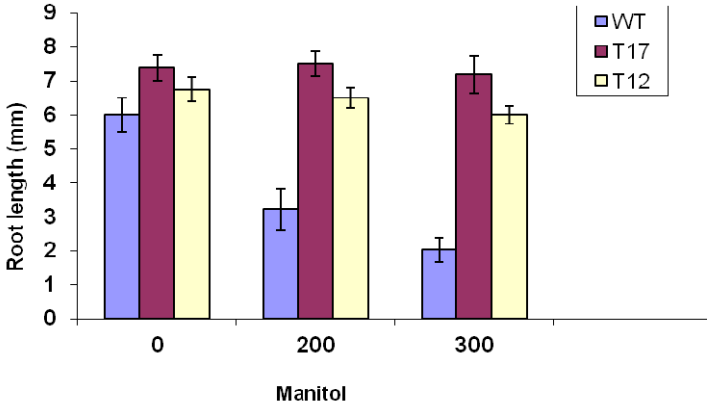

b)

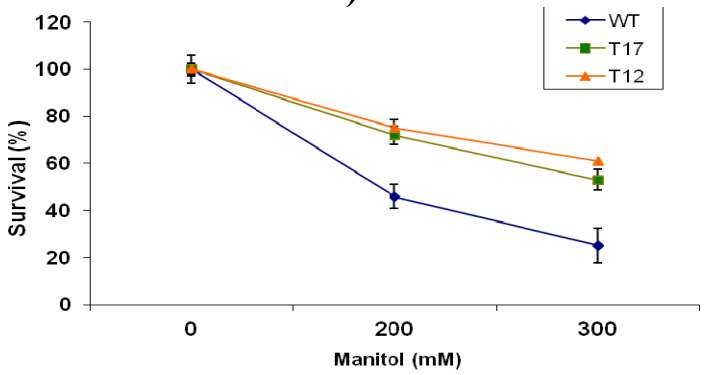

c)

Figure 5. Effect of drought stress on germination and seedling growth in WT and Re-transformed lines (T). Germination rate (**a)** and root length (**b**) of WT and transformed seeds grown on MS medium supplemented with 0, 200 and 300 mM mannitol for 14 days. **(c)** The seeds of WT and Re-transformed lines were grown on MS medium, the 3-day-old seedlings were transferred to medium containing different concentrations of mannitol and the survival rate of the seedlings were measured after 14 days. The data were obtained from three independent experiments. Data are means ± SE. WT wild type, T12 and T17 Re-transformed lines.

Table 1. Chlorophyll contents and enzyme activities in WT and Re-transformed lines (T) under salt stress

		Chlorophyll content (mg/g FW)				Enzyme activity (µmol min^{-1} mg $protein^{-1}$)		
	Salt (mM)	Chla	Chlb	Chla/b	Total Chl	Catalase	Peroxidse	Polyphenol oxidase
WT	0	0.58±0.04^{a}	0.25±0.02^{a}	2.3	0.75±0.05^{a}	0.33±0.03^{a}	37±4.6^{a}	3.6±0.36^{a}
	75	0.32±0.02^{b}	0.21±0.01^{b}	1.4	0.49±0.04^{b}	0.26±0.04^{a}	31.6±2.8^{b}	2.5±0.58^{b}
	100	0.24±0.05^{c}	0.11±0.02^{c}	2	0.24±0.03^{d}	0.15±0.04^{d}	24±3.7^{d}	1.9±0.44^{b}
T12	0	0.54±0.03^{a}	0.22±0.02^{a}	2.2	0.72±0.03^{a}	0.34±0.02^{a}	42.1±3.1^{a}	3.7±0.45^{a}
	75	0.59±0.03^{a}	0.29±0.02^{d}	2	0.77±0.02^{c}	0.44±0.02^{b}	48.5±2.4^{c}	4.1±0.21^{c}
	100	0.74±0.02^{d}	0.30±0.01^{d}	2.3	0.84±0.03^{e}	0.52±0.04^{bc}	60.1±2.4^{e}	4.8±0.34^{cd}
T17	0	0.56±0.04^{a}	0.26±0.02^{a}	2.1	0.74±0.04^{a}	0.36±0.03^{a}	41.17±5^{a}	3.9±0.32^{a}
	75	0.6±0.05^{a}	0.27±0.02^{d}	1.9	0.78±0.03^{c}	0.46±0.03^{b}	50±4.14^{c}	4±0.35^{c}
	100	0.72±0.03^{d}	0.31±0.02^{d}	2.1	0.86±0.03^{e}	0.54±0.04^{c}	59.5±2.8^{e}	5±0.36^{cd}

Seeds of WT and Re-transformed lines were grown on MS medium supplemented with 0, 75 and 100 mM salt for 14 days, then chlorophyll contents and enzymes activity were assayed. The data were obtained from three independent experiments. Data are means ± SE. Similar upper case letter in each column indicate no significant differences (Duncan test, P<0.05).

Table 2. Chlorophyll contents and enzyme activities in WT and Re-transformed lines (T) under drought stress.

		Chlorophyll content (mg/g FW)				Enzyme activity (µmol min^{-1} mg $protein^{-1}$)		
	Manitol (mM)	Chla	Chlb	Chla/b	Total Chl	Catalase	Peroxidse	Polyphenol oxidase
WT	0	0.58±0.02^{a}	0.25±0.02^{a}	2.3	0.75±0.05^{a}	0.33±0.03^{a}	37±4.6^{a}	3.6±0.36^{a}
	200	0.50±0.03^{b}	0.2±0.02^{b}	2.5	0.64±0.03^{b}	0.26±0.04^{c}	33±4.08^{a}	3.8±0.49^{ab}
	300	0.46± 0.05^{b}	0.14±0.03^{c}	3.1	0.58±0.05^{b}	0.1±0.03^{d}	30±2.9^{b}	3±0.41^{a}
T12	0	0.57±0.03^{a}	0.25±0.03^{a}	2	0.73±0.03^{a}	0.4±0.02^{b}	40.7±2.4^{a}	3.6±0.12^{a}
	200	0.6±0.02^{a}	0.32±0.02^{d}	1.9	0.78±0.02^{a}	0.48±0.02^{e}	51.7±2.8^{c}	4.4±0.28^{b}
	300	0.62±0.03^{a}	0.35±0.03^{d}	1.6	0.84±0.03^{c}	0.66±0.03^{f}	60.2±3.4^{d}	5.2±0.32^{bc}
T17	0	0.55±0.02^{a}	0.26±0.01^{a}	2.1	0.74±0.03^{a}	0.4±0.03^{b}	41.7±4.6^{a}	3.9±0.45^{a}
	200	0.6±0.01^{a}	0.3±0.02^{d}	1.9	0.8±0.03^{a}	0.47±0.04^{e}	54.3±3.2^{c}	4.5±0.5^{ab}
	300	0.63±0.05^{a}	0.34±0.02^{d}	1.5	0.89±0.05^{c}	0.65±0.04^{f}	62.5±3.7^{d}	5.7±0.4^{c}

Seeds of WT and Re-transformed lines were grown on MS medium supplemented with 0, 200 and 300 mM mannitol for 14 days, then chlorophyll contents and enzymes activity were assayed. The data were obtained from three independent experiments. Data are means ± SE. Similar upper case letter in each column indicate no significant differences (Duncan test, P<0.05).

Discussion

Drought and salinity are the major environmental limiting factors of agricultural production systems. To minimize yield losses, it is necessary to improve crop production under stressful conditions. One way is identification and over-expression of regulatory genes in signaling pathway that improve plant salt and drought tolerance. The obtained results indicated for the first time the involvement of *TRR14* in the plant response to the environmental stresses. In current study, we re-transformed *AtTRR14* into the *Arabidopsis* seedlings to study the physiological role of this novel gene in stress tolerance.

TRR14 expression level was very low in unstressed control plants. After treatment with 100 mM NaCl, transcript level increased in control plants (figure 2a). Drought stress also sharply induced expression of the *TRR14* gene in WT plants. The expression level of *TRR14* in manitol treatment was much higher than that in NaCl treatment (figure 2b). Similarly, *TRR14* expression was also induced by NaCl and Manitol treatment in the transformed plants.

Since salt and drought stress induced expression of TRR14, it was expected that *TRR14* could increase *Arabidopsis* seed germination under stressful conditions. Results obtained from seed germination on MS medium, supplemented with NaCl or mannitol, indicated that the transformed lines have higher germination rate than that of WT_s (figures 4a, 5a). The up-regulation of *TRR14* expression by salt or dehydration stress and the enhancement of germination rate of *TRR14* transformed lines under the salt or dehydration stress indicated that *TRR14* affects the germination of *Arabidopsis* in a positive way. But it is not known how *TRR14* affects germination and seedling growth under salt or dehydration stress conditions. These findings confirm our previous results that *TRR14* may affect seed germination in *Arabidopsis* (Aghdasi et al., 2012).

Abiotic stress affects different aspects of plant growth and development such as seed germination (Albuquerque and DeCarvalho, 2003), root length (Fan and Neumann, 2004; Fan et al., 2006; Jamil et al., 2006; Ma et al., 2006), photosynthetic activity, as well as chlorophyll synthesis (Agastian et al., 2000; Yang et al., 2006). Our data indicated that the transformed lines have unchanged root length, Chl a, Chl b and total chlorophyll level when grown on different concentrations of salt or manitol, compared with plants grown under normal condition. In addition, the observed unchanged chlorophyll contents of the transformed lines under stress may suggest that the transformed lines has unchanged photosynthetic capacities than WT. Reduction in chlorophyll and photosynthesis could be a reason for WT growth inhibition under stress.

One of the major effects of stress is induction of reactive oxygen species (ROS) production in plants (Smirnoff, 1996; Noctor and Foyer, 1998; Baier et al., 2005). Plants have enzymatic antioxidant defense system for scavenging of ROS (Blokhina et al., 2003). Our results showed that *TRR14* transformed lines have higher catalase and peroxidase activities than WT when plants grown under stress conditions (tables 1 and 2). It has been shown that tolerant cultivars have increased catalase activity under salt and drought stress (Hernandez and Almansa, 2002; Toorhan et al., 2006). Our results, which indicate an increase in peroxidase activity in transformed lines, are in accordance with those of Wang et al. (2009) and Toorhan et al. (2006), who found that salinity and drought stress lead to an increase in peroxidase activity in tolerant cultivars.

Trehalose is a non-reducing disaccharide which is one of the major osmoprotectants in nature (Crowe et al., 1998; Elbain, 2003). The role of trehalose in abiotic stress tolerance was demonstrated in many plants, but the detailed mechanism is not clear (Goddijn and Van Dun, 1999; Pramanic and Imai, 2005; Shima et al., 2007). Over-expression of trehalose-6-phosphate synthase (TPS) in tobacco and rice improved stress tolerance (Holmstrom et al., 1996; Garg et al., 2002; Jang et al., 2003). TRR14 is a novel protein that suppresses T6P-mediated growth arrest (our unpublished data). Characterization of TRR14 function will provide new insights into trehalose metabolism and stress pathway.

In conclusion, the present study has identified a novel gene, *TRR14,* that can be induced by salt and dehydration stress. The salt and dehydration tolerance of *TRR14* transformed *Arabidopsis* seedlings provide utility of this novel gene in genetic engineering to improve abiotic stress tolerance in plants. More investigation on the transformed plants of other *TRR14* family members will provide better understanding of the functional roles of *TRR14* in plants under abiotic stress conditions.

Acknowledgment

Authors wish to thank Golestan University for financial support.

References

1- Agastian P., Kingsley S. J. and Vivekababdan M. (2000) Effect of salinity on photosynthesis and biochemical characteristics in mulberry genotypes. Photosynthesis 38: 287-290.

2- Aghdasi M., Fazli F. and Bagherieh-Najar B. (2012) Analyses of Arabidopsis trr14 T-DNA insertion Mutants Reveal an Essential Role in Seed Germination. Plant Molecular Biology Reporter 30: 319-329.

3- Albuquerque F. M. C. and Decarvalho N. M. (2003) Effect of type of environmental stress on the emergence of sunflower (*Helianthus annuus* L.), soyabean (*Glycine max* (L.) Merril) and maize (*Zea mays* L.) seeds with different levels of vigor. Seed Science Technology 31: 465-467.

4- Baier M., Kandlbinder A., Golldack D. and Dietz K. J. (2005) Oxidative stress and ozone: perception, signalling and response. Plant Cell and Enviroment 28: 1012-1020.

5- Blokhina O. E., Virolainen E. and Fagerstedt K. V. (2003) Antioxidants, oxidative damage and oxygen deprivation stress: A review Annual Botany 91: 179-194.

6- Chance M. and Maehly A. C. (1955) Assay of catalases and peroxidases. Methods in Enzymology 2: 764–817

7- Crowe J. H., Carpenter J. F. and Crowe L. M. (1998) The role of vitrification in anhydrobiosis. Annual Review of Physiology 60: 73-103.

8- Dunwell J. M. (1998) Cupin: a new superfamily of functionally- diverse proteins that include germins and plant seed storage protein. Biotechnology Genetic Engineering Review 15: 1-32.

9- Dunwell J. M., Culham A., Carter C. E., Sosa-Aguirve C. R. and Goodenough P. W. (2001) Evolution of function divercity in the Cupin superfamily. Trends Biochemistry Science 26: 740-745.

10- Elbein A. D., Pan Y. T., Pastuzak I. and Carroll D. (2003) New insights on trehalose: a multifunctional molecule. Glycobiology 13: 17-27.

11- Fan L., Linker R., Gepstein S., Tanimoto E. and Yamaoto R. (2006) Neumann PM Progressive inhibition by water deficit of cell wall extensibility and growth along the elongation zone of maize roots is related to increased lignin metabolism and progressive

stelar accumulation of wall phenolics. Plant Physiology 140: 603–612.
12- Fan L. and Neumann P. M. (2004) The spatially variable inhibition by wate emergence of sunflower (*Helianthus annuus* L.), soyabean (*Glycine max* (L.) Merril) and deficit of maize root growth correlates with altered profiles of proton flux and cell wall pH. Plant Physiology 135: 2291–2300.
13- Gao M., Tao R., Miura K., Dandekar A. M. and Sugiura A. (2001) Tranformation of Japanese persimmon (Diospyros Kaki thumb) with apple cDNA encoding NADP-dependent sorbitol-6-phosphate dehydrogenase. Plant Science 160: 837-845.
14- Garg A. K., Kim J. K., Owens T. G., Ranwala A. P., Choi Y. D., Kochian, L. V. and Wu R. J. (2002) Trehalose accumulation in rice plants confer high tolerance levels to different abiotic stresses. Proceeding of The National Academy of Sciences 99: 15898-1590.
15- Goddijn O. and Van Dun K. (1999) Trehalose metabolism in plants. Trends Plant Science 4: 315-319.
16- Holmstrom K. O., Mantyla E., Welin B., Mandal A. and Palva E. T. (1996) Drought tolerance in tobacco. Nature 379: 683-684.
17- Holmstrom K. O., Somersalo S., Mandal A., Palva T. E. and Welin B. (2000) Improvement tolerance to salinity and low temperature in transgenic tobacco producing glycine betaine. Journal Experimental Botany 51:177-185.
18- Hernandez J. A. and Almansa M. S. (2002) Short-term effects of salt stress on antioxidant systems and leaf water relations of pea leaves. Plant Physiology 115: 251-257.
19- Jamil M., Lee D. B., Jung K. Y., Ashraf M., Lee S. C. and Rha E. (2006) Effect of salt (NaCl) stress on germination and early seedling growth of four vegetables species. Journal of Central European Agriculture 7: 273-282.
20- Jang I. C., Oh S. J., Seo J. S., Choi W. B., Song S. I., Kim C. H., Kim Y. S., Seo H. S., Choi Y. D., Nahm B. H. and Kim J. K. (2003) Expression of a bifunctional fusion of the E.coli genes for trehalose-6-phosphate phosphatase in Re-transformed rice plants increase trehalose accumulation and abiotic stress tolerance without stunting growth. Plant Physiology 131: 516-524.
21- Jeffery S. and Humphrey G. F. (1975) New spectrophotometric aquations determining chlorophyll a, b, c1 and c2 in higher plants, algae and phytoplankton. Plant Physiology 167:191-194.
22- Kar M. and Mishra D. (1976) Catalase, Peroxidase and Polyphenol oxidase activities during rice leaf senescence. Plant Physiology 57: 315-319.
23- Kishore P., Hong Z., Miao G. H., Hu C. and Verma D. (2004) Overexpression of [delta]-pyrroline-5-carboxylate synthase increases proline production and confers osmotolerance in transgenic plants. Plant Physiology 134: 43-58.
24- Ma S. S., Gon Q. and Bohnert H. J. (2006) Dissecting salt stress pathways. Journl Experimental Botany 57: 1097-1107.
25- Murashige T. and Skoog F. (1962) A revised medium for rapid growth and bioassays with tobacco tissue cultures. Plant physiology 15: 473-479.
26- Noctor G. and Foyer C. H. (1998) Ascorbate and glutathione: keeping active oxygen under control. Annual Review of Plant Molecular Biology 49: 249-279.
27- Pilson-Smits E., Ebskamp M., Paul M. J., Jeuken M., Weisbeek P. J. and Smeekens S. (1995) Improved performance of transgenic fructan-accumulating tobacco under drought stress. Plant Physiology 107: 125-130.
28- Pramanic M. H. and Imai R. (2005) Functional identification of a trehalose-6-phosphate phosphatase gene that is involved in transient induction of trehalose biosynthesis during chililing stress in rice. Plant Molecular Biology 58: 751-762.
29- Shima S., Matsui H., Tahara S. and Imai R. (2007) Biochemical characterization of rice trehalose-6-phosphate phosphatases supports distinctive functions of these plant enzymes. Federation of European Biochemical Sciences Journal 274: 1192.
30- Smirnoff N. (1996) The function and metabolism of ascorbic acid in plant. Annals of Botany 78: 661-669.
31- Toorhan E., Karni L., Astas H., Deventurero G., Chang D. C., Bartal A. and Aloni B. (2006) Apoplastic anti-oxidants in peper (C*apsicum Annum L.*) fruit and their relationship to blossom-end rot. Journal Horticulture Science biotechnology 81: 661-667.
32- Wang W. B., Kim Y. H., Lee H. S., Deng X. P. and Kwak S. S. (2009) Analysis of antioxidant enzyme activity during germination of alfalfa under drought stresses. Plant Physiology and Biochemistry 47: 570-577.
33- Yang X., Chen X., Ge Q., Li B., Tong Y., Zhang A., Li Z., Kuang T. and Lu C. (2006) Tolerance of photosynthesis to photoinhibition, high temperature and drought stress in flag leaves of wheat: a comparison between a hybridization line and its parents grown under field conditions. Plant Science 171: 389-397.
34- Zhu J. K. (2001) Plant salt tolerance. Trends Plant Science 6: 66-71.

Journal of Cell and Molecular Research (2012) 4 (1), 11-17

Organotypic brain slice culture promotes the transformation of haemopoietic cells to the microglial like cells

Roya Lari[1*], Jameel A. Khan[2] and Peter D. Kitchener[2]

[1]*Department of Biology, Faculty of Sciences, Ferdowsi University of Mashhad, Mashhad, Iran*
[2]*Department of Anatomy and Cell Biology, University of Melbourne, Parkville, Victoria 3010, Australia*

Received 3 June 2012 Accepted 12 July 2012

Abstract

The exact developmental origin of microglia is still under debate. In the present study we investigated which heamatopoietic tissues and which features of the organotypic brain slice culture promoted microglia ramification. The potential of cells derived from embryonic yolk sac, embryonic aorta-gonad-mesonephros and adult blood monocytes was examined. These tissues were co-cultured with brain slices after the brain slices had first been maintained *in vitro* for 1 day, 5 days and 9 days. When brain slices had been maintained in culture for 1 day before the donor cells were added, the donor cells took several days to ramify. However, when donor tissues were added to brain slices that had been 5 or 9 days maintained in culture, the donor cells exhibited a ramified morphology within a day. Therefore changes in organotypic brain slices had an effect on the transformation of cells to the microglial morphology. When adult blood monocytes were added to brain slice cultures there was no evidence of any tendency to ramify over 6 days of co-culture. This study did not support the suggestion that microglia cells derive from bone-marrow (BM) cells or from circulating monocytes.

***Keywords*:** Microglia, Macrophage, phagocyte, GFP, CSFE, in vitro, organotypic brain slices culture

Introduction

Microglial cells are considered to be a special form of phagocyte in central nervous system (CNS). They comprise around 10% to 15% of the total cell population of the CNS. Like macrophages in other parts of body, microglia respond to various kinds of CNS injury and, in their active state, can defend against microorganisms and remove dead cells by phagocytosis (Gehrmann et al., 1995).

The study of microglial cells, biology plays a key role in understanding of brain's fundamental tissue reaction against any kind of injuries and infections as well as cellular mechanisms of CNS development (Banati and Graeber, 1994). Although microglia have been known and studied for almost eighty years (Hortega, 1932), the origins of ramified microglia have been long-standing controversy. Several reports have described the existence of various types of microglia; resident parenchymal microglia and amoeboid microglia (Kaur et al., 2001; Monier et al., 2007). There are many lines of evidence showing that microglia cells belong to haematopoietic system, specifically to the myeloid lineages, which give rise to monocytes and macrophages. But the origin in terms of which haematopoietic tissue (or tissues) gives rise to these cells, and relationship between microglia and macrophages are still a matter of controversy (Prinz and Mildner, 2011).

Firstly it might be postulated that microglia, like macrophages in other tissue, belong to monocyte cycle and derive from bone marrow. Support for this suggestion was obtained by several studies that, after whole body irradiation, in these studies, the labelled bone marrow were transplanted to animals to examine the long-term fate of myeloid cells in the CNS (Eglitis and Mezey, 1997; Priller et al., 2001; Zeilhofer, 2008). As a result ramified labelled microglia could be observed in brain parenchyma (Eglitis and Mezey, 1997; Priller et al., 2001; Zeilhofer, 2008). On the other hand, the first microglial precursors appear in the mouse CNS at about E9, before the brain circulation is established and before production of monocytes begin - and certainly before there is any bone marrow (Cuadros and Navascues, 1998; Ginhoux et al., 2010). There

∗Corresponding author E-mail: royalari@gmail.com

are experiments that indicated after bone marrow transplantation only prevascular macrophages could be detected in CNS. For example in female patients who undergo sex-mismatched BM transplantation, only prevascular macrophages could be observed, but no cells with ramified microglia characteristics in the parenchyma could be detected (Unger et al., 1993). Also in the experiment by Ajami et al. (2007), the blood-stream of GFP-positive mice was connected with a GFP-negative animals and the presence of GFP-expressing mononuclear cells in the CNS of these animals was investigated. No evidences of microglia progenitor recruitment from the circulation in CNS were found (Ajami et al., 2007). It has been suggested that the engraftment of marrow-derived myeloid cells in the CNS is affected by the experimental conditions, e.g., irradiation (Prinz and Mildner, 2011). Increasing recent evidence supported that the microglial (and macrophages) are un-replenished by constant new arrivals and turnover, and the transient haemopoietic tissues are the origin of the entire microglia population (Ginhoux et al., 2010; Monier et al., 2007; Prinz and Mildner, 2011). In the present study we investigated which haemopoietic tissues and which features of the brain slice promoted microglia ramification. The organotypic brain slice cultures were co-culture with haematopoietic tissues after the brain slices had already been in culture for periods of 0, 1, 5 or 9 days.

Materials and Methods

Organotypic brain slice culturing

Brain slicing

Sparge Dawley rat pups age between postnatal day (P) 0 to 8 days old were used for brain slicing. In a laminar flow hood rat pups were sacrificed by decapitation. The head was placed in the ice-cold (4°C) hyperosmotic (>300 mOsm) slicing buffer. The brain were quickly desiccated from the head in the ice-cold slicing buffer and attached to a chuck with super glue. Warm agar (37-40°C) swirled around the brain to provide support for the brain during the cutting of 250 μm thick slices on a Leica VT 1000 vibratome. The chuck was placed in the slicing chamber that had been filled with ice-cold slicing buffer (4°C and pH 7.4) and the whole slicing chamber was packed in ice to keep it cold.

Brain culture

After cutting, the agar was gently removed from around the slices. 1 ml of cold (4°C) culture medium was placed in the wells of 6-well tray. Sterile Millicell-CM 30mm-diameter transparent culture inserts (Millipore) were used for brain slice culture. A glass pasture pipette was used to gently transfer the brain slices to the insert membrane. Usually, two slices were placed in each insert. The slices were keptat 4°C for next two hours, and then refreshed with a change of the MEM from cold 4°C to warm 37°C. The cultures were placed in an incubator at 37°C in a 5% CO_2 95% O_2 atmosphere. The MEM was changed every two days. The cultured tissue was kept in an incubator for 1 day, 5 days or 9 days before co-culturing with haematopoietic tissues.

Lectin staining for paraffin section

Paraffin sections of the cultured brain slice tissues that were 0 day in vitro (DIV), 1 DIV, 5 DIV and 9 DIV were de-waxed in Histolene and hydrated from absolute ethanol to 70% ethanol and then into phosphate buffer solution (PBS). Sections were incubated with biotinylated Lycopersicon esculentum agglutinin (LEA) lectin (vector Laboratories, Inc.CA). Lectin was made up at a diluted of 1:3000 in fish gelatin blocker. After 24-48 hours they washed (4x5 times) in 0.1 M PBS (0.1 M and pH 7.4). Lectin binding that remained after the washes was visualised by the avidin-biotin-HRP localisation of biotinylated lectins. A 1:100 dilute solution of Avidin Biotin Complex (ABC; vector Laboratories, CA) was made up in 0.1 M PBS and applied to the sections for 12-24 hours. The sections were washed again (4-5 times in PBS) and reacted with 0.05% of diaminobenzadine (DAB) and 0.01% hydrogen peroxide (H_2O_2) in PBS.

Haematopoietic tissues preparations

Haematopoietic tissues were dissected from embryos, taken by Caesarean section from deeply anaesthetised (100 mg/kg Nembutal i.p.) time-mated mothers. Time mating involved housing two female rats with a male for one hour in the morning and subsequently examined for vaginal plugs. The day of the appearance of vaginal plugs was designated as day 0. Embryos from 11 to 13 day of gestation (E11–E13) were obtained within sections of uterus and placed in a Petrie dish containing cold (4°C) sterile PBS, this dish was transferred to a laminar flow hood where subsequent dissection and washing took place. In warm MEM the embryos (in their yolk sacs) were dissected from the uterine tissues. Then, by using a plastic transfer pipette, the embryos were transferred to a separate Petrie dish containing warm MEM. After dissecting the yolk sac or AGM from embryo, scissors were carefully

cleaned to avoid transferring cell between haematopoietic tissues.

Vital labelling of embryonic haematopoietic tissues

To labell the haematopoietic tissues, they were infected with recombinant adenoviruses that encoded the gene for green fluorescent protein (adeno- GFP) (Kindly provided by Dr Steve Petrou from the department of Physiology University of Melbourne). The viral lysate was diluted 1:100 in MEM and added to haematopoietic tissue cultures. Tissues were left in incubator at 37°C in 5% CO_2 / 95% O_2 overnight to allow for infection.

Co-culturing the tissues

After 24 hours the infected tissue was washed 2-4 times with MEM to prevent transferring free virus to cultures. Then the infected haematopoietic tissues co-cultured with brain slices that have been 1, 5 or 9 DIV. These co-culture slices were harvested after 1 day, 3 day and 6 days (MEM was changed every two days).

In order to control for endogens infection with free viral particles, the culture medium from last wash of adeno-GFP infected haematopoetic tissues was added to one well of 1DIV organotypic brain slice culture. No infections were observed.

CFSE labelling the monocyte cells

Monocyte cells were resuspended in sterile PBS to 2 ml. A 2 ml stock solution of CFSE (5-(and –6)-carboxyfluorescein diacetate succiinimidyl ester, Molecular probes, Eugene, OR) in DMSO (stored desiccated at – 20 C) was added for 1 hour at room temperature. Then the monocytes were washed twice before added to brain slice culture.

Co- culture of organotypic brain slices with adult monocytes

In order to compare of adult monocytes with embryonic haematopoietic tissues in capacity of producing microglial like cells. Monocytes were separated from adult blood by using Boyum method (Boyum, 1968) and co-cultured with organotypic brain slices. Female adult rats were anesthetized by (1 ml) Nembutal. Via the cardiac 4-ml blood were drawn into the heparinized heparnized syringe. 3 ml of lymphocyte separation medium (LSM) were transferred to a 15- ml centrifuge tube and 4-ml blood diluted with 4 ml sterile PBS (0.1 M and PH 7.4). Supplemented the blood layered carefully over the LSM. The tube was centrifuged at 1200 H x g at room temperature for 20 minutes resulting a band of mononuclear lymphocytes observed between LSM and plasma. Top layer of clear plasma aspirated to 2-3 mm above lymphocytes layer aspirated the lymphocytes layer and half of the LSM below it transferred to centrifuge tube. The lymphocytes were washed several times by pelleting and resuspended in sterile PBS (0.1 M and PH 7.4).

Results

Endogenous microglia ramification in brain slice cultures

Endogenous microglial cells exhibited dramatic changes during the 9-days *in vitro*. At 0 DIV of the most of the LEA labelled cells had ramified processes typical of resting microglia (figure 1a), and some were macrophages. The great majority of macrophages were found in the white matter tracts and near the pial and ventricular surfaces, whereas microglia where seemingly evenly distributed throughout the parenchyma. After 1 DIV all of the Lectin labelled cells where rounded, consistent with a change of microglial which is the active phenotype (figure 1b). At 5 DIV some of the LEA labelled cells were ramified, some cells in intermediate phase, and macrophages were also observed (figure 1c). After 9 DIV most of the cells were highly ramified or had the intermediate phenotype, suggesting that the cells were still ramifying (figure 1d).

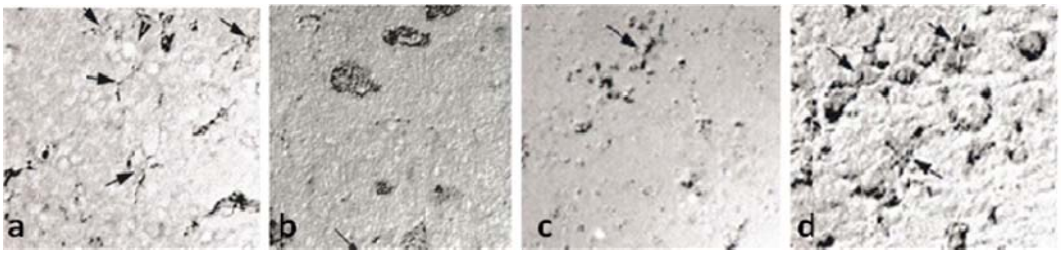

Figure 1. Endogenous microglial changes in brain slices culture In vitro (a) at 0 DIV ramified microglia stained with LEA (b) after 1 DIV all of the LEA labelled cells where rounded. (c) at 5 DIV some of the LEA labelled cells were ramified with short-branched processes. (d) At 9 DIV LEA stained highly ramified microglia with long multi-branched processes (arrows). Scale bar: 25 μm in all panel.

Brain slices co-cultured with yolk sac and AGM after one DIV

In this experiment five brain slices from a rat co-cultured with yolk sac and one slice co-cultured with AGM after one DIV. At day 1 of co-culture no ramified cells were observed. After six days of co-culturing the cultures were fixed. Fluorescent green protein (GFP) positive cells were found in both AGM and yolk sac co-cultured slices, mainly around the pial surface of the slices. In most of the cells the nuclei were brighter than the cytoplasm. Many of the GFP labelled cells were highly ramified. Also, some intermediate and round cells were observed, a few of which had one very long process along with some stout branches (figure 2 a, b).

Brain co-cultured with yolk sac and AGM after 5 DIV

In total eight brain slices were cultured for 5 days and then co-cultured with yolk sac or AGM. After one day co-culturing a great number of GFP labelled cells could be observed which distributed around the edges of the brain slices. Both AGM and yolk sac produced the fluorescent cells without any obvious distinction between them. Some of these cells were ramified with multi–branched cytoplasmic processes and strongly fluorescent green (figures 2 c, d). There were also some ramified and round cells with faint green fluorescent.

Brain co-cultured with yolk sac and AGM after 9 DIV

From a rat ten brain slices prepared and cultured. After 9 DIV the slices co-cultured with AGM or yolk sac. The co-cultured tissues were fixed in the following day. There were some haematopoietic-derived cells with highly green fluorescent in brain slices, many of which had a ramified morphology while others had a round appearance (figures 2 e, f). Some of the labelled cells had only weak green fluorescent. There was not any obvious difference between yolk sac and AGM in term of producing ramified cells. Density and morphology of the GFP labelled cells in this experiment resembled the GFP labelled cells of the 5 DIV co-cultures.

Co-culture the organotypic brain slices with adult monocytes for 6 days

In order to detect the potential of the precursor of definitive macrophages (monocytes) to produce the ramified type cells, the brain slices co-cultured with monocytes isolated from adult blood. The monocytes labelled by CFSE produced an intense green fluorescence not unlike that produced by GFP. Six brain slices of P6 rats co-cultured with adult monocytes after one DIV. The co-cultured tissues were fixed after 3 days or 6 days of co-culture. Fluorescent microscopy revealed the huge number of green fluorescent cells on the brain slices in both 3 and 6 days cultures. They had typical morphology of the monocytes, with round cell body and no branches. The density of the green cells after 6 days appeared to be higher than at 3 days in culture (figures 2 g, h).

Discussion

This and previous studies have demonstrated that the organotypic culture of neonatal brain slices provides an environment that maintains microglial cells and permits their reversible transformation from resting to active phenotypes (Coltman and Ide, 1996; Czapiga and Colton, 1999; Strassburger et al., 2008). This allows the brain slice to be employed in an assay for the microglial generating potential of candidate haemopoietic tissues. In this study, it was shown that both yolk sac and AGM from E12 rat embryos can produce vast numbers of microglia-like cells after being co-cultured for several days with brain slices. The observation that both yolk sac and AGM can produce these microglial-like cells does not address which one, or both, tissues was the ultimate origin of these cell, as they are connected by the circulation from E9, thus have the opportunity to mutually seed one another.

Although this study confirmed the previous report that embryonic tissue can give rise to microglial-like cells in brain slice cultures (Alliot et al., 1999; Prinz and Mildner, 2011), the positive characterisation of the ramified cells could not be extended beyond morphological features, as lectin labelling of these cells could not be achieved. It is important to note that while labelling with LEA did not label the "microglial-like" embryonic cells, this does not mean they did not express the carbohydrates that allow microglial labelling in paraffin sections. This is because the lectin labelling of the whole mount cultured slices (using fluorescent strepavidin to localise the biotinylated lectins) also failed to label the endogenous microglia of the host brain slice, which are readily labelled with lectin using the ABC technique on paraffin sections. Thus using the fluorescent methods to localise LEA ligands is not sufficiently sensitive to stain microglia in these whole-mount preparations. The option of paraffin processing was not available for this particular study, as it would result in the loss of the GFP fluorescence which identified the cells as being of donor origin.

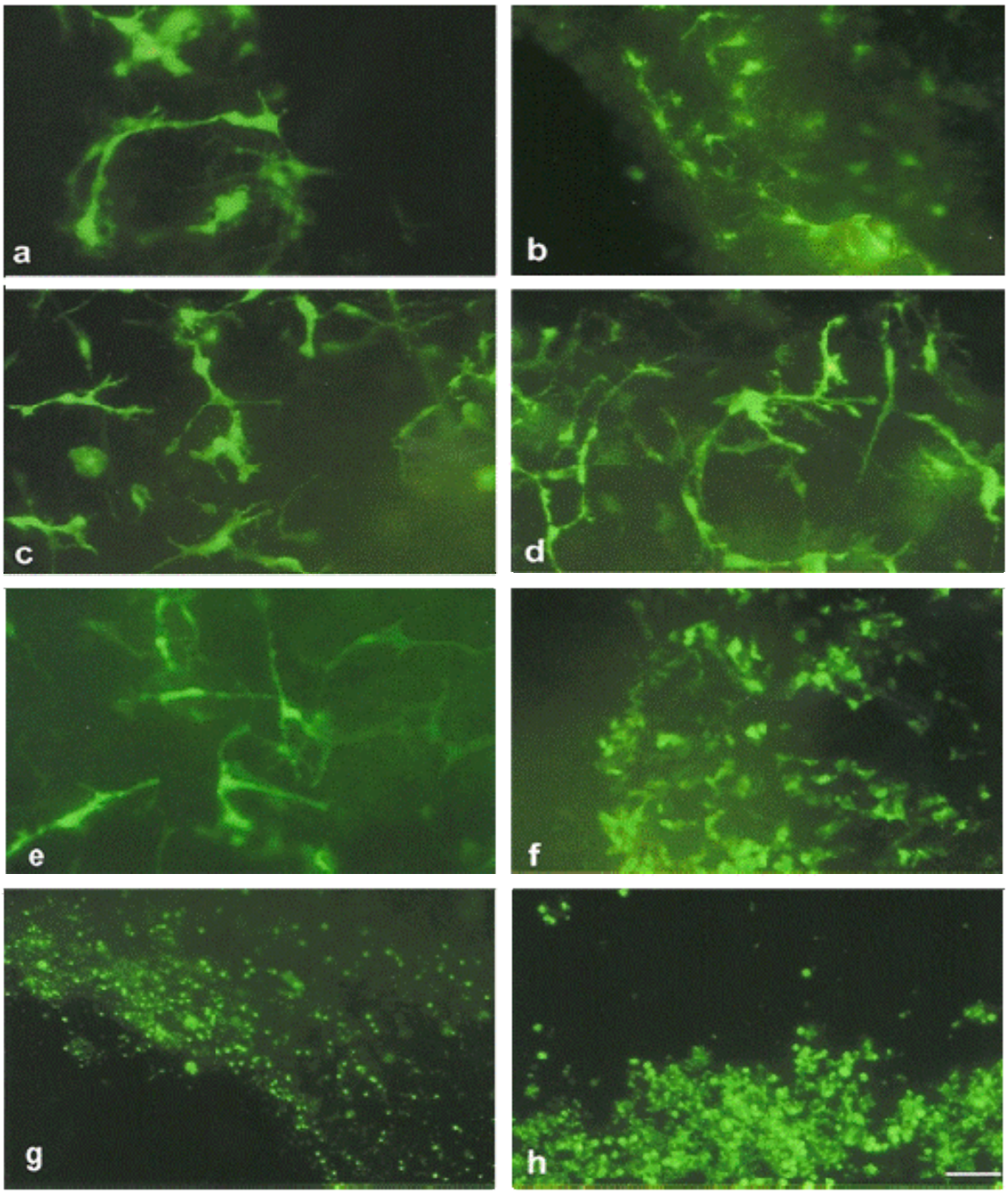

Figure 1. (a-b) brain slices co-cultured after one DIV with adeno-GFP-labelled E11 yolk sac (a) or AGM (b) and fixed after 6 days. Some ramified microglia like cells could be observed in both tissues. (c-d) brain slices co-cultured after 5 DIV with adeno-GFP-labelled yolk sac (c) or AGM (d) and fixed after one day. Some ramified microglia like cells could be observed in both tissues. Also some macrophages and some cells with fewer ramifications could be observed. (e-f) brain slices co-cultured after 9 DIV with adeno-GFP-labelled yolk sac and fixed after 1 day. Some ramified microglia like cells (e) and some macrophages (f) could be observed. (g-h) Organotypic brain slices co-cultured with CFSE labelled adult monocytes 3 days (g) or 6 days (h). No ramified microglia like cells could be observed.
Scale bar 50 mm in panel g and h, 25 mm in other panels.

While failing to provide cytological evidence of the microglial phenotype, other aspects of these cells were characterised in the present study. Khan's results showed that highly ramified donor derived cells were present after 6 days of co-culture (unpublished); this time *in vitro* could be effected by the state of the slice, or it may be that the expression of the ramified phenotype takes many days to emerge. As discussed above, the brain slice culture is an environment that induces activation of

phagocytes after cutting but subsequently this environment changes to be one which permits the re-ramification of microglia. The role of the state of the brain slice in the adoption of the ramified morphology was investigated by co-culturing the embryonic tissues with brain slices that had spend various times in culture before the donor tissues were added. It was clear that the ramified phenotype of donor cells could be observed within a day of co-culture if the brain slice was 5 or 9 days *in vitro* before the donor tissue was added.

This result strongly suggests that the status of the brain slice has a major influence on the adoption of the ramified phenotype. While the elimination of the dying and dead cells (caused by the slicing) might be why the older slices are more conducive to ramification, another possibility is that astrocyte proliferation may be the crucial factor facilitating the acquisition of the ramified phenotype. It has been reported that astrocyte monolayers induce ramification of isolated microglia, monocytes and macrophages (Wilms et al., 1997). The findings of Wilms et al. (1997) that not only microglia, but also macrophages and monocytes transform into a ramified phenotype suggest that the monocytes in our experiments should have ramified on the brain slices. However, monocytes isolated from the blood of adult rats did not exhibit the transformation into the ramified phenotype at any stage of co-culture (up to 6 days). A reason for this discrepancy might be that other factors are needed by monocytes that are not needed by the embryonic tissues. For example, monocytes and macrophages do not ramify if serum is present, unless astrocytes are included in the culture, but serum may in fact be required by monocytes for reasons unrelated to ramification, and thus the culture conditions employed in the present studies did not allow monocytes to differentiate to a stage where they could exhibit a ramified morphology.

The methods developed and characterised by this and other studies- such as brain slice cultures, serum free culture systems and the isolation of embryonic and adult haemopoietic tissues - will permit further elucidation of the identity, origin, nature and behavior of the brains immune cells.

Acknowledgment

This study was performed in the Department of Anatomy and Cell Biology, University of Melbourne, Australia.

References

1- Ajami B., Bennett J. L., Krieger C., Tetzlaff W. and Rossi F. M. (2007) Local self-renewal can sustain CNS microglia maintenance and function throughout adult life. Nature Neuroscience 10: 1538-1543.

2- Alliot F., Godin I. and Pessac B. (1999) Microglia derive from progenitors, originating from the yolk sac, and which proliferate in the brain. Brain Research Developmental Brain Research 117: 145-152.

3- Banati R. B. and Graeber M. B. (1994) Surveillance, intervention and cytotoxicity: is there a protective role of microglia? 'Developmental Neuroscience 16: 114-127.

4- Boyum A. (1968) Isolation of mononuclear cells and granulocytes from human blood. Isolation of monuclear cells by one centrifugation, and of granulocytes by combining centrifugation and sedimentation at 1 g. Scandinavian Journal of Clinical and laboratory Investigation. 97: 77-89.

5- Coltman B. W. and Ide C. F. (1996) Temporal characterization of microglia, IL-1 beta-like immunoreactivity and astrocytes in the dentate gyrus of hippocampal organotypic slice cultures. International Journal of Developmental Neuroscience 14: 707-719.

6- Cuadros M. A. and Navascues J. (1998) The origin and differentiation of microglial cells during development. Progress in Neurobiology 56: 173-189.

7- Czapiga M. and Colton C. A. (1999) Function of microglia in organotypic slice cultures. Journal of Neuroscience Research 56: 644-651.

8- Eglitis M. A. and Mezey É. (1997) Hematopoietic cells differentiate into both microglia and macroglia in the brains of adult mice. Proceedings of the National Academy of Sciences 94: 4080-4085.

9- Gehrmann J., Matsumoto Y. and Kreutzberg G. W. (1995) Microglia: intrinsic immuneffector cell of the brain. Brain Research Reviews 20: 269-287.

10- Ginhoux F., Greter M., Leboeuf M., Nandi S., See P., Gokhan S., Mehler M. F., Conway S. J., Ng L. G., Stanley E. R., Samokhvalov I. M. and Merad M. (2010) Fate mapping analysis reveals that adult microglia derive from primitive macrophages. Science 330: 841-845.

11- Hortega D. R. (1932) Cytology and cellular pathology of the nervous system. Hober, New York 2: 481-534.

12- Kaur C., Hao A. J., Wu C. H. and Ling E. A. (2001) Origin of microglia. Microscopy Research and Technique 54: 2-9.

13- Monier A., Adle-Biassette H., Delezoide A. L., Evrard P., Gressens P. and Verney C. (2007) Entry and distribution of microglial cells in human embryonic and fetal cerebral cortex. Journal of Neuropathology and Experimental Neurology 66: 372.

14- Priller J., Flugel A., Wehner T., Boentert M., Haas C. A., Prinz M., Fernandez-Klett F., Prass K., Bechmann I., de Boer B. A., Frotscher M., Kreutzberg G. W., Persons D. A. and Dirnagl U. (2001) Targeting gene-modified hematopoietic cells to the central

nervous system: Use of green fluorescent protein uncovers microglial engraftment. Nature Medicine 7: 1356-1361.

15- Prinz M. and Mildner A. (2011) Microglia in the CNS: immigrants from another world. Glia 59: 177-187.

16- Strassburger M., Braun H. and Reymann K. G. (2008) Anti-inflammatory treatment with the p38 mitogen-activated protein kinase inhibitor SB239063 is neuroprotective, decreases the number of activated microglia and facilitates neurogenesis in oxygen-glucose-deprived hippocampal slice cultures. European Journal of Pharmacology 592: 55-61.

17- Unger E. R., Sung J. H., Manivel J. C., Chenggis M. L., Blazar B. R. and Krivit W. (1993) Male donor-derived cells in the brains of female sex-mismatched bone marrow transplant recipients: a Y-chromosome specific in situ hybridization study Journal of Neuropathology and Experimental Neurology 52: 460-470.

18- Wilms H., Hartmann D. and Sievers J. (1997) Ramification of microglia, monocytes and macrophages in vitro: influences of various epithelial and mesenchymal cells and their conditioned media. Cell and Tissue Research 287: 447-458.

19- Zeilhofer H. U. (2008) Loss of glycinergic and GABAergic inhibition in chronic pain--contributions of inflammation and microglia. International Immunopharmacology 8: 182-187.

Journal of Cell and Molecular Research (2012) 4 (1), 18-27

Critical and synergy nodes in insulin-EGF signaling network

Hassan Monhemi[1], Mohammad Reza Housaindokht[1,2], Mohammad Reza Bozorgmehr[3] and Ahmad Reza Bahrami[2,4]*
[1]Biophysical Chemistry Laboratory, Department of Chemistry, Faculty of Science, Ferdowsi University of Mashhad, Mashhad, Iran
[2] Cell and Molecular Biotechnology research group, Institute of Biotechnology, Ferdowsi University of Mashhad, Mashhad, Iran
[3]Department of Chemistry, Faculty of Science, Islamic Azad University, Mashhad Branch, Mashhad, Iran
[4]Department of Biology, Faculty of Science, Ferdowsi University of Mashhad, Mashhad, Iran

Received 25 March 2012 Accepted 11 June 2012

Abstract

Signaling pathways are not isolated from their surroundings. They are also intervened by other signaling pathways known as "crosstalk mechanism". One of the most important crosstalk mechanisms is the insulin-EGF network. Although insulin and epidermal growth factor (EGF) networks have some complexity in their isolated forms, their complexities will grow in the crosstalk network. In this study, we used the analytical tools of the systems biology workbench for elucidating some ambiguities of the insulin-EGF crosstalk. Based on sensitivity analysis, we reconstructed an elucidated model with 51 chemical reactions in comparison with the previous model with 111 chemical reactions. Interestingly, this reduced model reproduces the results of the original model in synergy conditions. We noticed two controlling pathways with direct participation of phosphorylated insulin and EGF receptors that involve Insulin Receptor Substrate (IRS) and Src kinase modules. Also, insulin pathway by producing phosphatidylinositol-3, 4, 5-triphosphate (PIP3), and EGF pathway by activation of GAB1, control the downstream events and lead to potentialities in the mitogenic signal. Surprisingly, Shc and phosphatase SHP2-dependent reactions have no significant roles in the synergy conditions and are not involved in the reduced model. Regarding sensitivity analysis, all Ras/ERK cascade reactions are crucial for signal transduction and were kept in the reduced model.

***Keywords*:** Signaling pathways, crosstalk, computational modeling, systems biology, insulin-EGF networks, sensitivity analysis, targeted drug therapy

Introduction

Since the 1990s, modeling has appeared as a novel tool to perform the abundant information on the molecular parts list and the troublesome complex interaction circuitry of signaling networks (Kholodenko, 2006). Signal is transuded along a complex pathway of molecular interactions; this leads to distinct biological responses and different functions of the cells. Signaling pathways depend very much on various species, interactions, and parameters of such busy pathways and it is difficult to identify conserved signaling modules and those specific control mechanisms that modulate the strength of any signaling. On the other hand, the crosstalk between heterologous pathways increases the complexity of the integrated signaling pathways.

Moreover, in these years, study about the mechanisms of cross talking among signaling pathways becomes an interesting research area in medicine and cell biology (Borisov et al., 2009; Sasagawa et al., 2005; SureshBabuCV et al., 2008; Yu et al., 2006; Zhu and Kyprianou, 2008). Thereby, some strategies are required to reduce the complexity of a crosstalk model and characterize the possible synergy effects. Mathematical modeling emerged as a solution to study the complex behavior of networks (HarshaRani et al., 2005; Orton et al., 2005). One of the most popular analytical tools for model reduction and identifying the controlling nods of a pathway is sensitivity analysis (Birtwistle et al., 2007; Bornheimer et al., 2007; Chen et al., 2009; Ihekwaba et al., 2004; Kinzer-Ursem and Linderman, 2007; Liu et al., 2005; Mahdavi et al., 2007; Mauch et al., 1997; Maurya et al., 2005; Zhang et al., 2009; Zheng and Rundell, 2006). Sensitivity analysis is an important tool in the studies of the dependence of a system on external parameters (Ingalls and Sauro, 2003). With this modeling technique, it is possible to predict the main routs of any pathway and reduce the complexities. This approach could be especially useful for studying the complex crosstalk mechanism.

One of the most important crosstalk mechanisms that involve such complexities is insulin-EGF network. Although insulin and EGF networks have some complexity in their isolated forms, these complexities will grow in the crosstalk

∗Corresponding author E-mail:
h_monhemi_chem@ymail.com

network (Avruch, 1998; Kholodenko et al., 1999; Schoeberl et al., 2002; Taniguchi et al., 2006). Insulin is a well-described anabolic agonist. The main physiological function of insulin signaling is metabolic, involving the control of glucose metabolism and stimulation of protein and lipid synthesis (Cheatham and Kahn, 1995). Other important functions of insulin are to enhance, or potentiate, the effects of growth factors such as epidermal growth factor (EGF), particularly in relation to cell proliferation, extracellular signal-regulated kinase (ERK) activation and DNA synthesis (Chong et al., 2004; Crouch et al., 2000; Ediger and Toews, 2000). On the other hand, EGF can negatively regulate insulin signaling and in some conditions can evoke metabolic responses, e.g., GLUT4 translocation (Gogg and Smith, 2002; Gual et al., 2003; Ishii et al., 1994). The epidermal growth factor receptor (EGFR) and the insulin receptor (IR) networks share many downstream components and can be considered as integrative cellular signaling network (Borisov et al., 2009). However, this crosstalk with combinatorial complexity of molecular interactions and a variety of feedback and feed-forward loops has imposed some limitation on our ability to understand their functionality and how they affect the robustness of the overall pathway. The formulation and study of such models must also be reduced as far as possible to cope with the increasing complexity demanded and exponential of metabolic reconstruction, computed from sequenced genomes (Goryanin et al., 1999). Also identifying the synergy sites of such systems has crucial roles in development of the future studies and therapeutic usage such as targeted diabetes (Carlson et al., 2003) or cancer (hornberg et al., 2006) therapy.

Therefore, in this paper we used the robust and new model of this crosstalk mechanism constructed by Brisov et al. (Borisov et al., 2009), and employed sensitivity analysis to identify those reactions that exert the greatest control on the activation of ERK. Using obtained results, we reproduced a reduced model that contains controlling reactions in synergy condition. Then, with parameter variation, we signalized the roles of synergic and essential reactions of this mechanism.

Materials and Methods

Model reconstruction

As a template for analysis, we use the new and robust insulin-EGF crosstalk model of Borisov et al. (Borisov et al., 2009). This model contains 111 processes and several of these processes have some sub processes, too. Therefore, they have named their model “minimal” (Borisov et al., 2009). We converted the processes of the template model into the ordinary differential equations (ODEs) form. The construction and further analysis of the model was carried out by Matlab simbiology toolbox. This toolbox can perform time-dependent sensitivity analysis.

Sensitivity analysis

We considered one simplification in calculating sensitivity coefficients and did not consider the mass balance for EGF (Borisov et al., 2009). Other aspects of the template model are conserved. For each process, we computed the time-dependent sensitivity coefficients for the parameters such as the rates of reaction, forward and backward rate constants, k_{cat}, and Michaelis-Menten constants during activation of signal. The number of the studied sensitivity coefficients depends on the choice of system variables and system parameters. These coefficients also vary with both time and stimulus dosage. For illustrative figures, we assigned sensitivity coefficients in two time domains: *i)* maximum sensitivity of each reaction before and after maximal activation of ERK *ii)* in maximal activation of ERK (figure 1). Dose-dependencies may lead to the wrong results in calculation of sensitivity coefficients (Liu et al., 2005). Some reactions have a high flux but not a high sensitivity coefficient while these reactions may be critical in the signaling pathway. Moreover, in particular concentration of stimulus, addition of excessive dose does not change the maximal activation and only leads to increment of the flux. To handle this problem, we calculated the dose-response curves for insulin and EGF network and then assigned the doses in which the maximal activation is not saturated. Therefore, for computation of all sensitivities, we used 0.05 nM and 30 nM doses for EGF and insulin, respectively (figure 2).

Results

Reduced model of Insulin-EGF network

Using sensitivity analysis we were able to reconstruct a reduced replica of the original model of insulin-EGF crosstalk mechanism. Browsing in time-dependent sensitivity coefficients showed that more than one-half of reactions have the sensitivity coefficients equal or near to zero. With some simplifications, reactions that have non zero sensitivity coefficients, are gathered in a reduced model. Thus, in this model, only the necessary

reactions that have a noticeable role in the activation of phosphorylated ERK are considered. The graphical representation of this reduced model shown in figure 3 and its SBML file (HarshaRani et al., 2005) is provided. The model is initiated by ligand binding to Insulin and EGF receptors and autophosphorylation of the ligand-receptor complexes. Further details, approximations and explanations of isolated or crosstalk models of insulin and EGF are discussed in the literatures (Avruch 1998; Borisov et al., 2009; Cheatham and Kahn, 1995; Crouch et al., 2000; Johnston et al., 2003; Kholodenko et al., 1999; Schoeberl et al., 2002).

Validation and scope of reduced model

Not with standing all changes in the original model that were discussed above, simulation of reduced model versus original model (Borisov et al., 2009) in different doses of insulin and EGF confirm the reliability of the model (figure 4). For simulations, we utilized the same doses as used in original model (Borisov et al., 2009). On the other hand, sensitivity coefficients were obtained in the synergy conditions (Co-stimulation of both stimuli), because we are interested in the study of synergy effects. So, the model is reconstructed for the study of the synergy effects and only works correctly by co-stimulation. Also, at high concentrations of each stimulus, variations from the original model are not negligible (figure 4 (1 nM EGF and 100 nM insulin)). This is due to notability of deleted reactions (especially inhibition reactions) in regulation of high concentrations of each stimulus.

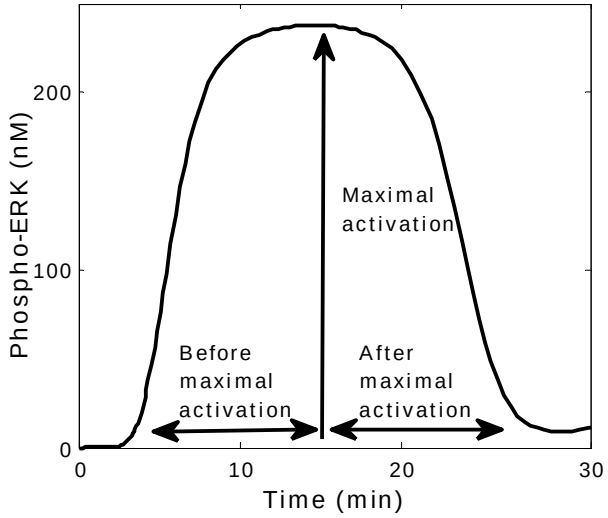

Figure 1. Time regions for calculation of sensitivity coefficients.

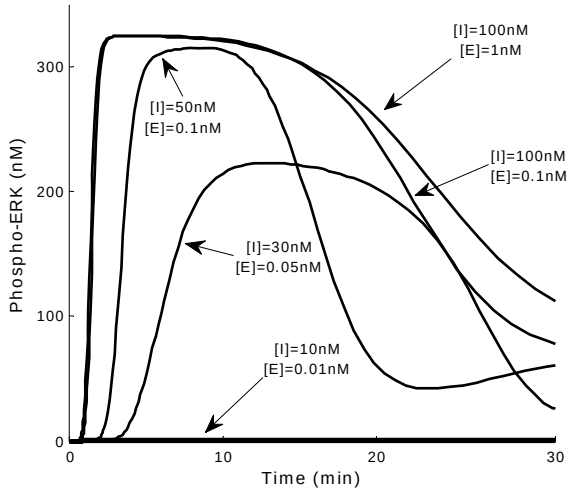

Figure 2. Dose response curve of ERK activation. [E] And [I] represent concentrations of EGF and insulin respectively.

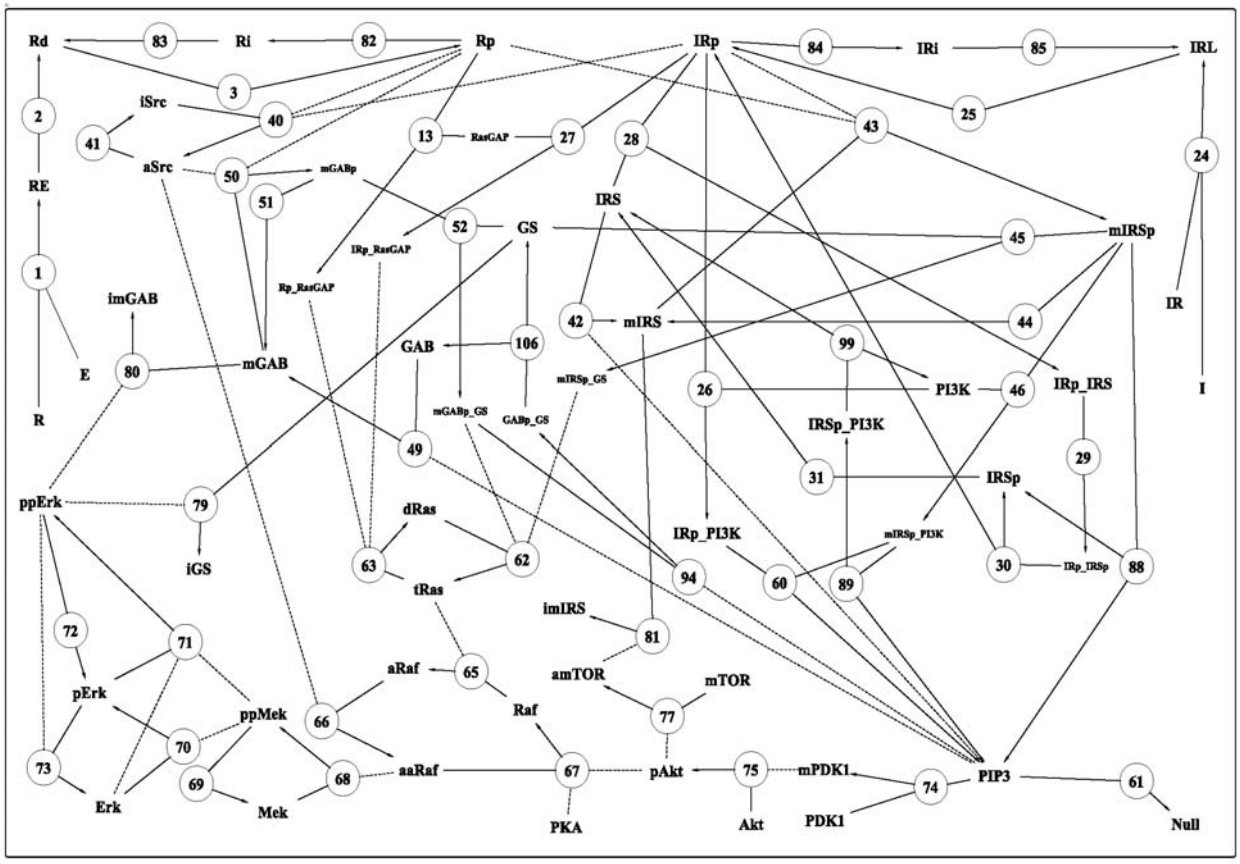

Figure 3. Graphical representation of the reduced Insulin-EGF model. The circles show the number of each reaction. Reactions are numbered according to the original model developed by Brisov et al. (Borisov et al., 2009) (All reactions, rate constant parameters and abbreviations are presented in supplementary table S1) and only operative reactions with respect to their sensitivity coefficients are considered. The dotted lines show the activation and inhibition interactions. Phosphorylation of ERK is the end point of the pathway.

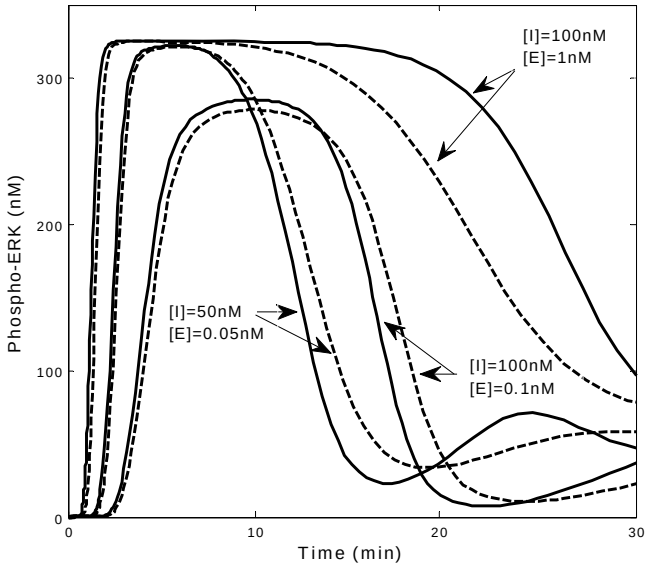

Figure 4. Dynamics of EGF and insulin-induced ERK activation. The dashed lines show the time courses calculated by the original model and the solid lines show the time courses calculated by the reduced model. Calculations were performed with different co-stimulation of EGF and Insulin. [E] And [I] represent concentrations of EGF and insulin, respectively.

Discussion

Unlike the original model (Borisov et al., 2009), the reduced model does not consider direct binding of EGFR to Shc, Grb2–SOS, PI3K, protein phosphatase SHP2 and also binding of phosphorylated insulin receptor to phosphatase SHP2. Instead, phosphorylated EGFR only participates on the activation of Src (reaction 40), phosphorylation of membrane associated IRS (reaction 43), and GAB1 (reaction 50) and binds to RasGAP (reaction 13). Also, Phosphorylated insulin receptor activates Src, phosphorylation of membrane associated IRS and binds to the IRS, PI3K and RasGAP. Surprisingly, all Shc and SHP2-dependent reactions are eliminated in the reduced model. All Ras/ERK cascade reactions are conserved in the reduced model. Activation of ERK was the main purpose in derivation of sensitivity coefficients and thus, some reactions of PI3K/AKT cascade that have no impressive role in activation of ERK, are omitted. Moreover, all degradation reactions and useless complexes are deleted. Now, the model is elucidated to some extent and therefore, it is ready for further discussion, experimentation or analysis.

Synergy nodes in the model-direct participation of insulin and EGF in the crosstalk

Two distinct synergy nodes, with direct participation of the phosphorylated insulin and EGF receptors, appear in the reduced model and involve activation of Src (reaction 40) and phosphorylation of membrane associated IRS (reaction 43, figure 3). Sensitivity coefficients of these two processes in maximal activation of ERK show the emphasis of reaction 40 in comparison with reaction 43 (figure 7A). Parameter variation in different conditions also indicate this result (figures 5 A and B). Diminution of the rate has more destructive effects for reaction 40 than that for reaction 43. Src activation ultimately leads to Raf activation (figure 3). There are some evidences indicating that the application of Src inhibitors, lead to the improvement of tumor cells in some extent (Chen et al., 2008; Koga et al., 2006). This shows the fragility and important role of Src kinase in signaling pathways in different cells which is also in agreement with our results.

The roles of phosphatidylinositol-3, 4, 5-triphosphate (PIP3) in the ERK activation

Clearly, the reduced model shows that PIP3 can negatively (reactions 74 and 94) or positively (reaction 42 and 49) induces the ERK activation. PIP3 induces conversion of cytoplasmic IRS and GAB1 to their membrane associated states that ultimately leads to activation of Ras. The extent and manner of this activation through these two reactions can be elucidated with parameter variation (figure 6A and B). Simulations in the different conditions of these reactions (without, half and complete inhibition) showed that by complete inhibition of the reaction 49, the signal is attenuated near to zero (figure 6A). However, half and non inhibition conditions produce similar results. This means that in the synergy conditions, despite the notability of reaction 49 in the pathway, the signal is promoted by a small performance of this reaction. On the other hand, the signal has some sensitivity to the variation in the rate parameters of reaction 42 (figure 6B). These results are reflected in sensitivity coefficients, too. Maximal signal has no sensitivity to reaction 49; but reaction 49 has a sensitivity coefficient of about 0.45 (figure 7A).

Variations in the rate parameters of the reaction 74 do not change the signal amplitude considerably (data not shown); instead the reaction 94 has a high regulatory role in the model (figure 6C).

The reduced model predicts that interactions of PI3K with phosphorylated Insulin receptor and IRS are responsible reactions for PIP3 production. However, the original model has also been considered the interactions of GAB1 and phosphorylated EGFR (reaction 12 and 53 in the supplement, table S1). These results reveal some key mechanistic elucidation of crosstalk pathways in the reduced model. EGF network, by activation of Src and GAB1 modules can positively regulate the ERK activation while the insulin network activates this signal by production of PIP3. This molecular trade leads to potentialities in the mitogenic signal.(Borisov et al., 2009; Chong et al., 2004; Crouch et al., 2000).

Critical nods of the model

We conserved all reactions of Ras/ERK cascade in the reduced model (reactions 63-73). This is due to the high amounts of sensitivity coefficients for the reactions of this cascade. The coefficients also show the fragility of each reaction (figure 7 A and B). Thus, like Src kinase, these fragilities lead to the appearance of new points for drug targeting (Amit et al., 2007; Roberts and Der, 2007; Scaltriti and Baselga, 2006; Zhu and Kyprianou, 2008). However, the sensitivity coefficients for the crosstalk mechanism, rather than for each isolated pathway, are to some extent decreased (Data not shown). This shows that the co-stimulation of insulin and EGF decreases the stress on the Ras/ERK cascade and corroborates the synergy

results in the integrated crosstalk mechanism (Borisov et al., 2009). Other substantial reactions are in upstream of the insulin and EGF networks (reaction 1 and 24). Reaction 1 has the highest sensitivity coefficient in the maximal ERK activation (figure 7A), whereas reaction 24 has the highest sensitivity coefficient before maximal activation of ERK (figure 7B). Parameter variation shows that the role of the reaction 1 is more critical than reaction 24 (figure 8 A and B). This confirms the valuably of sensitivity coefficients in maximal ERK activation relative to the other time regions.

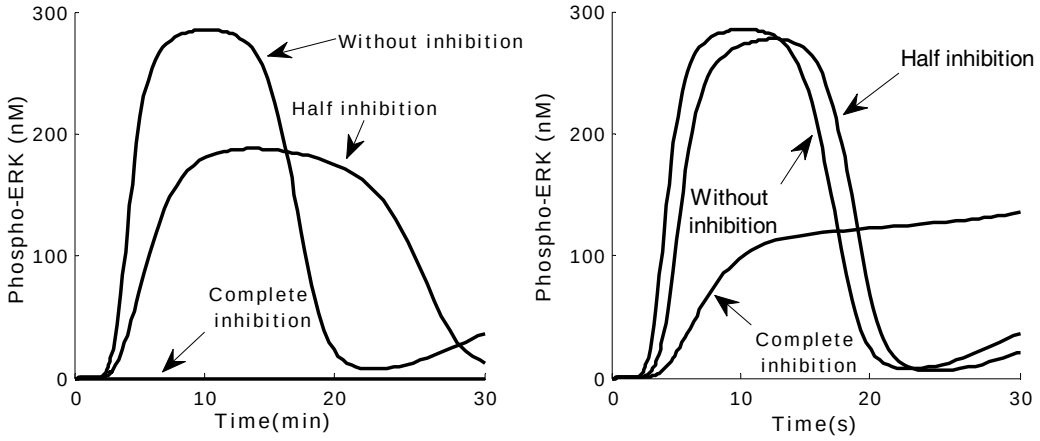

Figure 5. Activation of ERK in response to changes in the reaction 40 (A) and reaction 43 (B) in various levels of inhibition.

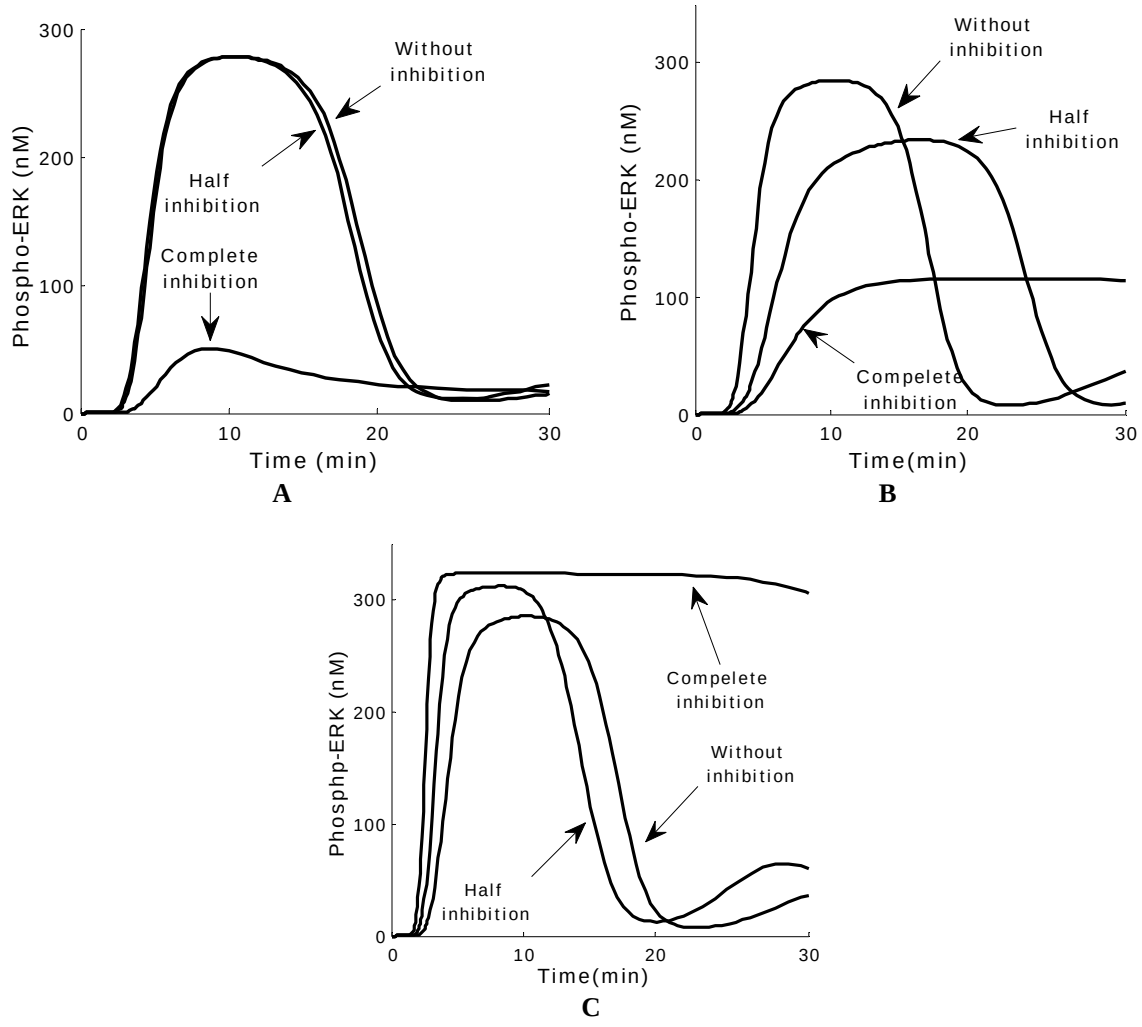

Figure 6. Activation of ERK in response to changes in the reaction 49 (A), reaction 42(B) and reaction 94 (C) in various levels of inhibition.

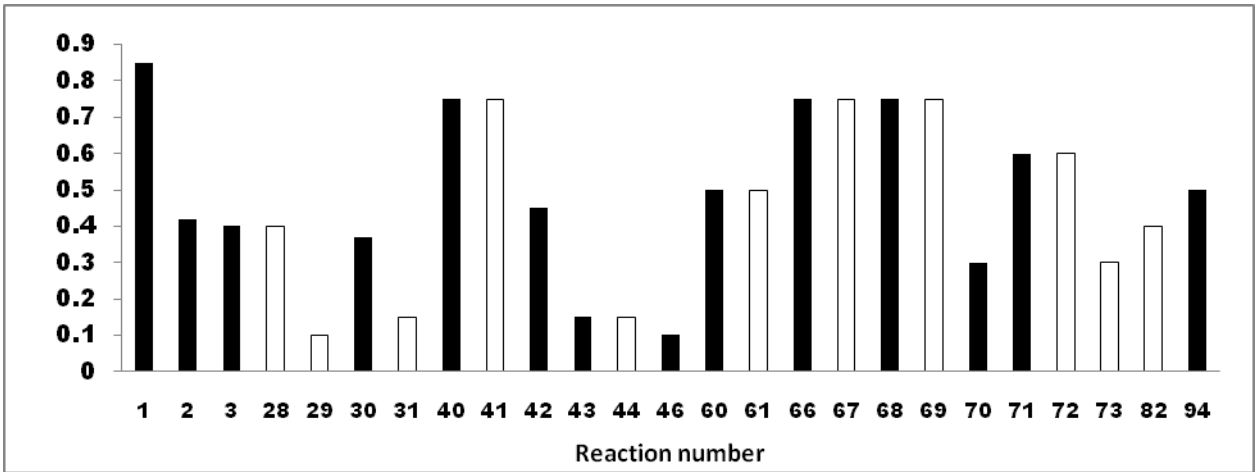

A

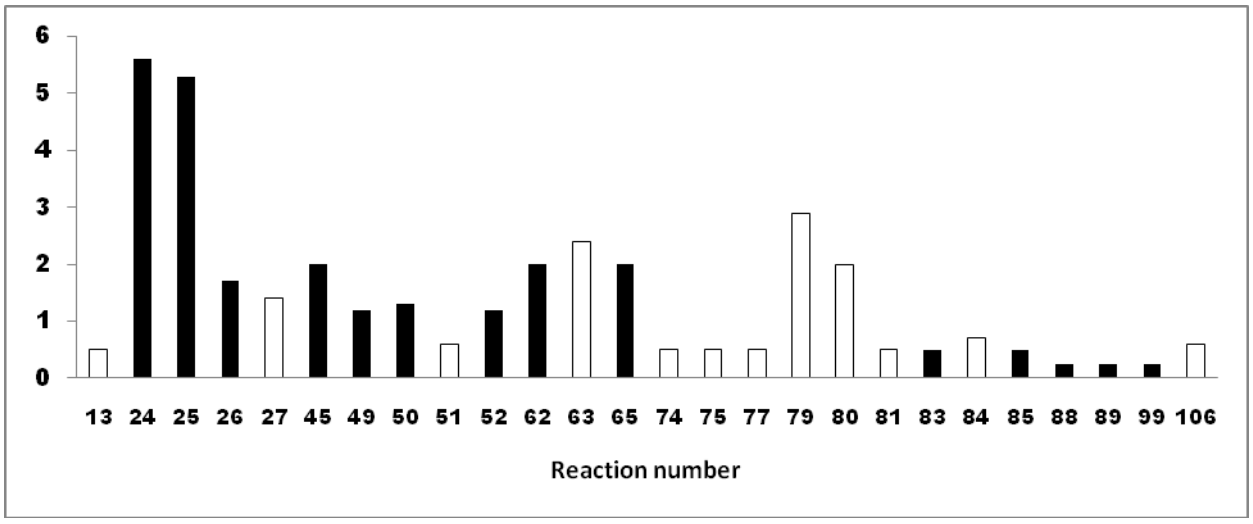

B

Figure 7. Sensitivity coefficients of the operative reactions of insulin-EGF crosstalk. (A) Reactions that have some sensitivity in maximal ERK activation. (B) Reactions that have no sensitivity in maximal ERK activation but have some sensitivity before and after it. (The bars with black and white colors represent minus and plus sensitivity coefficients, respectively.

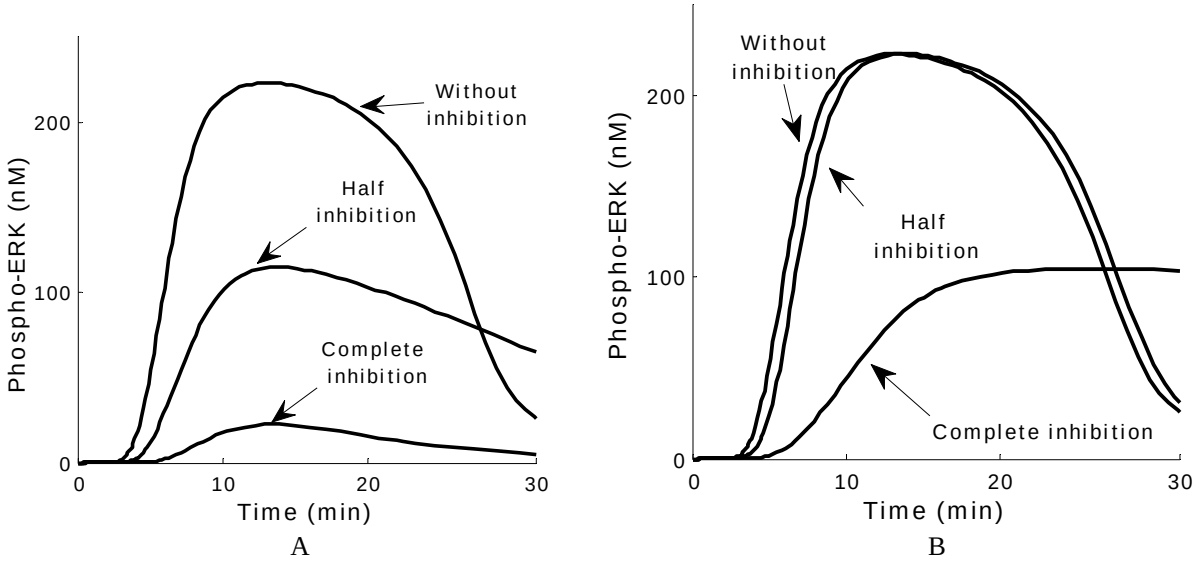

Figure 8. Activation of ERK in response to changes in the reaction 1 (A), reaction 24 (B) in various levels of inhibition.

In summary, the main aims of the current study are to reproduce an elucidated model of insulin-EGF networks and reliably determine the controlling and synergy nods of this crosstalk. Major effects of EGF pathway appear in participation of the phosphorylated EGF receptor in the activation of Src kinase and GAB1. Src kinase is a crucial and synergic nod of the crosstalk. Activation of Src leads to Raf activation and its downstream events. Thereby, signal is destructed by complete inhibition of Src activation. Roles of insulin pathway are reflected in recruitments IRS and PIP3 by phosphrylated insulin receptor. These two modules influence Ras and GAB1 activation, respectively. Finally, all of these solidarities are emerged with regard to activation of Ras–Raf–MEK–ERK cascade. The high amounts of sensitivity coefficients of the cascade reactions confirm these objectivities. Also, the recent therapeutic reports indicated that the targets of many anti-cancer drugs are within the Ras–Raf–MEK–ERK cascade. These reports are repeated for Src and GAB1, too. We hope that the results of this paper and other similar studies would elucidate some ambiguities of the drug targeting mechanisms.

Acknowledgment

We gratefully acknowledge financial support from the Research Councils of Ferdowsi University of Mashhad.

References

1-Amit I., Wides R. and Yarden Y. (2007) Evolvable signaling networks of receptor tyrosine kinases: relevance of robustness to malignancy and to cancer therapy. Molecular Systems Biology 3: 1-14.

2- Avruch J. (1998) Insulin signal transduction through protein kinase cascades. Molecular and Cellular Biochemistry 182: 31-48.

3- Birtwistle M. R., Hatakeyama M., Yumoto N., Ogunnaike B. A., Hoek J. B. and Kholodenko B. N. (2007) Ligand-dependent responses of the ErbB signaling network: experimental and modeling analyses. Molecular Systems Biology 3: 1-16.

4- Borisov N., Aksamitiene E., Kiyatkin A., Legewie S., Berkhout J., Maiwald T., Kaimachnikov N. P., Timmer J., Hoek J. B. and Kholodenko B. N. (2009) Systems-level interactions between insulin–EGF networks amplify mitogenic signaling. Molecular Systems Biology 5: 1-15.

5- Bornheimer S., Maurya M., Farquhar M. and Subramaniam S. (2004) Computational modeling reveals how interplay between components of a GTPase-cycle module regulates signal transduction. Proceedings of the National Academy of Sciences 101: 15899–15904.

6- Carlson C. J., Oterski S. K., Sciotti R. J., Poccard G. and Rondinone C. M. (2003) Enhanced basal activation of mitogen-activated protein kinases in adipocytes from type 2 diabetes: potential role of p38 in the downregulation of GLUT4 expression. Diabetes 52: 634–641.

7- Cheatham B. and Kahn C. R. (1995) Insulin action and the insulin signaling network. Endocrine Reviews 16: 117–142.

8- Chen J. Y. F., Hung C. C., Huang K. L., Chen Y. T., Liu S. Y., Chiang W. F., Chen H. R., Yen C. Y., Wu Y. J., Ko J. Y. and Jou Y. S. (2008) Src Family Kinases Mediate Betel Quid–Induced Oral Cancer Cell

Motility and Could Be a Biomarker for Early Invasion in Oral Squamous Cell Carcinoma1. Neoplasia 10: 1393–1401.

9- Chen W. W., Schoeberl B., Jasper P. J., Niepel M., Nielsen U. B., Lauffenburger D. A. and Sorger P. K. (2009) Input–output behavior of ErbB signaling pathways as revealed by a mass action model trained against dynamic data. Molecular Systems Biology 5: 1-19.

10- Chong M. P., Barritt G. J. and Crouch M. F. (2004) Insulin potentiates EGFR activation and signaling in fibroblasts. Biochemical and Biophysical Research Communications 322: 535–541.

11- Crouch M. F., Davy D. A., Willard F. S. and Berven L. A. (2000) Insulin induces epidermal growth factor (EGF) receptor clustering and potentiates EGF-stimulated DNA synthesis in Swiss 3T3 cells: A mechanism for costimulation in mitogenic synergy. Immunology and Cell Biology 78: 408–414.

12- Ediger T. and Toews M. (2000) Synergistic stimulation of airway smooth muscle cell mitogenesis. Journal of Pharmacology and Experimental Therapeutics 294: 1076–1082.

13- Gogg S. and Smith U. (2002) Epidermal growth factor and transforming growth factor mimic the effects of Insulin in human fat cells and augment Downstream Signaling in Insulin Resistance. Journal of Biological Chemistry 277: 36045–36051.

14- Goryanin I., Hodgman T. C. and Selkov E. (1999) Mathemacal simulation and analysis of cellular metabolism and regulation. Bioinformatics 15: 749-758.

15- Gual P., Gremeaux T., Gonzalez T., Marchand-Brustel Y. L. and Tanti J. (2003) MAP kinases and mTOR mediate insulin-induced phosphorylation of insulin receptor substrate-1 on serine residues. Diabetologia 46: 1532–1542.

16- HarshaRani G. V., Vayttaden J. S. and Bhalla U. S. (2005) Electronic Data Sources for Kinetic Models of Cell Signaling. J Biochem 137: 653–657.

17- Hornberg J. J., Bruggman F. J., Westerhoff H. V. and Lankelma J. (2006) cancer: A Systems biology disease. Biosystems 83: 81-90.

18- Ihekwaba A. E. C., Broomhead D. S., Grimley R. L., Benson N. and Kell D. B. (2004) Sensitivity analysis of parameters controlling oscillatory signalling in the NF-kB pathway: the roles of IKK and IkBa. Systms Biology 1: 93-103.

19- Ingalls B. P. and Sauro H. M. (2003) Sensitivity analysis of stoichiometric networks: an extension of metabolic control analysis to non-steady state trajectories. Journal of Theoritical Biology 222: 23–36.

20- Ishii K., Kamohara S., Hayashi H., Todaka M., Kanai F., Imanaka T. and Ebina Y. (1994) Epidermal growth factor triggers the translocation of insulin-responsive glucose transporter (GLUT4). Biochemical and Biophysical Research Communications 205: 857-863.

21- Johnston A. M., Pirola L. and Obberghen E. V. (2003) Molecular mechanisms of insulin receptor substrate protein-mediated modulation of insulin signalling. Federation of the Societies of Biochemistry and Molecular Biology Letters 546: 32-36.

22- Kholodenko B. N. (2006) Cell signalling dynamics in time and space. Nature Reviews Molecular Cell Biology 7: 165-176.

23- Kholodenko B. N., Demin O. V., Moehren G. and Hoek J. B. (1999) Quantification of Short Term Signaling by the Epidermal Growth Factor Receptor. Journal of Biological Chemistry 274: 30169–30181.

24- Kinzer-Ursem T. L. and Linderman J. J. (2007) Both Ligand- and Cell-Specific parameters control ligand agonism in a kinetic model of G protein–coupled Receptor signaling. Public Library of Science Computational Biology 3: 84-94.

25- Koga F., Xu W., Karpova T. S., McNally J. G., Baron R. and Neckers L. (2006) Hsp90 inhibition transiently activates Src kinase and promotes Src-dependent Akt and Erk activation. Proceedings of the National Academy of Sciences 103: 11318–11322.

26- Liu G., Swihart M. T. and Neelamegham S. (2005) Sensitivity, principal component and flux analysis applied to signal transduction: the case of epidermal growth factor mediated signaling. Bioinformatics 21: 1194-1202.

27- Mahdavi A., Davey R. E., Bhola P., Yin T. and Zandstra P. W. (2007) sensitivity analysis of intracellular signaling pathway kinetics predicts targets for Stem Cell fate control. Public Library of Science Computational Biology 3: 1257-1267.

28- Mauch K., Arnold S. and Reuss M. (1997) Dynamic sensitivity analysis for metabolic systems. Chemical Engineering Science 52: 2589–2598.

29- Maurya M. R., Bornheimer S. J., Venkatasubramanian V. and Subramaniam S. (2005) Reduced-order modeling of biochemical networks: Application to the GTPase-cycle signaling module. Systems Biology 152: 229–242.

30- Orton R. J., Sturm O. E., Vyshemirsky V., Calder M., Gilbert D. R. and Kolch W. (2005) Computational modelling of the receptor-tyrosine-kinase-activated MAPK pathway. Biochemical Journal 392: 249–261.

31- Roberts P. and Der C. (2007) Targeting the Raf-MEK-ERK mitogen-activated protein kinase cascade for the treatment of cancer. Oncogene 26: 3291–3310.

32- Sasagawa S., Ozaki Y., Fujita K. and Kuroda S. (2005) Prediction and validation of the distinct dynamics of transient and sustained ERK activation. Nature Cell Biology 7: 365–373.

33- Scaltriti M. and Baselga J. (2006) The epidermal growth factor receptor pathway: a model for targeted therapy. Clinical Cancer Research 12: 5268-5272.

34- Schoeberl B., Eichler-Jonsson C., Gilles E. and Muller G. (2002) Computational modeling of the dynamics of the MAP kinase cascade activated by surface and internalized EGF receptors. Nature Biotechnology 20: 370-375.

35- SureshBabu C. V., Babar S. M. E., Song E. J., Oh E. and Yoo Y. S. (2008) Kinetic analysis of the MAPK and PI3K/Akt signaling pathways. Molecular Cells 25: 397-406.

36- Taniguchi C. M., Emanuelli B. and Kahn C. R. (2006) Critical nodes in signalling pathways: insights into insulin action. Molecular and Cellular Biology 7: 85-96.

37- Yu Y., Hao Y. and Feig L. A. (2006) The R-Ras GTPase mediates cross talk between Estrogen and Insulin signaling in breast cancer cells. Molecular and Cellular Biology 26: 6372-6380.

38- Zhang T., Song K. W., Hekmat-Nejad M., Morris D. G. and Wong B. R. (2009) A modeling-derived hypothesis on chronicity in respiratory diseases: desensitized pathogen recognition secondary to hyperactive IRAK/TRAF6 signaling. Public Library of Science One 4: 1-7.

39- Zheng Y. and Rundell A. (2006) Comparative study of parameter sensitivity analysis of the TCR-activated Erk–AMPK signaling pathway. Systems Biology 153: 201–211.

40- Zhu M. L. and Kyprianou N. (2008) Androgen receptor and growth factor signaling cross-talk in prostate cancer cells. Endocrine-Related Cancer 15: 841–849.

Journal of Cell and Molecular Research (2012) 4 (1), 28-33

The effect of pH and temperature on spatial variation of *Acidobacteria* /*Actinobacteria* communities from Alpine soil

Bahar Shahnavaz [1] and Roberto A. Geremia [2]

[1] *Department of Biology, Faculty of Science, Ferdowsi university of Mashhad, Mashhad, Iran*
[2] *Laboratoire d'Ecologie Alpine UJF/ CNRS, Université de Grenoble, 2233, rue de la Piscine, BP 53 Bat D Biologie, Grenoble F-38041, France*

Received 30 April 2012 Accepted 11 June 2012

Abstract

Bacteria play a major role in environmental processes. However, the spatial and seasonal variations and environmental impact factors on different bacterial groups have been poorly studied. In the present study, we compared the spatial and seasonal variations of two bacterial groups (*Acidobacteria*, *Actinobacteria*) from Early Snow Melt and Late Snow Melt locations in Alpine tundra by CE-SSCP method. We examined correlation between the two groups and environmental factors. The results revealed that pH of soil is the essential factor for structure of two bacterial groups. The SSCP pattern of *Acidobacteria* is very similar to the overall bacterial communities in our previous study, while both bacterial communities are highly influenced by seasonal variations with an independent pattern.

***Keywords*:** Alpine soil, Single Strand Conformation Polymorphism (SSCP), Acidobacteria, Actinobacteria, pH

Introduction

Bacteria play a key role in carbon biogeochemical cycle; therefore it is important to identify their origins and functions in different environments such as Alpine soils. In the recent decades, developments in molecular technology provide an increase in literature. These studies indicate that environmental variables can be influenced by bacterial communities. It is known that presence or absence of different plant species provide different conditions for bacterial groups in soil (Harris and Tibbles, 1997; Kowalchuk et al., 2002; Yergeau et al., 2007). Plants can structure bacterial communities through the root exudation or their litter. In addition, the quality or quantity of the root exudates may vary with plants and physiological conditions or age of plants can influence the bacterial communities (Eviner and Chapin, 2003, Graystone et al., 1996; Maloney et al., 1997). Certain studies showed that soil properties, for example, soil texture, pH, and organic carbon/nitrogen have strong effects on soil bacteria (Marschner et al., 2003; Sessitsch et al., 2001; Girvan et al., 2003). However, impacts of these environmental conditions on different bacterial groups are poorly investigated.

Alpine ecosystems present a high spatial heterogeneity and its topography is characterized by the absence of trees. In fact, topographic context leads to differential snow deposition with the concomitant changes in soil characteristics, lengthening of seasonal vegetation, diversity in plant species composition, vegetation and microbial communities (Olear and Seastedt, 1994; Korner, 1995; Litaor et al., 2001; Choler, 2005). These ecosystems are the best models to investigate the effect of environmental conditions on the bacterial community.

In this framework, we selected two locations in the Alpine ecosystem. Despite their vicinity to each other topographically, they are different in the duration of snow-cover, type of vegetation, Soil Organic Matter (SOM) content, soil texture, and pH. The Early Snow Melt (ESM) location presents a weakly snow cover, in which the cycles of freezing and thawing are accruing. In contrast, the soils of Late Snow Melt (LSM) location are protected in winter with a snowpack. These regimes strongly influence the snow cover and consequently generate a mosaic plant cover typical for Alpine ecosystems.

Recent studies using PLFA (Phospholipid Fatty Acid), 16s rRNA and Single Strand Conformation Polymorphism (SSCP) demonstrated some spatial

∗Corresponding author E-mail: shahnavaz@um.ac.ir

and seasonal variations in Alpine ecosystems (Bjork et al., 2008; Lipson et al., 2002; Lipson and Schmidt, 2004; Zinger et al., 2009). In a previous work (Zinger et al., 2009), we found that all of bacterial communities were submitted to spatial and temporal variations. In present work, we investigate how changes over space/seasons can drive *Acidobacteria* and *Actinobacteria* groups that were the most bacterial groups presented in our locations and second to investigate the environmental conditions causing the pattern similar between these bacterial groups.

Materials and Methods

Site characterization and sample collection

The study area is located in the Grand Galibier massif (south-western Alps, France, 45°05' N, 06°37' E). The sampling site is a topographical gradient comprising two neighboring habitats: an Early Snow Melt and Late Snow Melt location, with less than 100 m^2. Table 1 shows the soil characteristics for each location. The slow-growing, stress-tolerant plants (*Kobresia myosuroides, Dryas octopetala, Carex curvula All. subsp. rosae)* dominate ESM, while LSM is covered by fast-growing species (*Carex foetida, Salix herbacea L., Alopecurus alpinus Vill., Alchemilla pentaphyllea L.*). Summer length and growing season is longer in ESM than LSM. In winter harsh condition resulted from snow-cover in LSM plays a protective role for bacterial communities and keeps soil temperature approximately 0°C in LSM. Conversely, the soils from ESM are under freeze-thaw condition because of absence of snow-cover. Five soil samples from each location were collected in June (spring), August (top of growing season), October (after litter-fall), and in May (late winter). During May (latest days of the winter in our site) at a course of 10 days the mean soil temperature of ESM became above 0°C and those of LSM got around 0°C. The LSM soil was covered by >2 m of snow pack, but already waterlogged. The sampled soils were immediately transported to the laboratory in a sterile condition before DNA extraction. Soil pH was measured after mixing 5 grams of it with 12.5 ml of distilled water (adapted from Yan et al., 1996). Soil organic matter content (SOM) was determined by loss-on-ignition according to Schulte and Hopkins (1996).

Soil DNA extraction and Capillary Electrophoresis-SSCP analysis of Acido- and Actionbactria community

Extraction of total soil DNA has already been described (Zinger et al., 2009). Briefly, three replicates 250 mg of soil from each sample were extracted using Power Soil™ Extraction Kit (MO BIO Laboratories, Ozyme, St Quentin en Yvelines, France) according to manufacturer's instructions. To minimize the location heterogeneity, DNA derived from the five replicates was pooled to obtain one sample location/date. The V3 of 16S rRNA genes was amplified with specific primer pA (5'-GCCTGAGAGGGCRC-3') (Barn 1999) and W104-FAM (5'-TTACCGCGGCTGGCAC-3') (Delbes 1998) for *Acidobacteria* whereas F243 (5'-GGATGAGCCCGCGGCCA-3') and R513-FAM (5'-CGGCCGCGGCTGCTGGCACGTA-3') (Heuer, 1997) for *Actinobacteria*. PCRs were performed with 2.5 mM $MgCl_2$, 0.1 mM each dNTP, 0.2 mM of each primer, 1 U AmpliTaq Gold™ polymerase, 10X buffer provided by the manufacturer, 20g.l^{-1} of bovine serum albumin and 10 ng of DNA template. The thermal PCR profile was as following: initial denaturation at 95°C for 10 min, 30 cycles of amplification: denaturation at 95°C for 30 s, annealing at 59°C (for *Acidobacteria*) or 56°C (for *Actinobacteria*) for 15s and extension 72°C for 15s, and a final elongation at 72°C for 7 min. PCRs were carried out by triplicating to limit the influence of PCR biases.

PCR products were checked on a 1.5% agarose gel. CE-SSCP conditions were performed on an ABI Prism 3130 XL genetic analyzer (Applied Biosystems, Courtaboeuf, France), as previously described in (Zinger et al., 2008). For analysis, initially, an informatics tool was applied that allow retrieving the digital data of obtained CE-SSCP profiles. In a second step, these dates were normalized in order to reduce the variations of fluorescence intensity among profiles. Finally, standardization of data allows us to calculate a distance matrix by Edwards' distance between the different profiles and a dendrogram constructed by Neighbor-Joining with 1000 bootstrap replications (package ade4). These analyses were carried out with the R software (The R Development Core Team, 2007).

Linking bacteria composition with environmental parameters

We performed mantel tests to exam if the pattern similarity between bacterial communities were associated with two environmental variations (soil temperature and pH). This test carried out using the Spearman rank correlation method (999 permutations) that allowed examining correlation between distance obtained from each group bacterial community and distance of environmental factors.

Results

Variation of Acidobacteria and Actinobacteria with CE-SSCP

At the previous work (Zinger et al., 2009), we found that bacterial communities from ESM and LSM are different. The *ssu* sequence data (see more information in Zinger et al., 2009) indicated that ESM location is co-dominated by *Acidobacteria*, *Acitnobacteria* and *α-proteobacteria*, while *Acidobacteria* is dominant in LSM location. In order to test if seasonal variations of *Acidobacteria* and *Actinobacteria* are periodic over the years, and if environmental variation has the same effect for different bacterial communities, we performed SSCP analysis using primers specific of these two phyla and measured significance among environmental variations and bacteria communities. As shown in figure 1, two bacterial communities were separated from ESM and LSM. This discrepancy was noticed for all sampling date for two bacterial communities. During the growing season (June/August) and plant senescence period (October), ESM *Acidobacteria* were grouped together (figure 1a), while in LSM location *Acidobacteria* communities were grouped in all seasons. During May ESM community showed a shift toward the LSM community. The obtained profiles by *Acidobacteria* populations exhibited same pattern presented for total bacteria (Zinger et al., 2009). Thus, the largest distance between ESM and LSM was observed in June and August and decreased from October to May. Present SSCP pattern by *Actinobacteria* from ESM and LSM location displayed mirror to *Acidobacteria*. Similar to *Acidobacteria*, the *Actinobacteria* dendrogram (figure 1b) during May showed a convergence between two locations with tendency of *Actinobacteria* from LSM to ESM location. However, the lowest distance between two locations from each bacterial community was pronounced during May, though the pattern observed from bacterial communities was not similar.

Microbial communities and environmental conditions

In order to test the significance relation between two bacterial communities and soil abiotic factors we examined the effects of soil temperature and pH on bacteria communities. *Acidobacteria* displayed strong correlation with soil pH ($p \leq 0.001$) and temperature ($p \leq 0.004$), while *Actionbacteria* were only correlated with soil pH ($p \leq 0.009$) (table 2).

Table 1. Characteristic of soil samples gathered from Early and Late Snow Melt locations. Soil temperatures are average from May 1999 to May 2007 in same months of sampling date.

Sample	Date	pH (H_2O)	Soil Temp. (°C)	Granulometry (%) Clay (<2µm) Silt (2-50 µm) Sand (50-2000) µm	SOM (%)	Summer length (d)
ESM	June	6.74 ± 0.16^a	9.45 ± 1.86	9.7 (0.5) 41.4 (1.0) 48.6 (1.2)	15.7 ± 4.7	170 ± 3
	August	6.5 ± 0.32^a	10.88 ± 1.58			
	October	6.7 ± 0.16^a	3.66 ± 1.63			
	May	5.2 ± 0.1^b	3.49 ± 2.18			
LSM	June	5.56 ± 0.09^c	5.34 ± 2.32	26.4 (2.6) 61.7 (2.0) 11.9 (4.5)	8.7 ± 2.5	125 ± 3
	August	5.33 ± 0.2^c	11.04 ± 1.33			
	October	5.45 ± 0.09^c	3.07 ± 1.58			
	May	5.96 ± 0.1^d	0.98 ± 2.67			

Table 2. Correlation between bacterial communities (*Acido- and Actinobacteria*) with environmental conditions. Correlation significances were assessed with 1000 permutations and are indicated as follows: * P<0.05, ** P<0.01, *** P<0.001.

Bacterial groups	Environmental conditions Spearman rank ρ values (Significance)	
	Soil pH	Temperature
Acidobacteria	0.7(0.001)***	0.2(0.004)**
Actinobacteria	0.2(0.009)**	0.02(0.3)

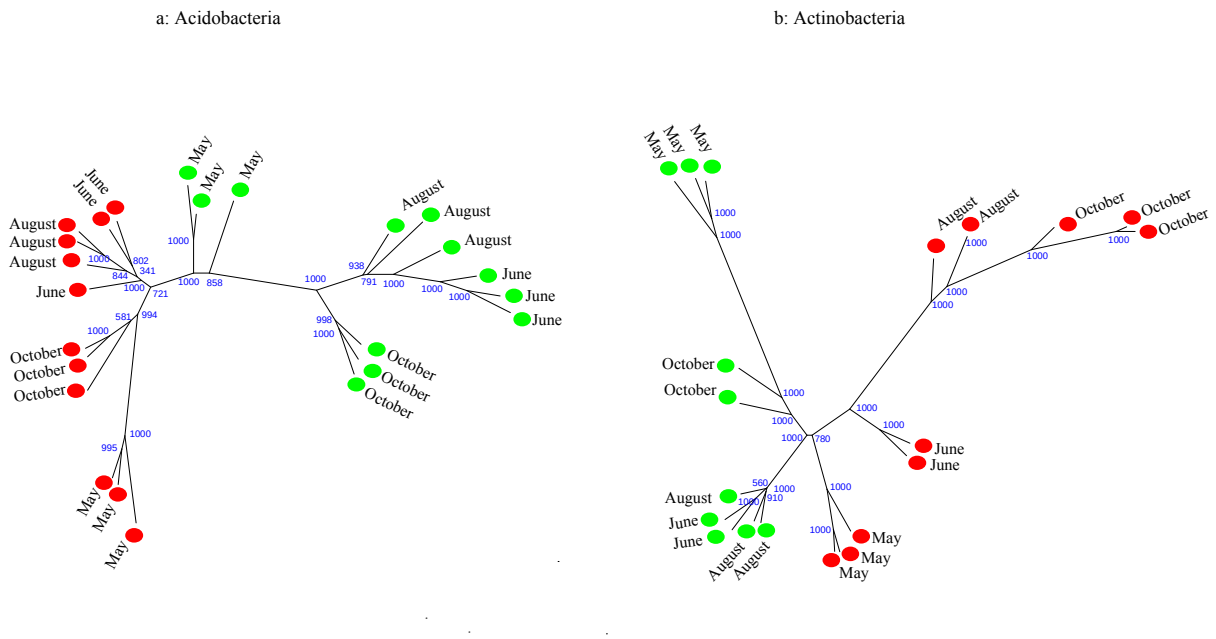

Figure 1. Obtained Dendrograms from a) *Acido* and b) *Actinobacteria* show seasonal variation in two different locations (Early and Late Snow Melt). These dendrograms were obtained from the molecular profiles of bacterial communities as described in Material and Methods. The ESM and LSM locations are represented in green and red colours, respectively. Bootstraps values (1000) are indicated by blue.

Discussion

At the previous work, we found snow cover effects on microbial communities by CE-SSCP method and *ssu* sequences (Zinger et al., 2009) and bacterial phylogenetic structure (Shahnavaz et al., 2012). *Actinobacteria* (co-dominant in ESM location) are active in decomposition of organic material in soil such as lignin and other recalcitrant polymers (Crawford, 1988). The members of this phylum are sources of antibiotics and enzymes (Srinivasan et al., 1991; Trujillo, 2008; Stach et al., 2003). They are dominant in any ecosystems (Axelrood et al., 2002) and cold ecosystems (Tian et al., 2007; Bai et al., 2006). These bacteria are widely distributed in soil so that the resulted probability shows the importance of their ecological role in recycling nutrient and degradation of xenobiotic compounds (Trujillo, 2008).

The Phylum of *Acidobacteria* is one of the most distributed bacterial species in a wide variety of environment including different types of soil, sediments, fresh water and marine ecosystems (Hugenholtz et al., 1998; Janssen, 2006; Barn et al., 2007; Kleinsteuber et al., 2008). It is very difficult to cultivate and isolate members of the phylum *Acidobacteria* in the laboratory. They are often distributed in low pH soils (Sait et al., 2006; Lauber et al., 2008). Thus the knowledge of their morphological and biological properties, their consequences as well as their ecological roles is poorly known. Although certain studies showed that members of this phylum are metabolically active in rhizosphere soil (Lee et al., 2008), many authors have been presented that soil chemical and physical properties e.g. water content, pH, texture, nutrient and mineral availability and its creation of different ecological niches lead to different distribution of bacterial communities (Ulrich and Becker, 2006). The obtained patterns by *Acidobacteria* phylum were very similar to other bacteria indicating the abundance of this group of bacteria in both locations. Thus, in *Acidobacteria* phylum the largest distance between ESM and LSM in the growing season can be corresponded with plant cover. The root exudation from different plant species that vary with plant age and root zone (Graystone et al., 1996; Maloney et al., 1997) can form the bacterial community. LSM and ESM location display different plant cover that can recruit different bacterial phylotype. A correlation between plant species and bacterial groups in Alpine tundra (Yergeau et al., 2007a; Yergeau et al., 2007b) and other ecosystems (Buyer et al., 2002) has been known. This pattern was observed for *Actiobacteria* phylum except in LSM location, where the samples collected in June were far from

those gathered in August and October. It has been suggested that *Actionbacteria* phylotypes gathered in May are not very different from those gathered in June and new phylotypes adapted to plant cover do not appear. In any of bacterial groups, the lowest distance between bacterial groups was observed in May (end of winter in Alpine soil) according to Zinger et al. observations (2009) for overall bacterial groups. As described in the previous studies for overall bacterial communities, the low pH in ESM, weak temperature and absence of plant during May lead to *Acidobacteria* tendency from ESM to LSM and a convergence of *Actinobacteria* in LSM to ESM. Again, this pattern supports that behaviour of two bacterial groups is a little different in a given environment.

In this study, we attempted to examine impacts of abiotic factors (soil pH and temperature) on different bacterial groups (*Acido-* and *Actinobacteria*) by fingerprinting method. Consistent with other studies (Fierer and Jackson 2006; Lauber et al., 2008), our results showed that soil pH acts as main driver of two bacterial phyla though temperature can significantly affect *Acidobacteria* (Bryant et al., 2008). Differences in reactions of bacterial phyla to environmental factors may refer to their different morphological and physiological characteristics, although our information about *Acidobacteria* characteristic is somehow little.

Acknowledgment

I appreciate Lucie Zinger, Abderrahim Bouasria for statistical works. Philippe Choler and the staff of Station Alpine J. Fourier for providing logistic facilities during the fieldwork.

References

1- Axelrood P. E., Chow M. L., Clarke S. A., Lu K., McDermott J. M. and Davies J. (2002) Cultivation dependent characterization of bacterial diversity from British Columbia forest soils subjected to disturbance. Canadian Journal of Microbiology 48: 643-654.

2- Bai Y., Yang D., Wang J., Xu S., Wang X. and An L. (2006) Phylogenetic diversity of culturable bacteria from alpine permafrost in the Tianshan Mountains, northwestern China. Research in Microbiology 157: 741-751.

3- Barns S. M., Takala S. L. and Kuske C. R. (1999) Wide distribution and diversity of members of the bacterial kingdom Acidobacterium in the environment. Applied and Environmental Microbiology 65: 1731-1737.

4- Barns S. M., Cain E. C., Sommerville L. and Kuske C. R. (2007) Acidobacteria phylum sequences in uranium-contaminated subsurface sediments greatly expand the known diversity within the phylum. Applied and Environmental Microbiology 73: 3113-3116.

5- Bjork R. G., Bjorkman M. P., Andersson M. X. and Klemedtsson L. (2008) Temporal variation in soil microbial communities in Alpine tundra. Soil Biology and Biochemistry 40: 266-268.

6- Bryant J. A., Lamanna C., Morlon H., Kerkhoff A. J., Enquist B. J. and Green J. L. (2008) Microbes on mountainsides: Contrasting elevational patterns of bacterial and plant diversity. Proceedings of the National Academy of Sciences (PNAS) 105: 11505-11511.

7- Choler P. (2005) Consistent shifts in Alpine plant traits along a mesotopographical gradient. Arctic, Antarctic and Alpine Research 37: 444-453.

8- Crawford D. L. (1978) Lignocellulose decomposition by selected streptomyces strains. Applied and Environmental Microbiology 35: 1041-1045.

9- Delbes C., Moletta R. and Godon J. J. (2000) Monitoring of activity dynamics of an anaerobic digester bacterial community using 16S rRNA polymerase chain reaction– single strand conformation polymorphism analysis., Environmetal Microbiology 2: 506-515.

10- Eviner V. T. and Chapin F. S. (2003) Functional matrix: A conceptual framework for predicting multiple plant effects on ecosystem processes. Annual Review of Ecology Evolution and Systematics 34: 455-485.

11- Fierer N. and Jackson R. B. (2006) The diversity and biogeography of soil bacterial communities. Proceedings of the National Academy of Sciences (PNAS) 103: 626-631.

12- Girvan M. S., Bullimore J., Pretty J. N., Osborn A. M. and Ball A. S. (2003) Soil type is the primary determinant of the composition of the total and active bacterial communities in arable soils. Applied and Environmental Microbiology 69: 1800-1809.

13- Grayston S. J., Wang S. Q., Campbell C. D. and Edwards A. C. (1998) Selective influence of plant species on microbial diversity in the rhizosphere. Soil Biology and Biochemistry 30: 369-378.

14- Harris J. M. and Tibb B. J. (1997) Factors Affecting Bacterial Productivity in Soils on Isolated Inland Nunataks in Continental Antarctica. Microbial Ecology 33:106-123.

15- Heuer H., Krsek M., Baker P., Smalla K. and Wellington E. M. (1997) Analysis of actinomycete communities by specific amplification of genes encoding 16S rRNA and gel electrophoretic separation in denaturing gradients. Applied and Environmental Microbiology 63: 3233-3241.

16- Hugenholtz P., Goebel B. M. and Pace N. R. (1998) Impact of culture-independent studies on the emerging phylogenetic view of bacterial diversity. Journal of Bacteriology 180: 4765-4774.

17- Janssen P. (2006) Identifying the Dominant Soil Bacterial Taxa in Libraries of 16S rRNA and 16S rRNA Genes. Applied and Environmental

Microbiology 72: 1719-1728.
18- Kleinsteuber S., Muller F. D., Chatzinotas A., Wendt-Potthoff K. and Harms H. (2008) Diversity and in situ quantification of Acidobacteria subdivision 1 in an acidic mining lake. FEMS Microbiology Ecology 63: 107-117.
19- Körner C. (1995) Alpine plant diversity: a global survey and functional interpretations. In Arctic and Alpine biodiversity. Chapin, F.S.a.K., CH. (ed). Berlin: Springer, 45-62 pp.
20- Kowalchuk G. A., Buma D. S., Boer W., Klinkhamer P. G. L. and Veen J. A. (2002) Effects of above-ground plant species composition and diversity on the diversity of soil-borne microorganisms. Antonie van Leeuwenhoek 81: 509-520.
21- Lauber C. L., Strickland M. S., Bradford M. A. and Fierer N. (2008) The influence of soil properties on the structure of bacterial and fungal communities across land-use types. Soil Biology and Biochemistry 40: 2407-2415.
22- Lee S. H., Ka J. O. and Cho J. C. (2008) Members of the phylum Acidobacteria are dominant and metabolically active in rhizosphere soil. FEMS Microbiology Letters 285: 263-269.
23- Lipson D. A. and Schmidt S. K. (2004) Seasonal changes in an alpine soil bacterial community in the colorado rocky mountains. Applied and Environmental Microbiology 70: 2867-2879.
24- Lipson D. A., Schadt C. W. and Schmidt S. K. (2002) Changes in soil microbial community structure and function in an alpine dry meadow following spring snow melt. Microbial Ecology 43: 307-314.
25- Litaor M. I., Seastedt T. R. and Walker D. A. (2002) Spatial analysis of selected soil attributes across an alpine topographic/snow gradient. Landscape Ecology 17: 71-85.
26- Maloney P. E., Bruggen A. H. C. and Hu S. (1997) Bacterial community structure in relation to the carbon environments in lettuce and tomato rhizospheres and in bulk soil. Microbial Ecology 34: 109-117.
27- Marschner P., Kandeler E. and Marschner B. (2003) Structure and function of the soil microbial community in a long-term fertilizer experiment. Soil Biology and Biochemistry 35: 453-461.
28- Olear H. A. and Seastedt T. R. (1994) Landscape Patterns of Litter Decomposition In Alpine Tundra. Oecologia 99: 95-101.
29- Sait M., Davis K. E. R. and Janssen P. H. (2006) Effect of pH on isolation and distribution of members of subdivision 1 of the phylum Acidobacteria occurring in soil. Applied and Environmental Microbiology 72: 1852-1857.
30- Schulte E. E. and Hopkins G. G. (1996) Estimation of organic matter by weight loss-onignition. In Soil organic matter: Analysis and interpretation. Magdoff, F.R.e.a. (ed): SSSA spec. Publ. 46. SSSA, Madison, WI, 21-31 pp.
31- Sessitsch A., Weilharter A., Gerzabek M. H., Kirchmann H. and Kandeler E. (2001) Microbial population structures in soil particle size fractions of a long-term fertilizer field experiment. Applied and Environmental Microbiology 67: 4215-4224.
32- Shahnavaz B., Zinger L., Lavergne S., Choler P., and Geremia R. A. (2012) Phylogenetic Clustering Reveals Selective Events Driving the Turnover of Bacterial Community in Alpine Tundra Soils. Arctic, Antarctic, and Alpine Research. 44 (2): 232-238
33- Srinivasan M. C., Laxman R. S. and Deshpande M. V. (1991) Physiology and nutritional aspects of actinomycetes: an overview. World Journal of Microbiology and Biotechnology 7: 171-184.
34- Stach T. E. M., Maldonado L. A., Ward A. C., Goodfellow M. and Bull A. T. (2003) New primers for the class Actinobacteria: application to marine and terrestrial environments. Environmental Microbiology 5: 828-841.
35- The R Development Core Team. (2007) R: A language and environment for statistical computing. R Foundation for statistical computing: Wien.
36- Tian X., Cao L., Tan H., Han W., Chen M., Liu Y. and Zho S. (2007) Diversity of Cultivated and Uncultivated Actinobacterial Endophytes in the Stems and Roots of Rice. Microbial Ecology 53: 700-707.
37- Trujillo M. E. (2008) Actinobacteria. Encyclopedia of Life Sciences (ELS). John Wiley and Sons, Ltd: Chichester.
38- Yan F., Schubert S. and Mengel K. (1996) Soil pH increase due to biological decarboxylation of organic anions. Soil Biology and Biochemistry 28: 617-624.
39- Yergeau E., Newsham K. K., Pearce D. A. and Kowalchuk G. A. (2007) Patterns of bacterial diversity across a range of Antarctic terrestrial habitats., Environmental Microbiology 9: 2670-2682.
40- Zinger L., Shanhavaz B., Baptist F., Geremia R. A. and Choler P. (2009) Microbial diversity in alpine tundra soils correlates with snow cover dynamics. International Society for Microbial Ecology Journal 3: 850-859
41- Zinger L., Gury J., Alibeu O., Rioux D., Gielly L., Sage L., Pompanon F. and Geremia R. A. (2008) CE-SSCP and CE-FLA, simple and high-throughput alternatives for fungal diversity studies. Journal of Microbiological Methodes 72: 42-53.

Journal of Cell and Molecular Research (2012) 4 (1), 34-42

Deletion mutagenesis in the streptomycin biosynthesis regulatory gene (*strR*) isolated from Iranian *Streptomyces griseus* PTCC1127 and cloning of the new construct in *E. coli*

Somayeh Panahi Moghadam, Zohreh Hojati* and Majid Motovali-Bashi

Department of Biology, Faculty of Sciences, University of Isfahan, P.O. Box 81746-73441, Isfahan, I.R. Iran

Received 23 May 2012 Accepted 12 July 2012

Abstract

StrR is a putative pathway specific regulator of streptomycin production in *Streptomyces griseus*. Because of finding new spo0j domain in *strR* by bioinformatics methods, the purpose of this study was to suggest another role for *strR* gene. This domain can be seen in proteins that are involved in initiation of sporulation and normal chromosome partitioning. So, 51 bps of *strR* in accordance to spo0j domain was deleted to investigate effects of deletion mutation in StrR functions. A unique specific procedure, including three consecutive PCRs, known as SOEing PCR were used here for site directed mutagenesis. Application and feasibility of this PCR was studied here. Bioinformatic studies were carried out for comparison of the sequence similarities between StrR and Spo0J proteins. An exclusive procedure, including three consecutive PCRs, was designed here in order to delete a 51 bp from the native *strR*. Other PCRs such as Semi-Nested PCR and RFLP PCR were used for *strR* isolation and structural confirmation of the isolated *strR* and deleted *strR* genes. Routine genetic engineering procedures were conducted in order to clone the native and deleted *strR* genes into *E. coli*. Obtained sequence information, from Conserved Domains Database (CDD) and Clustal W program, revealed that the StrR is similar to members of ParB family. Here, the *strR* was initially isolated from Iranian strain of *Streptomyces griseus* (PTCC1127). It was then confirmed as *StrR* by Semi-Nested PCR and RFLP-PCR. A 51 base pair region of the *strR* gene was deleted by specifically designed overlapped primers. A ten nucleotide overlap region was considered for a set of these primers. The recombinant cassette pSPM*strR*Δ17 was constructed and cloned in *E. coli*. The sequencing results showed that a specific deletion is produced in the desired site and region in the *strR* gene. Therefore the designed three steps PCRs (known as SOing PCR) is a very rapid, cheap, and precise method for introducing such a deletion in any preferred gene.

Keywords**:** *deletion mutation, SOEing PCR, StrR protein, Streptomyces griseus, ParB nuclease*

Introduction

Soil-dwelling actinobacteria of the genus *Streptomyces* are mycelial sporulating organisms that produce more than 70% of the commercially available antibiotics (Li et al., 2006; Weber et al., 2003). Triggering of the physiological differentiation (secondary metabolism) in *Streptomyces* is linked with initiation of the morphological differentiation, and both processes are under control of common physiological and environmental signals such as A-factor (2-isocapryloyl-3Rhydroxymethyl-g-butyrolactone) from *Streptomyces griseus* (Li et al., 2006).

Streptomycin antibiotic is the most notable secondary metabolite produced by *S. griseus*. In the regulatory network of streptomycin biosynthesis, the A-factor> ArpA> adpA activates *strR* gene transcription (Hara et al., 2009; Komatsu et al., 2010; Ohnishi et al. 1999; Hirano et al., 2006). The streptomycin biosynthetic gene cluster, with total length of 32.5 kb, is regulated by streptomycin gene expression Regulator (StrR) as a unique transcriptional activator (Retzlaff and Distler, 1995; Tomono et al., 2005).

The events in *Streptomyces* that convert aerial hyphae into chains of pre-spore compartments such as development of spores into branched, filamentous, multinucleoidal, in one hand and the large size and linearity of the *Streptomyces* chromosome (~9.0 Mb) (Boccard et al., 1988; Hopwood, 1999) from other hand, suggest that *Streptomyces* chromosome partitioning is a complex and interesting issue. Dozens of linear chromosomes ought to be condensed and segregated accurately and synchronously during sporulation to ensure that each spore receives a single copy of the chromosome (Jakimowicz et al., 2005; Kois et al., 2009; Ohnishi et al., 2008). Thus,

*Corresponding author E-mail: z.hojati@sci.ui.ac.ir

we can assume that a complex interaction between functionally different proteins involves in partitioning of chromosomal DNA in *S. griseus*.

The number of recombinant proteins used in academic research, and therapeutic applications has increased dramatically. Therefore, the demand for manipulating proteins has also been elevated significantly. The available procedures for engineering the protein structures and functions are also increasing. On the other hand, PCR has made these techniques easier, quicker and more flexible. There is a specific PCR procedure for deleting a defined region in a desired protein. This technique is known as splicing by overlap extension (SOEing). SOEing PCR has been used recently for making various mutations in different proteins and peptides (Enshell-Seijffers et al., 2001). This technique relies on using three sets of PCR primers (Enshell-Seijffers et al., 2001; McPherson and Moller, 2000; Horton., 1993; Senanayake and Brian, 1995). Here, we aimed in designing a perfect SOEing PCR protocol for introducing a deletion in the desired region on *strR* gene. Four specific primers were designed using appropriate PCR primer design software and *strR* sequence (available from NCBI). Using this specifically designed SOEing PCR, a 51-bp region from parB like nuclease domain of *strR* gene was successfully deleted without any frame shift. The *strR*Δ17 was ligated into a *Streptomyces* specific vector, pMA::hyg, and finally transformed to *E. coli* competent cell. The performance and accuracy of this deletion were confirmed using DNA sequencing.

Materials and Methods

Bacterial strains and growth conditions

S. griseus PTCC1127 was purchased from IROST (Iranian Research Organization for Science and Technology), IR, Iran; and *S. griseus* ATCC1952 was obtained from UMIST University, UK. Glucose with Yeast and Malt Extract Agar medium (GYM) was used for *Streptomyces* strains (Kieser et al., 2000). Furthermore, *S. grisues* strains were grown in Yeast Extract-Malt Extract medium (YEME) for DNA isolation (Kieser et al., 2000). *E. coli* XL1Blue was purchased from CinnaGen IR, Iran. LB and LB agar media were used for *E. coli*. Ampicilin (100 µg/ml) was used when required.

Bioinformatic analysis

Genetic sequence database (NCBI) was used to pull out the *strR* nucleotide and amino acid sequences (NC_010572.1 GI: 182433793). Clustal W program was used for searching a conserved portion in StrR Protein sequence (figure 1) (Thompson et al., 1994). Conserved Domains database revealed that StrR protein has "ParB-like nuclease" domain in accordance to that maintained portion.

PCR and cloning of the strR gene

Chromosomal DNA was isolated from *S. griseus* strains as described for CTAB method (Cullings, 1992). An 1134-bp fragment (including *strR* gene, 1053 bp without promoter region) was amplified by using the primers SP_1F, SP_2R and *pfu* polymerase (Fermentas, Germany). The sequences of these two primers are as follows: CCGGATCCTAGAAGTCGCAAGCAT as SP_1F and TATCTAGACCGCCCGCATCCGACAT as SP_2R (figure 2). Final reaction volume was 25 µl containing 1 µl PCR buffer (stock solution concentration: 500 mM KCl and Tris-HCl), 1 mM $MgCl_2$, 0.8 pmol/l of each primer, 0.4 mM of each dNTP, 1U *Pfu* DNA polymerase, and 50 ng of the genomic DNA. The PCR conditions consisted of 95°C for 5 min, 30 cycles of denaturation at 94°C for 1min, annealing for 1:30 min at 63°C, and extension at 72°C for 3 min, followed by a final extension at 72°C for 15 min. The amplified fragment was confirmed as *strR* by using different strategies such as restriction digestion analysis (RFLP), and Semi-Nested PCR (data not shown). Treatment of PCR product and pMA::hyg plasmid with restriction enzymes (*Xba*I and *BamH*I; Fermentase, Germany), agarose gel purification and ligation with T4 DNA ligase (Ferments, Germany) were performed by the protocols recommended by manufacturers. Plasmid pMA::hyg was kindly provided by Colin P. Smith (University of Surrey, UK). This plasmid encodes for hygromycin resistance (*hyg*) and ampicilin (betalactam) resistance (*BLA*). The multiple cloning site of this vector contains the recognition sites for *Bam*HI, *Xba*I, *Sal*I, *Pst*I, and *Hind*III. To prevent re-circularization or self-ligation of the vector, two different restriction sites (*BamH*I and *Xba*I) were designed at 5' end of the primers SP_1F and SP_2R, respectively. The two recognition sites for *Bam*HI and *Xba*I are located adjacent to each other in vector. The resulting plasmid (pSP*strR*) was transformed and cloned in *E. coli* XL1Blue competent cells. *E. coli* competent cell preparation and the transformation procedure were carried out according to the $CaCl_2$ protocol (Sambrook and Russell, 2001). The structure of the recombinant colonies were confirmed by colony-PCR and restriction digestion analysis (data wasn't shown).

Deletion mutation on strR gene by SOEing PCR

A three consecutive PCRs technique known as gene splicing by overlap extension (SOEing), was designed here to create a 1083-bp fragment containing an in frame 51-bp deletion in "parB like nuclease" domain of the *strR* gene. The primers' locations and sequences are schematically drawn in figure 2. Inner primers SP_1R and SP_2F represent the junction region of the deletion. Primers SP_1R and SP_2F have a complement region extending to 10 base pairs, as shown in figure 2. Here are the primer's sequences:

SP_1F, CCGGATCCTAGAACGCCGAAGCAT; SP_1R, **CGATCTCGGT**CTCGCTGGTGGG; SP_2F, **ACCGAGATCG**CCCGCCAGTATTTC; SP_2R, TATCTAGACCGCCCGCATCCGACAT.

The 5' portion of primer SP_1R contained the final 12 bases of the upstream 308-bp section of *strR*, followed by 10 bases that are complementary to the 5' portion of primer SP_2F (complement nucleotides are bolded). The following 14 bases of the primer SP_2F are the same as the first 14 bases of the downstream 785-bp section after the region desired to be deleted from *strR*. Using the pSP*strR* plasmid as template, the SP_1F and SP_1R primers were used to amplify a 308-bp upstream fragment, and the SP_2F and SP_2R primers were used to amplify a 785-bp downstream fragment (the SP_2F and SP_2R primers have a 10 bp overlapped portion as show in figure 2, so 308-bp and 785-bp PCR products have also that same overlapped portion). Then, following the gel purification (gel purification kit, Qiagene) of two amplified fragments, these PCR products were mixed together as the templates in another round of PCR. Final reaction volume was 25 µl containing 1 µl PCR buffer (stock solution concentration: 500 mM KCl and Tris-HCl), 1.5 mM $MgCl_2$, 20 pmol of each primer, 0.4 mM of each dNTP, 0.3U *Pfu* DNA polymerase and 20 ng of plasmid DNA. This PCR reaction was carried out using the outer primers, SP_1F and SP_2R, with the following conditions: 95° C for 5 min, 15 cycles of denaturation at 94°C for 1 min, annealing at 65° C for 1min, and extension at 72°C for 3 min, followed by a final extension at 72° C for 10 min. For cloning purpose, two recognition sites, *BamH*I and *Xba*I, were introduced into the 5' ends of SP_1F and SP_2R primers respectively. The obtained 1083-bp product, the *strR*Δ17, was purified from 0.8 % agarose gel, treated with *Xba*I and *BamH*I restriction enzymes and ligated into the pMA::hyg plasmid, according to routine DNA manipulation techniques described before (Enshell-Seijffers et al., 2001). The resulting plasmid (pSPM*strR*Δ17) was transformed into *E. coli* XL_1Blue competent cells. Then supercoiled pSPM*strR*Δ17 plasmid, was purified from *E. coli* using boiling method as previously described (Holmes, 1981).

DNA sequencing

This was carried out using the ABI system (Bioneer, Italy).

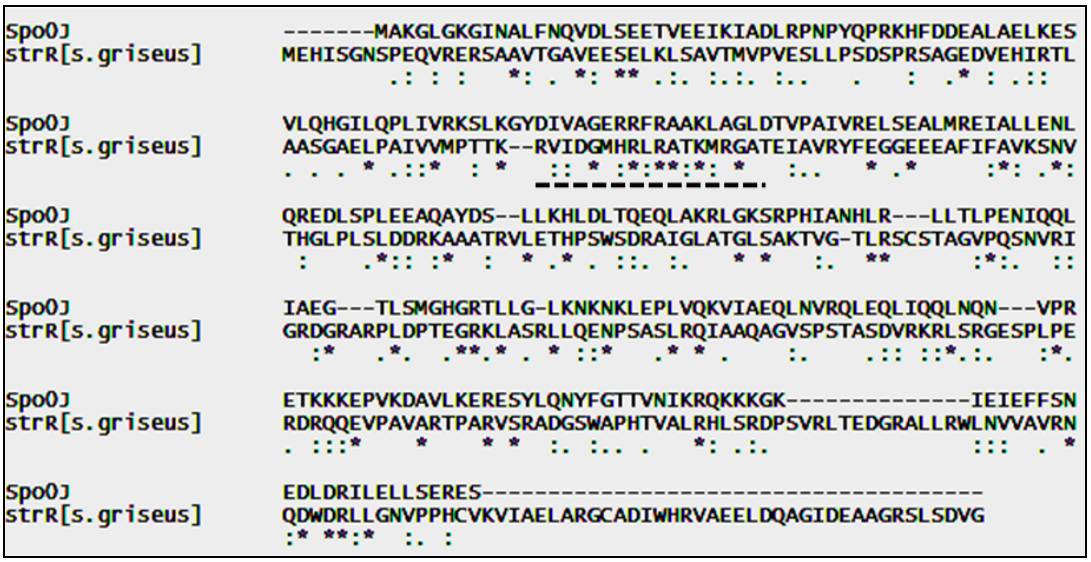

Figure 1. Amino acid sequence alignment by using Clustal W program. 17 amino acid residues were selected for deletion, these amino acids are underlined by (---) and located from 78 to 94, (this region is a part of parB like nuclease domain which is highly conserved). (*****): Same residues, (**:**):High similar residues, and (**.**):Similar residues.

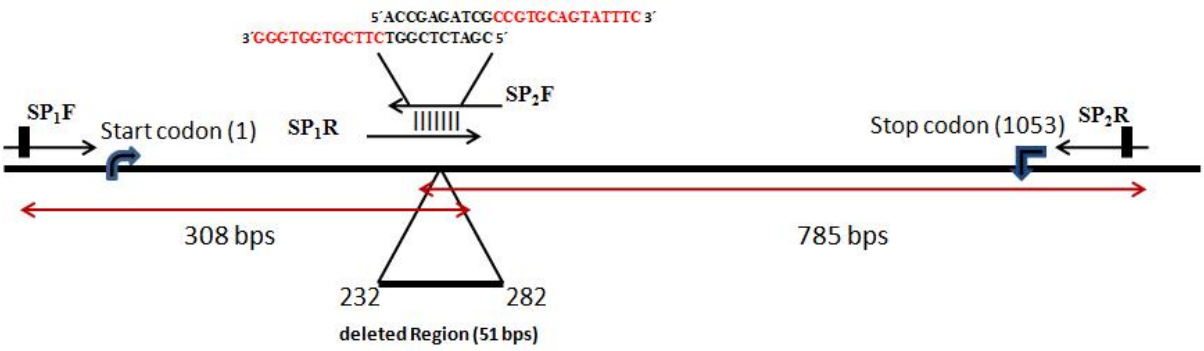

Figure 2. The *strR*Δ17 gene schematic map. Sequence and position of primers and deleted region are shown here (two inner primers have a ten bp overlapped region , for more information read the text).

Results

A 22 amino acids conserved domain was found for the StrR protein by using clustal W program (figure 1). More investigations in Conserved Domains database (NCBI) revealed that StrR protein had "ParB-like nuclease" domain in accordance with that 22 amino acids. This domain belongs to parB. This domain has been selected to be partially deleted by PCR aided site directed mutagenesis to investigate effects of that mutation in initiation of sporulation and chromosome partitioning in *S. griseus.*

Isolation of strR gene from S. griseus using PCR

In a PCR reaction using SP_1F and SP_2R primers, a 1134-bp *strR* fragment was produced (figure 3). The amplified fragment, *strR* gene, was initially confirmed by RFLP-PCR. According to the restriction map of the *strR* gene sequence, *Nla*III was chosen. *Nla*III cuts the amplified *strR* fragment at positions 287 and 317 that leaves three fragments with different sizes (287, 30 and 817 bps), (data not shown). The integrity of the amplified fragment was then confirmed using Semi-Nested-PCR, as illustrated in figure 4. Hence, the isolated *strR* fragment was used as a template, and primers SP_1F and SP_1R were used in the Semi-Nested PCR reaction.

Cloning of strR in E. coli XL$_1$Blue using pMA::hyg vector

The amplified *strR* fragment has preferred *BamH*I and *Xba*I restriction sites at 5' and 3' ends, respectively (these sites have been added to the designed primers). PCR product from each strain was ligated to pMA::hyg vector, separately. Then *E. coli* transformation was carried out using two new constructs.

Deletion of 51-bp region from strR gene

A 17- amino acid region from parB like nuclease domain of StrR was selected for deletion. This amino acid sequence has high similarity to a region from Spo0J domain in *Bacillus subtilis* Spo0J protein (figure 1). Six specific primers were appropriately designed using Oligo® primer design software and *strR* sequence (NC_010572.1 GI:182433793), as illustrated schematically in figure 2. The overlapped region is also shown on this figure. Ten nucleotide overlaps were considered for two primers SP_1R and SP_2F. These primers were initially used two by two, for amplification of the SOEing products. These overlapped-amplified fragments were used in a further PCR reaction to amplify the deleted PCR product (figure 5). Each PCR reaction was carried out, in particular conditions using two specific primers. Therefore, this exclusively designed SOEing PCR was conducted for deletion a 51-bp region from parB like nuclease domain of *strR* gene. In order to verify this deletion, its deleted version has to be cloned. A *Streptomyces* specific plasmid, pMA::hyg was selected as a cloning vector. This is a shuttle vector, capable of propagating in either *E. coli* or *Streptomyces.* The *strR*Δ17 gene was ligated to the pMA::hyg vector and transformed into the *E. coli* competent cells. Figure 6 shows the ligation and transformation results confirmed by 1% agarose gel electrophoresis. The plasmid containing *strR*Δ17 was isolated from the recombinant *E. coli.* A genetic map of the constructed recombinant vector pSPM*strR*Δ17 was drawn using plasmid draw software and illustrated in figure 7. The deleted region of *strR*Δ17 gene was confirmed by sequenc analysis (figure 8). On the other hand, the sequencing data was shown that the desired deletion had been introduced in the *strR* gene.

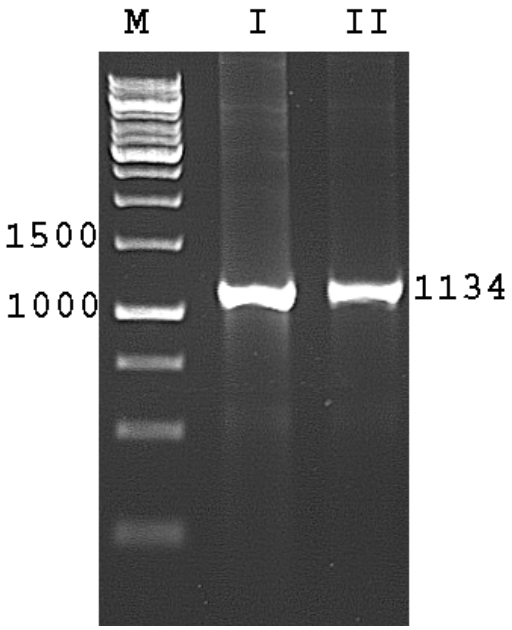

Figure 3. Isolation and amplification of the *strR* gene from *S. griseus*. Total DNA was isolated from two different strains of *S. griseus* and used in the PCR reaction using primers SP_1F and SP_2R. lane I: *strR* from *S. griseus* ATCC1952 ; lane II: : *strR* from *S. griseus* PTCC1127;M: Marker (1kb DNA ladder). Fragments sizes are in base pair (bp).

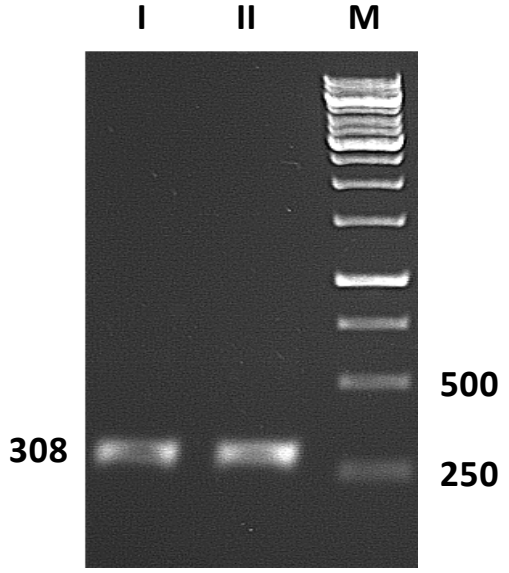

Figure 4. Confirmation of the isolated *strR* gene using Semi-Nested PCR. The *strR* amplified fragment used as a template (lane I: PTCC1127; lane II: Repeat (with the same PCR conditions). 308-bp fragment was amplified as expected from the *strR* sequence data. M: Marker (1kb DNA ladder). Fragments sizes are in base pair (bp).

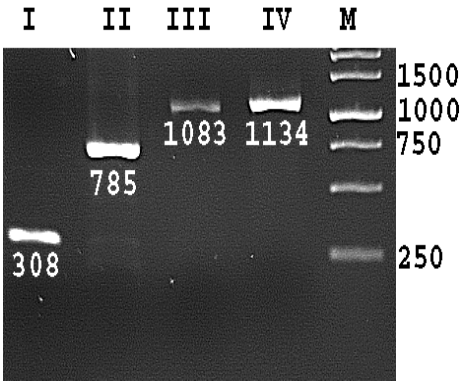

Figure 5. SOEing PCR product of *strR* gene from PTCC1127 strain. Lane I: the 308-bp fragment from left side of *strR* gene. Lane II: the 785-bp fragment from right side of *strR* gene after deleted region. Lane III: the final SOEing PCR product (*strR*Δ17) in comparison with intact *strR* gene (lane IV, 1083 + 51). Definitely, the 51-bp different in length between *strR* and *strR*Δ17 couldn't be detected on 1.5% agarose gel.

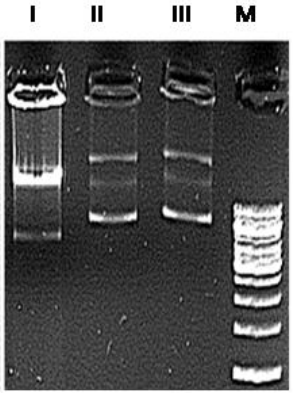

Figure 6. Isolation of the recombinant vector from the transformed *E. coli*. Lane II and III pSPM *strR*Δ17 vector (isolated from two different transformed strains), lane I: pMA::hyg as a control which is lighter than recombinant vectors.

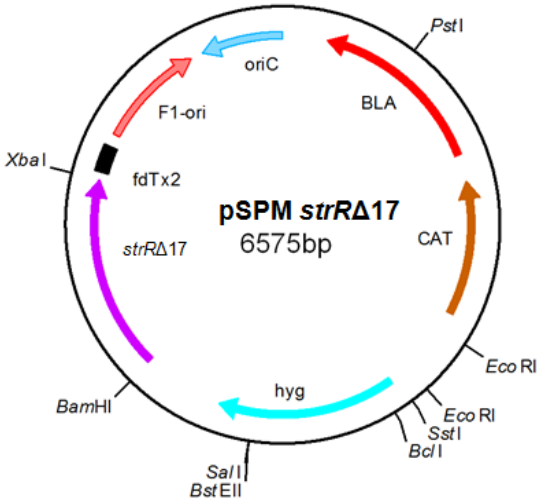

Figure 7. The genetic map of pSPM*strR*Δ17 vector. The resistance to ampicilin, chloramphenicol and hygromycin are shown by *BLA*, *CAT*, and *hyg*, respectively. The *strR*Δ17 gene is inserted between Hyg and fdTx2. The origin of replication in *E. coli* is also illustrated as *oriC*.

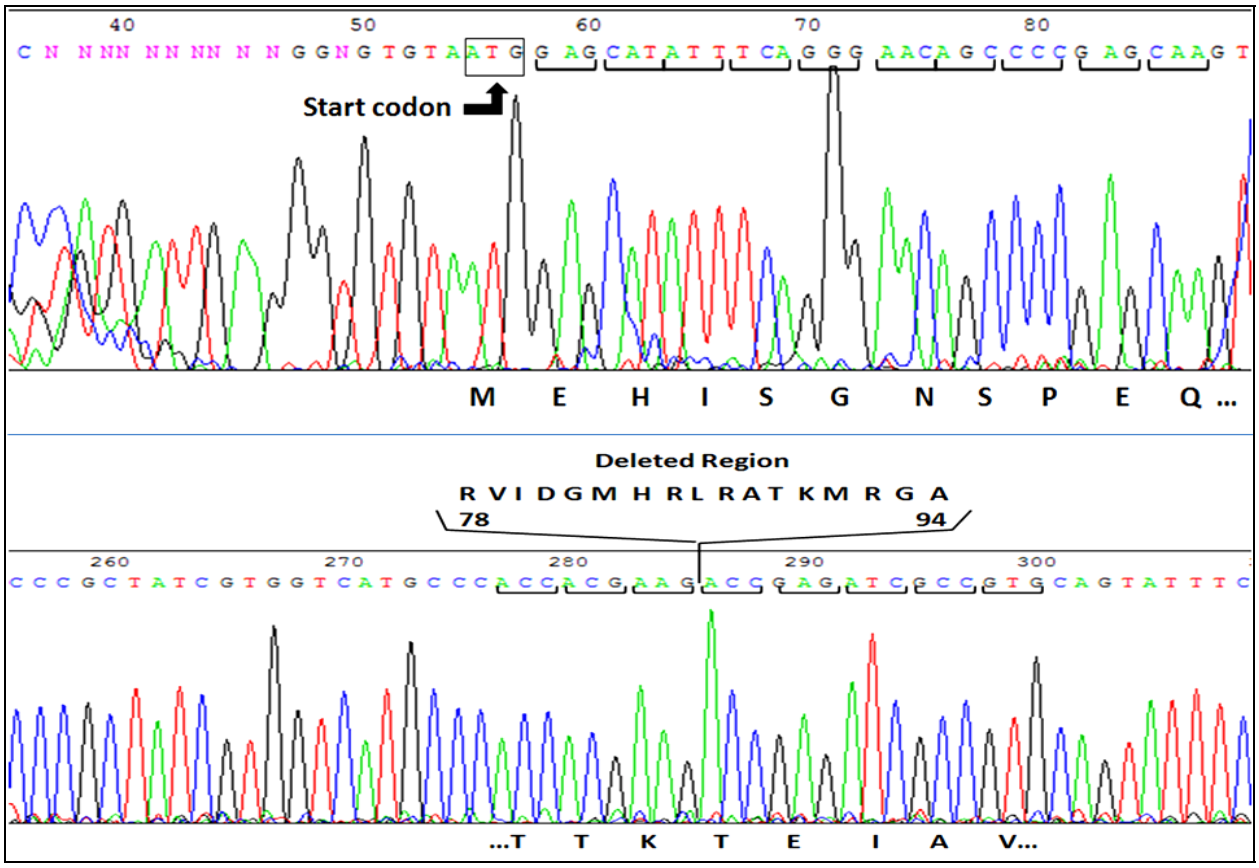

Figure 8. Confirmation of the SOEing deleted region using sequencing result. The amino acid sequence of the in frame deleted region is shown (17 amino acids from 78 to 94).

Discussion

StrR is known as a pathway specific activator required for regulation of streptomycin biosynthesis gene cluster transcription. A 22 amino acids conserved portion was found in this protein. More investigations have revealed that StrR protein has "ParB-like nuclease" domain in accordance with that 22 amino acids. This domain belongs to parB family. Proteins containing this domain appear to be related to the *Escherichia coli* protein ParB, which preferentially cleaves single-stranded DNAs (http://pfam.sanger.ac.uk/family?acc=PF025). Spo0J protein is another member of the parB family. The spo0J domain was found in Spo0J protein, which is required for normal chromosome partitioning, during vegetative growth and initiation of sporulation in *Bacillus subtilis*. Spo0J is a member of ParB superfamily (Jakimowicz et al., 2005; McLeod and Spiegelman, 2005). ParB like nuclease family control partitioning of several bacterial plasmids. Ireton et al. (1994) and Mysliwiec et al. (1991) have shown that deletion of the sequence responsible for Spo0J results in a phenotype with a low frequency of anucleate cells accumulation during growth and a block to sporulation before stage II (Ireton et al., 1994; Mysliwiec et al., 1991). Kois et al. showed the same results for *Streptomyces coelicolor* by introduction of deletions in *parB*, *parA*, and *smc* proteins (Kois et al., 2009).

Amino acid sequence information of StrR revealed that the product of this gene is similar to the members of parB superfamily including Spo0J, IncC and KorB (Ireton et al., 1994). Using the Conserved Domains database (CDD) and pfam databases, the parB like nuclease domain in StrR was identified. Then, the amino acid sequence of StrR and Spo0J from *B. subtilis*, were analyzed by Clustal W program. The result showed high similarity between amino acid sequences of these proteins (figure 1). This similarity was significant, especially in parB like nuclease and Spo0J domains from StrR and Spo0J proteins, respectively. According to this homology, a 17- amino acid region from StrR was selected for deletion.

Here, a deletion was introduced into the *strR* gene, using SOEing PCR. Two different sets of designed primers were accompanied with a specific strategy in order to delete the selected region from the *strR* gene. This deletion eventually produces a recombinant StrR protein. We used a very efficient,

precise and rapid procedure for site directed mutagenesis Enshell-Seijffers et al. (2001), Balasingham et al. (2007), and the others used this procedure for their researches. This procedure and protocol could be applied for varieties of gene and proteins in various organisms. Our sequencing results have also shown that a specific deletion is produced in the desired site and region in the *strR* gene without any frame shift.

Unlike the transformation of pSPM *strR*Δ17 to the *E.coli*, the transformation of this construct to *S.griseus* protoplasts was unsuccessful. This is originated from very robust restriction barriers in *Streptomyces* family especially in *S.griseus* (Kato et al., 2005K; Kong et al., 2000; wak et al., 2002). Efforts to overcome these barriers are continued.

Three separate achievements were considered here: At first, The StrR regulatory protein has a putative conserved domain known as Spo0J domain. Second, this domain was subjected to deletion using SOEing PCR. Different sets of SOing PCR primers should be designed precisely in order to introduce the desired mutation in the gene. About 10 bp ought to be considered for the overlapped region in one set of primers. Third, characterization of the isolated *strR* from the *S. griseus* was carried out here, using molecular studies. Cloning of the deleted gene was conducted using a dual action shuttle vector pMA::hyg. So, the structural analysis of the overproduced StrRΔ17 protein (in *E. coli*) could be studied later. pMA::hyg is a *Streptomyces* specific vector, containing a multiple cloning site (MCS), three selection markers (*hyg;* Hygromycin, *BLA;* Ampiclin and *CAT;* Chloramphenicol) and two origins of replication (*oriC* in *E. coli* and *F1-ori* in M13 phage). All of these features make it efficient for site directed mutagenesis and gene replacement strategies in *Streptomyces*.

Acknowledgment

This study was performed at the University of Isfahan and financially supported by the Graduate Studies Office of the University of Isfahan.

References

1- Balasingham S. V., Collins R. F., Assalkhou R., Homberset H., Frye S. A., Derrick J P., and Tonjum T. (2007) Interactions between the lipoprotein PilP and the secretin PilQ in *Neisseria maeningitides*. Journal of Bacteriology 189: 5716–5727.

2- Boccard F., Pernodet J., Friedmann A. and Guerineau M. (1988) Site specific integration of plasmid pSAM2 in *Streptomyces lividans* and *S. ambofaciens.* Molelucar and General Genetics 212: 432–439.

3- Cullings K. W. (1992) Design and testing of a plant-specific PCR primer for ecological and evolutionary studies. Molecular Ecology 1: 233–240.

4- Enshell-Seijffers D., Smelyanski L. and Gershoni J. M. (2001) The rational design of a 'type 88' genetically stable peptide display vector in the filamentous bacteriophage. Nucleic Acids Research 15: 29(10): E50-0.

5- Hara H., Ohnishi Y. and Horinouchi S. (2009) DNA microarray analysis of global gene regulation by A-factor in *Streptomyces griseus*. Microbiology 155: 2197–2210.

6- Hirano S., Kato J., Ohnishi Y. and Horinouchi S. (2006) Control of the *Streptomyces* subtilisin inhibitor gene by AdpA in the A-Factor regulatory cascade in *Streptomyces griseus*. Journal of Bacteriology 188: 6207–6216.

7- Holmes D. S. and Quigley M. (1981) A rapid boiling method for the preparation of bacterial plasmids. Analytical Biochemistry 114: 193–197.

8- Hopwood D. A. (1999) Forty years of genetics with *Streptomyces*: from in vivo through in vitro to in silico. Microbiology 145: 2183–2202.

9- Horton R. M. (1993) PCR protocols: Current methods and applications. In White B. A. (ed), Methods in Molecular Biology. Humana Press, New Jersey, USA, 251–261 pp.

10- Ireton K., Gunther N. W. and Grossman A. D. (1994) SpoOJ is required for normal chromosome segregation as well as the initiation of sporulation in *Bacillus subtilis*. Journal of Bacteriology 176: 5320–5329.

11- Jakimowicz D., Gust B., Zakrzewska-Czerwinska J. and Chater K. F. (2005) Developmental-stage-specific assembly of parB complexes in *Streptomyces coelicolor* hyphae. Journal of Bacteriology 187: 3572–3580.

12- Kato J. Y., Chi W. J., Ohnishi Y., Hong S. K. and Horinouchi S. (2005) Transcriptional control by A-factor of two trypsin genes in Streptomyces griseus. Journal of Bacteriology 187(1): 286–295.

13- Kieser T., Bibb M. J., Buttner M. J., Charer K. F. and Hopwood D. A. (2000) Practical *Streptomyces* Genetics. John Innes Foundation, Norwich, England.

14- Kois A., Swiatek M., Jakimowicz D. and Zakrzewska-Czerwinska J. (2009) SMC protein-dependent chromosome condensation during aerial hyphal development in *Streptomyces*. Journal of Bacteriology 191: 310–319.

15- Komatsu M., Uchiyama T., Omura S., Canec D. E. and Ikedaa H. (2010) Genome-minimized *Streptomyces* host for the heterologous expression of secondary metabolism. Proceedings of the National Academy of Sciences 107: 2646–2651.

16- Kong H., Lin L. F., Porter N., Stickel Sh., Byrd D., Posfai J. and Roberts R. J. (2000) Functional analysis of putative restriction-modification system genes in the *Helicobacter Pylori* J99 genome. Nucleic Acids Research 28: 3216–3223.

17- Kwak J., Jiang H. and Kendrick K. E. (2002)

Transformation using in vivo and in vitro methylation in *Streptomyces griseus*. Federation of European Microbiological Societies Microbiology Letters 209: 243–248.

18- Li W., Ying X., Guo Y., Yu Zh., Zhou X., Deng Z., Kieser H., Chater K. F. and Tao M. (2006) Identification of a gene negatively affecting antibiotic production and morphological differentiation in *Streptomyces coelicolor*. Journal of Bacteriology 187: 8368–8375.

19- McLeod B. N. and Spiegelman G. B. (2005) Soj antagonizes Spo0A activation of transcription in *Bacillus subtilis*. Journal of Bacteriology 187: 2532–2536.

20- McPherson M. J. and Moller S. G. (2000) PCR (Basics: from Background to Bench), 1st Ed. BIOS Scientific Publishers, Ltd. Oxford, UK, 143–148 pp.

21- Mysliwiec T. H., Errington J., Vaidya A. B. and Bramucci M. G. (1991) The *Bacillus subtilis* spo0J gene: evidence for involvement in catabolite repression of sporulation. Journal of Bacteriology 173: 1911–1919.

22- Ohnishi Y., Kameyama S., Onaka H. and Horinouchi S. (1999) The A-factor regulatory cascade leading to streptomycin biosynthesis in *Streptomyces griseus*: identification of a target gene of the A-factor receptor. Molecular Microbiology 34: 102–111.

23- Ohnishi Y., Ishikawa J., Hara H., Suzuki H., Ikenoya M., Ikeda H., Yamashita A., Hattori M. and Horinouchi S. (2008) Genome sequence of the streptomycin -producing microorganism *Streptomyces griseus* IFO 13350. Journal of Bacteriology 190: 4050–4060.

24- Retzlaff L. and Distler J. (1995) The regulator of streptomycin gene expression, StrR, of *Streptomyces griseus* is a DNA binding activator protein with multiple recognition sites. Molecular Microbiology 18: 151–162.

25- Sambrook J. and Russell D. (2001) Preparation and transformation of competent *E. coli* using callcium chloride. In: Spedding G (ed). Molecular Cloning (A Laboratory Manual). Cold Spring Harbor Laboratory Press. Cold Spring Harbour, New York, USA, 116–118 pp.

26- Senanayake S. D. and Brian D. A. (1995) Precise large deletions by the PCR-based overlap extension method. Molecular Biotechnology 4: 13–15.

27- Thompson J. D., Higgins D. G. and Gibson T. J. (1994) CLUSTAL W: improving the sensitivity of progressive multiple sequence alignment through sequence weighting, position-specific gap penalties and weight matrix choice. Nucleic Acids Research 22(22): 4673–4680.

28- Tomono A., Tsai Y., Yamazaki H., Ohnishi Y. and Horinouchi S. (2005) Transcriptional control by A-factor of StrR, the pathway-specific transcriptional activator for Streptomycin biosynthesis in *Streptomyces griseus*. Journal of Bacteriology 187: 5595–5604.

29- Weber T., Welzel K., Pelzer S., Vente A. and Wohlleben W. (2003) Exploiting the genetic potential of polyketide producing *Streptomycetes*. Journal of Biotechnology 106: 221–232.

Journal of Cell and Molecular Research (2012) 4 (1), 43-49

The role of over expression of P5CS gene on proline, catalase, ascorbate peroxidase activity and lipid peroxidation of transgenic tobacco (*Nicotiana tabacum L.*) plant under *in vitro* drought stress

Somayyeh Zarei, Ali Akbar Ehsanpour* and Jalil Abbaspour

Department of Biology, Faculty of Science, University of Isfahan, Isfahan, Iran

Received 30 May 2012 Accepted 12 July 2012

Abstract

In this study proline content and activity of catalase (CAT), and ascorbate peroxidase (APX) and level of lipid peroxidation in terms of malondialdehyde (MDA) content were measured in transgenic tobacco (*Nicotiana tabacum* cv. Wisconsin), over expressing a Δ-1-pyrroline-5-carboxylate synthase (P5CS) gene, and non transgenic plants as control. Drought stress was applied using polyethylene glycol (PEG) 6000 at concentrations of 217, 264, 320, 637, 1292 mmol/kg equal to (0, 5, 10, 20, 30% respectively). Proline content, especially in transgenic plants, was increased in leaves and roots significantly. CAT and APX activities increased under drought stress and the highest activity was observed in 10 and 20% of the PEG treatment. MDA content was increased by increasing of PEG and the highest MDA content was revealed in transgenic and non transgenic plants at 20% and 30%, respectively. Our results suggest that P5CS is an inducible gene and over production of proline and induction of CAT and APX activities are involved in drought tolerance mechanism.

***Keywords*:** Tobacco, drought stress, proline, catalase, ascorbate peroxidase, P5CS gene

Introduction

One of the most important abiotic stress is drought, which results in the disruption of water potential slopes, loss of turgor and decreasing of pressure potential. Abiotic stresses and osmotic adjustment contributes to pressure potential maintenance and stress tolerance of plants (Cherian et al., 2006). In response to water stress, plants accumulate osmolytes and protect themselves against drought stress. Proline is one of the most common compatible osmolytes and plays an overriding role in osmotic pressure adjustment (Yamch et al., 2005). Proline allows many plant species to survive under stress without interfering with the normal biochemical reactions (Stewart, 1981). The most important function of proline is turgor maintenance and scavenging the excess reactive oxygen species (ROS). It stabilizes protein, enzyme and other subcellular structures such as membranes. Proline also act as an antioxidant, and regulates cellular redox status under stress condition (Chinnusamy et al., 2005). The first response of plants to drought stress is closure of stomata and a decrease in CO_2 concentration in leaf mesophyll tissue. Due to decrease in CO_2 concentration, accumulation of NADPH and loss of $NADP^+$ occur and oxygen accepts electrons and leads to ROS formation (Sairam et al., 1998; Asada, 1999). ROS results in injury to vital molecules such as nucleic acids, proteins, structural carbohydrates, and lipids (Mittler, 2002; Daveis, 1987). Lipid peroxidation of cellular membranes is the most important effect of ROS that finally leads to disruption of plant growth and development (Chen et al., 2000; Sreenivasulu et al., 1999).

Plants prevent or alleviate ROS damages by antioxidants protection system which provides protection against oxidative stress. Antioxidants are non enzymatic including glutathione, ascorbate and carotenoids, and enzymatic such as catalase (CAT), ascorbate peroxidase (APX), superoxide dismutase (SOD) and glutathione reductase (GR) (Apel and Hirt, 2004; Bhardwaj et al., 2007).

Ascorbate peroxidases have been found in higher plants, algae and some cyanobacteria (Sano et al., 2001; Sharma and Dubey, 2004). Ascorbate, as an electron donor, is utilized in reduction of hydrogen peroxide (Shigeoka et al., 2002). CAT and APX reduce H_2O_2 to water and O_2 (Gratao et al., 2005). Unlike APX, CAT acts without any electron donor

*Corresponding author E-mail: ehsanpou@sci.ui.ac.ir

or reducing agent (Mallick and Mohn, 2000).

In some plants such as *Vigna aconitifolia* and *Arabidopsis thaliana* reduction of glutamate to its semialdehyde intermediate is catalyzed by a single bifunctional enzyme, Δ-1-pyrroline-5-carboxylate synthase (P5CS), whose transcription is induced in plants subjected to salt and drought stress (Yoshiba et al., 1995). Furthermore, data indicated that, over expression of *V. aconitifolia* P5CS (VaP5CS) in transgenic tobacco plants increased proline level and rendered plants less sensitive to the osmotic stress (Kishor et al., 1995). However, there is a controversy discussion in balance activity of P5CS and P5CR enzyme (Verbruggen, 1995). It has been documented that transgenic plants, over expressing the P5CS gene, increases concentration of proline and resulted in more resistance to both drought and salt stress (Kishore et al., 1995). The objective of this work was to understand better the relationship between drought tolerance and proline content, the CAT and APX activity and lipid peroxidation in transgenic tobacco plants over expressing P5CS gene.

Materials and Methods

Plant materials and treatment

Transgenic tobacco plants (*Nicotiana tabacum* cv. Wisconsin) (T1 seeds) carrying P5CS gene were surface sterilized in 70% ethanol and then grown on MS medium (Murashige and Skoog, 1962) and kept in the growth chamber (16/8 h light and dark respectively, with approximately 40 µm photon $m^{-2}s^{-1}$ light density) at 25°C. After 18-20 days, seedlings were transferred to MS medium supplemented with PEG (217, 264, 320, 637, 1292 mmol/kg). After 4 weeks proline content, CAT and APX activities and lipid peroxidation were measured in leaves and roots.

Proline measurement

Free proline accumulation was estimated using ninhydrin reaction based on method described by Bates (1973). A small portion (0.04 g) of leaves or roots was homogenized with 1.7 ml of 3% (w/v) sulphosalicylic acid (Merk). The homogenate was centrifuged at 13000 rpm for 20 min. Then ninhydrin reagent (1 ml) (Sigma) and glacial acetic acid (1 ml) were added to 1 ml of the centrifuged extract. The mixture was boiled for 1 h in a water bath and then cooled on ice. Then 2 ml toluene was added to each tube, and tubes were placed in the dark for 1 h. Absorption of chromophore was determined at 520 nm by spectrophotometer (Shimadzu UV-160, Japan). Toluene was used as blank. Proline content was calculated using L-proline (Sigma) as a standard curve.

Enzyme assays

For enzyme extraction, fresh samples of leaves from control and stressed seedlings (0.1 g) were homogenized in an ice bath in 1 mL of phosphate buffer saline (PBS, pH:7.4) containing NaCl (8 g/l), KCl (0.2 g/l), Na_2HPO (41.44 g/l), KH_2PO_4 (24 g/l) and polyvinylpyrrolidone (PVP, 1%). The homogenate was centrifuged at 14000 rpm at 4 °C for 20 min. The supernatant was collected and used for enzyme (CAT and APX) activity analysis.

Catalase (EC 1.11.1.6)

The CAT activity was determined by measuring the decomposition of H_2O_2. The reaction mixture contained 50 mM potassium phosphate buffer (pH 7.4), 10 mM H_2O_2, and 0.05 ml of the enzyme extract (Aebi, 1984). Then the absorbance at 240 nm was recorded every 10 sec. up to 1 min. The CAT activity was calculated and expressed as U/g FW^{-1} min^{-1} (One unit of CAT activity is defined as the amount of enzyme required to consume 1 µmole H_2O_2 min–1). CAT activity was calculated using the coefficient of absorbance of 0.0394 mM^{-1} cm^{-1} by spectrophotometer (Shimadzu).

Ascorbate peroxidase (EC 1.11.1.11, APX)

APX was estimated by slightly modified procedure of Nakano and Asada (1981). APX activity was determined by measuring the consumption of ascorbate. Reaction mixture containing 25 mM potassium phosphate buffer (pH 7.0), 0.5 mM ascorbic acid, 0.2 mM EDTA, 0.1 mM H_2O_2, 50 µl of BSA, and 0.05 ml of the enzyme extract. The absorbance at 290 nm was recorded every 10 sec up to 1 min. One unit of APX activity was defined as the amount of enzyme required to consume 1 µmole ascorbate min^{-1}. Ascorbate peroxidase activity was calculated using the coefficient of absorbance of 2.8 mM^{-1} cm^{-1}.

Lipid peroxidation

Fresh plant material (0.1 g) was homogenized in 2.5 ml 0.1% (w/v) trichloroacetic acid (TCA). The level of lipid peroxidation was measured using the malondialdehyde (MDA), thiobarbituric acid (TBA) reaction based on method of Heath and Packer (1968). Lipid hydroperoxides resulting from peroxidation of the cell membrane react with thiobarbituric acid (TBA) to form MDA, which is a crystalline pink pigment with absorption from 525 to 535 nm (Persky et al. 2000). The absorbance of extract was measured at 532 and 600 nm. The amount of MDA-TBA complex was calculated

from the coefficient of absorbance 155 $mM^{-1}cm^{-1}$.

Statistical analysis

All experiments were carried out in a completely randomized design. The mean values of proline, CAT and APX activity and lipid peroxidation level were taken from the measurements of four replicates and the "Standard Error" of the means was calculated. Two-way ANOVA was applied to determine the mean between different treatments and then Tukey test was performed and significance was determined at $P < 0.05$. All statistical analyses were carried out using SPSS Software program version 10.

Results

Proline content

As the PEG concentration increased, proline level of shoot in transgenic and non transgenic plants, was increased significantly. In transgenic plants, either in leaf or root the proline content was significantly higher than non transgenic (figures 1A and 1B). In both plant types, 20 and 30% PEG showed the highest level of proline content. In the root, proline content was increased (1.3 and 1.2 fold) by increasing of PEG particularly in the highest level at 20 and 30% PEG compared to non transgenic plants.

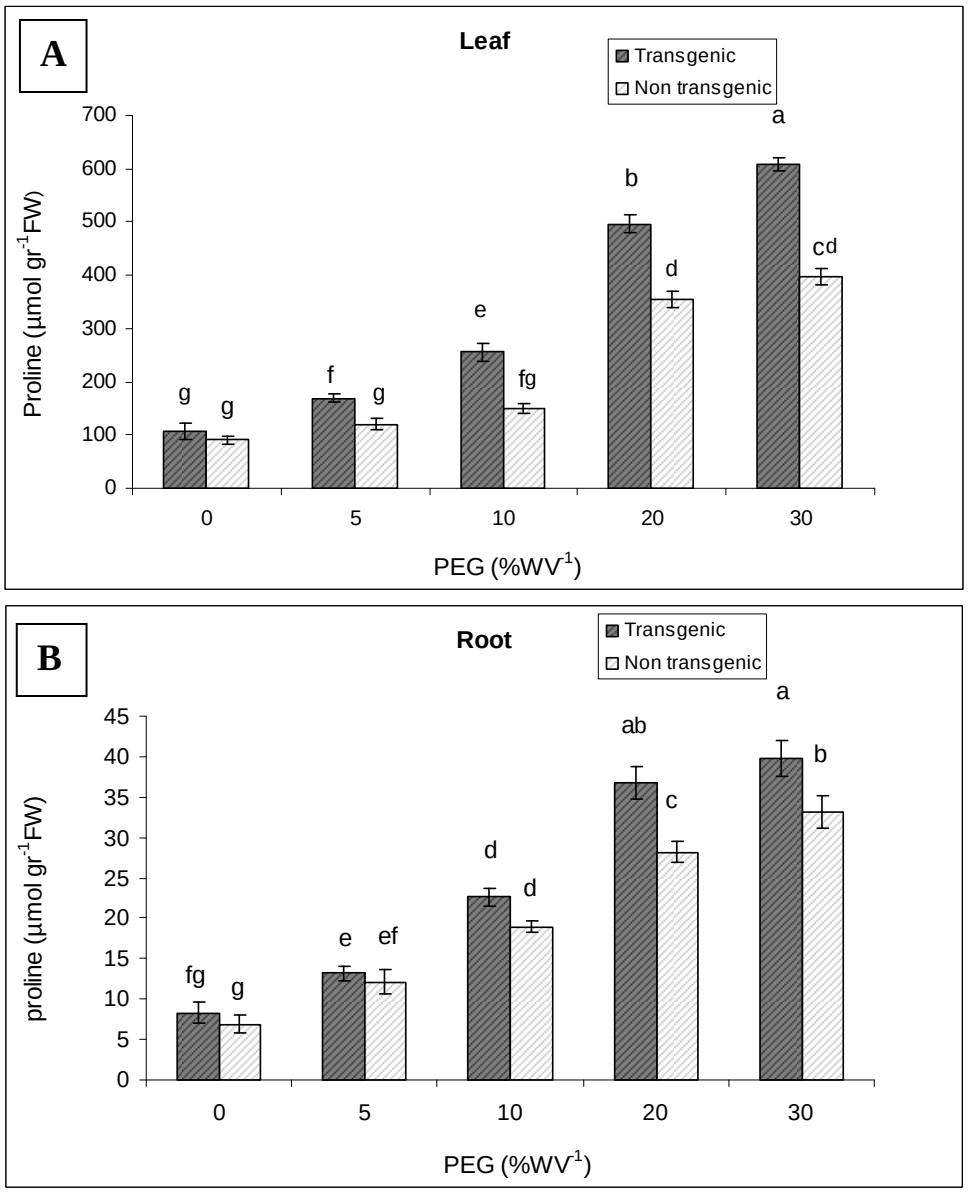

Figure 1. Proline content in shoot (A) and roots (B) of transgenic and non transgenic tobacco seedlings. Values are means ± Sd. Uncommon letters are significant based on Tukey test ($P < 0.05$). 0, 5, 10, 20 30% of PEG are equal to 217, 264, 320, 637, 1292 mmol/kg respectively.

APX activity

The APX, showed a high significant activity by increasing of PEG up to 20% either in transgenic or non transgenic plants. Transgenic plants showed higher APX activity than non transgenic plants in all PEG concentrations. In transgenic plants, both plant types, the APX activity decreased at 30% PEG. (figure 2).

CAT activity

Results indicated that the CAT activity was increased by increasing of PEG concentration. In transgenic plants, CAT activity at 5, 10 and 20% PEG while in non transgenic plants at 10 and 20% PEG increased significantly however, at 30% the activity of CAT decreased compared to the control plants (figure 3).

Lipid peroxidation

Lipid peroxidation data (measured as MDA content), showed a significant increase in both plant types in 10, 20 and 30% of PEG. MDA was increased significantly in comparison to control plants. In non transgenic plants at 10 and 20% PEG it was significantly higher than transgenic ones (figure 4).

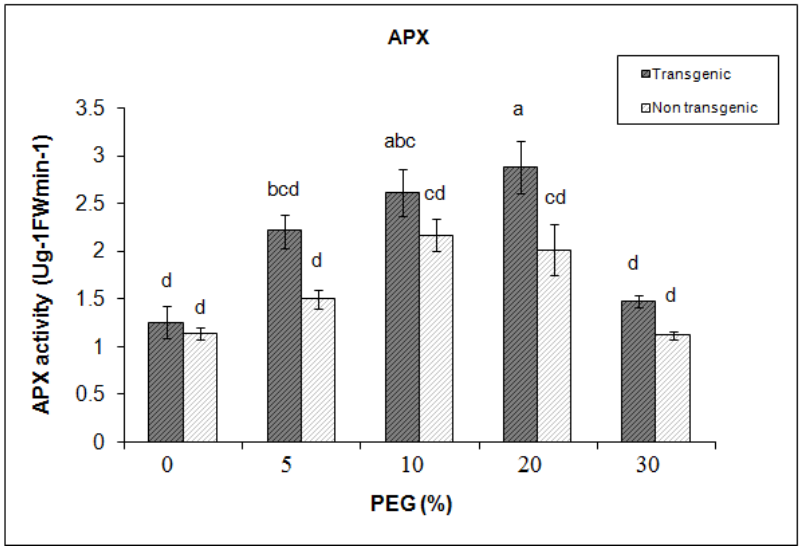

Figure 2. Ascorbat peroxidase (APX) activity of leaves of tobacco seedlings in response to drought stress. Values are means ± SE. Uncommon letters are significant based on Tukey test ($P < 0.05$). 0, 5, 10, 20 30% of PEG are equal to 217, 264, 320, 637, 1292 mmol/kg respectively.

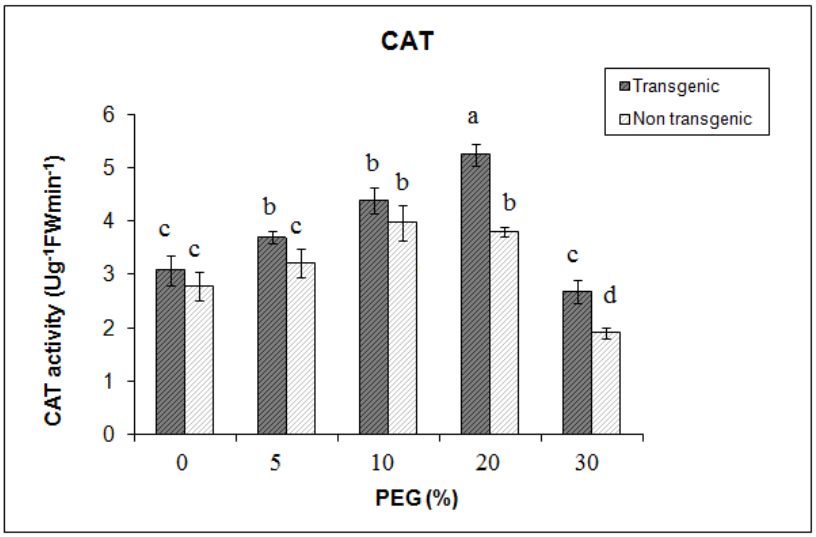

Figure 3. Catalase (CAT) activity of leaves of tobacco seedlings. Values are means ± SE. Uncommon letters are significant based on Tukey test ($P < 0.05$). 0, 5, 10, 20 30% of PEG are equal to 217, 264, 320, 637, 1292 mmol/kg respectively.

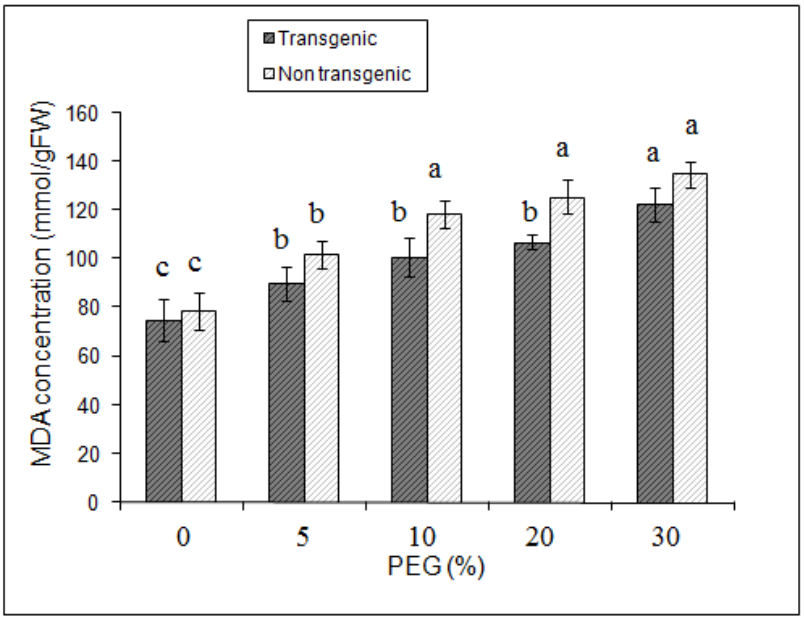

Figure 4. Effect of PEG on MDA content in transgenic and non transgenic tobacco plants. Values are means ± SE. Similar letters indicate not significant based on Tukey test ($P < 0.05$). 0, 5, 10, 20 30% of PEG are equal to 217, 264, 320, 637, 1292 mmol/kg respectively.

Discussion

Results of this study showed that proline was accumulated in shoot and roots of transgenic and non transgenic plants when subjected to drought stress. Accumulation of proline in shoots and roots of the transgenic plants was much higher than that in non transgenic plants. It seems that over expression of P5CS gene in transgenic plants, have a remarkable role in proline synthesis and accumulation. As P5CS gene is a rate-limiting enzyme in the proline biosynthetic pathway in plants and has an important role in transgenic plants over expressing P5CS gene, it is expected to be responsible for more proline accumulation in the transgenic plants. As proline plays an important role in osmotic adjustment as well as membrane protection, free radical scavenging, and redox buffering (Verbruggen and Hermans, 2008; Kishor et al., 2005), high level of proline, accumulation by over expression of P5CS, can tolerate plants against osmotic stress (Hank and Hwang, 2003). Similar data was obtained when our transgenic and non transgenic tobacco plants exposed to osmotic (PEG) stress. These results are in agreement with the report from Kishore et al. (2005). Transgenic tobacco in the present study, plants of the over expressing P5CS gene, produced a high level of the antioxidant enzymes and synthesized more proline than the controls.

Our results showed that drought stress changed antioxidant enzymes, activity in leaves of both plant types. APX and CAT activities were induced in leaves of the transgenic plants compared to the control ones. These finding are in accordance to the results obtained by Khedr et al. (2003) and Ghorbanli et al. (2004). On the other hand, it has been known that abiotic stresses, including drought stress, induce ROS accumulation, resulting oxidative damage to the membrane lipids, proteins, and nucleic acids (Smirnoff, 1993). Plants increase activity of detoxifying enzymes such as superoxide dismutase, catalase, and ascorbat peroxidase to combat oxidative stress. Proline has a role in scavenging ROS and protect proteins against denaturation (Alia et al., 1991), increasing of CAT and APX activities may cooperates with the other antioxidant enzymes for giving more tolerance to drought stress in our tobacco plants.

It is well known that ROS induce lipid peroxidation of the membranes. The change in MDA content is often used as an indicator of oxidative damage (Sung, 1996; Goel and Sheoran, 2003). Our data showed that MDA content enhanced by increasing of drought stress intensity. It has been reported that MDA content, as lipid peroxidation criteria, in the transgenic plants was lower than non transgenic plants (Smirnoff and Cumbes, 1989; Matysik et al., 2002). It has been shown that proline can reduce lipid peroxidation in alga cells, exposed to heavy metals (Mehta and Gaur, 1999). Therefore it can be speculating that similar role might be responssible for proline accumulation due to P5CS over expression in tobacco plants too. The lower level of

lipid peroxidation in leaves of the transgenic plants suggests that, these plants are better protected from the oxidative damage under drought stress than non transgenic ones. It can be concluded that over expression of the P5CS gene in tobacco plants and consequent proline accumulation along with alleviation of with CAT and APX activities increase drought tolerance in tobacco plants.

Acknowledgment

Authors wish to thank University of Isfahan and Plant Stress Center of Excellence (PSCE) for their support.

References

1- Aebi H. (1984) Catalase in vitro. Methods of Enzymology 105: 121-126.

2- Alia P. S. P., Pardha S. P. and Mohanty P. (1991) Proline enhances primary photochemical activities in isolated thylakoid membranes of Brassica juncea by arresting photoinhibitory damage. Biochemical and Biophysical Research Communications 181: 1238–1244.

3- Apel K. and Hirt H. (2004) Reactive oxygen species: metabolism, oxidative stress, and signal transduction. Annual Review of Plant Biology 55: 373-399.

4- Asada K. (1999) The water- water cycle in chloroplast; scavenging of active oxygen and dissipation of excess photons. Annual Review of Plant Physiology and Plant Molecular Biology 50: 601- 639.

5- Bates L. S. (1973) Rapid determination of free proline for water-stress studies. Plant and Soil 39: 205-207.

6- Bhardwaj R. N., Arora P., Sharma H. and Arora K. (2007) Effects of 28-homobrassinolide on seedling growth, lipid peroxidation and antioxidative enzyme activities under nickel stress in seedlings of *Zea mays* L. Asian Journal of plant Science 6: 756-772.

7- Chen W. P., Li P. H. and Chen T. H. H. (2000) Glycinebetaine increases chilling tolerance and reduces chilling-induced lipid peroxidation in *Zea mays* L. Plant Cell Environment 23: 609-618.

8- Cherian S., Reddy M. P. and Ferreira R. B. (2006) Transgenic plants with improved dehydration- stress tolerance: Progress and future Prospects. Biologia Plantarum 50: 481- 495.

9- Chinnusamy V., Jagendorf A. and Zhu J. K. (2005) Understanding and improving salt tolerance in plants. Crop Science 45: 437–448.

10- Davies K. J. (1987) Protein damage and degradation by oxygen radicals. I. General aspects. Journal of Biological Chemistry 262: 9895-9901.

11- Goel A. and Sheoran L. S. (2003) Lipid peroxidation and peroxide scavenging enzymes in cotton seeds under natural ageing. Biologia Plantarum 46: 429–434.

12- Ghorbanli M., Ebrahimzadeh H. and Sharifi M. (2004) Effects of NaCl and mycorrhizal fungi on antioxidative enzymes in soybean. Biologia Plantarum 48: 575-581.

13- Gratao P. L., Polle A., Lea P. J. and Azevedo R. A. (2005) Making the life of heavy metal-stressed plants a little easier. Functional Plant Biology 32: 481–494.

14- Hank H. and Hwang C. H. (2003) Salt tolerance enhanced by transformation of a P5CS gene in carrot. Journal of Plant Biotechnology 5: 149–153.

15- Heath R. L. and Packer L. (1969) Photoperoxidation in isolated chloroplast. I. Kinetics and stoichiometry of fatty acid peroxidation. Archives of Biochemistry and Biophysics 125: 189-198.

16- Kavi Kishor P. B., Sangam S., Amrutha R. N., Laxmi P. S., Naidu K. R., Rao K. R. S. S., Rao S., Reddy K. J., Theriappan P. and Sreenivasulu N. (2005) Regulation of proline biosynthesis, degradation, uptake and transport in higher plants: its implications in plant growth and abiotic stress tolerance. Current Science 88: 424-38.

17- Khedr A. H. A., Abbas M. A., Wahid A. A. A., Quick W. P. and Abogadallah G. M. (2003) Proline induces the expression of salt-stress-responsive proteins and may improve the adaptation of Pancratium maritmum L. to salt stress. Journal of Experimental Botany 54: 2553-2562.

18- Kishore B., Hong Z., Miao G., Hu C. and Verma D. (1995) Over expression of Δ- Pyrroline-5-carboxylate synthetase increase proline production and confers osmotolerance in transgenic plants. Plant Phsiology 108: 1387-1394.

19- Kishore P. B. K., Sangam S., Amrutha R. N., Laximi P., Naidu K., Rao K. R., Rao S., Reddy K. J., Theriappon P. and Sreenivasula N. (2005) Regulation of proline biosynthesis, degredation, uptake and transport in higher plants: its implication in plant growth and abiotic stress tolerance. Current Science 88: 427-438.

20- Mallick N. and Mohn F. H. (2000) Reactive oxygen species: Response to algal cells. Journal of Plant Physiology 157: 183-193.

21- Matysik J., Alia B. B. and Mohanty P. (2002) Molecular mechanisms of quenching of reactive oxygen species by proline under stress in plants. Current Science 82: 525-532.

22- Mehta S. K. and Gaur J. P. (1999) Heavy metal-induced proline accumulation and its role in ameliorating metal toxicity in Chlorella vulgaris. New Phytologist 143: 253-259.

23- Mittler R. (2002) Oxidative stress, antioxidntas and stress tolerance. Trends in Plant Science 7: 405-410.

24- Murashige T. and Skoog F. (1962) A revised medium for rapid growth and bioassays with tobacco tissue cultures. Physiologia Plantarum 15: 473-497.

25- Nakano Y. and Asada K. (1987) Purification of ascorbate peroxidase in spinach chloroplasts: its inactivation in ascorbate-depleted medium and reactivation by monodehydroascorbate radical. Plant and Cell Physiology 28: 131-140.

26- Sairam R. K., Deshmukh P. S. and Saxna D. C. (1998) Role of antioxidant systemes in wheat genotype tolerance to water stress. Biologia Plantarum

41: 387-394.
27- Savouré A., Jaoua S., Hua X. J., Ardiles W., Van Montagu M. and Verbruggen N. (1995) Isolation, characterization, and chromosomal location of a gene encoding the 11-pyrroline-5-carboxylate synthase in *Arabidopsis thaliana*. Federation of European Biochemical Societies (FEBS) Letter 372: 13–19
28- Sano S., Ueda M., Kitajima S., Takeda T., Shigeoka S., Kurano N., Miyachi S., Miyake C. and Yokota A. (2001) Characterization of ascorbate peroxidases from unicellular red alga Galdieria partita. Plant and Cell Physiology 42: 433–440.
29- Sharma P. and Dubey R. S. (2004) Ascorbate peroxidase from rice seedlings: properties of enzyme isoforms, effects of stresses and protective roles of osmolytes. Plant Science 167: 541–550.
30- Shigeoka S., Ishikawa T., Tamoi M., Miyagawa Y., Takeda T., Yabuta Y. and Yoshimura K. (2002) Regulation and function of ascorbate peroxidase isoenzymes. Journal of Experimental Botany 53: 1305–1319.
31- Smirnoff N. and Cumbes Q. J. (1989) Hydroxyl radical scavenging activity of compatible solutes. Phytochemistry 28: 1057-1060.
32- Smirnoff N. (1993) The role of active oxygen in the response to plants to water deficit and desiccation. New Phytologist 125: 27-58.
33- Sreenivasulu N., Ramanjulu S., Rmachandra-Kini K., Prakash H. S., Shekar-Shetty H., Savithri H. S., Sudhakar C. (1999) Total peroxidase activity and peroxidase isoforms as modified by salt stress in two cultivars of fox-tail millet with differential salt tolerance. Plant Science 141: 1-9.
34- Stewart C. R. (1981) Proline accumulation, Biochemical aspects. In: Paleg L. G., Aspinall D. (Eds), Physiology and Biochemistry of drought resistance in plants 243-251 pp.
35- Sung J. M. (1996) Lipid peroxidation and peroxide-scavenging in soybean seeds during aging. Physiologia Plantarum 97: 85–89.
36- Verbruggen N. and Hermans C. (2008) Proline accumulation in plants: a review. Amino Acids 35: 753-759.
37- Yamchi A., Rastgar Jazii F., Ghobadi C., Mousavi A. and Karkhanehee A. A. (2005) Increasing of tolerance to osmotic stresses in tobacco *Nicotiana tabacum* cv. xanthi through overexpression of p5cs gene. Journal of Science and Technology of Agriculture and Natural Resources 8: 40- 49.
38- Yoshiba Y., Kiyosue T., Katagiri T., Ueda H., Mizoguchi T., Yamaguchi-Shinozaki K., Harada Y., Shinozaki K. (1995) Correla- tion between the induction of a gene for 11-pyrroline-5- carboxylate synthase and the accumulation of proline in *Arabidopsis thaliana* under osmotic stress. Plant Journal 7: 751–760**.**

Scientific Reviewers

MANUSCRIPT PREPARATION

Manuscripts should be prepared in accordance with the uniform requirements for Manuscript's Submission to **"Journal of Cell and Molecular Research".**

Language. Papers should be in English (either British or American spelling). The past tense should be used throughout the results description, and the present tense in referring to previously established and generally accepted results. Authors who are unsure of correct English usage should have their manuscript checked by somebody who is proficient in the language; manuscripts that are deficient in this respect may be returned to the author for revision before scientific review.

Typing. Manuscripts must be typewritten in a font size of at least 12 points, double-spaced (including References, Tables and Figure legends) with wide margins (2.5 cm from all sides) on one side of the paper. The beginning of each new paragraph must be clearly indicated by indentation. All pages should be numbered consecutively at the bottom starting with the title page.

Length. The length of articles should be restricted to ten printed pages. Short communication should not exceed five pages of manuscript, including References, Figures and Tables.

GENERAL ARRANGEMENT OF PAPERS

Title. In the first page, papers should be headed by a concise and informative title. The title should be followed by the authors' full first names, middle initials and last names and by names and addresses of laboratories where the work was carried out. Identify the affiliations of all authors and their institutions, departments or organization by use of Arabic numbers (1, 2, 3, etc.).

Footnotes. The name and full postal address, telephone, fax and E-mail number of corresponding author should be provided in a footnote.

Abbreviations. The Journal publishes a standard abbreviation list at the front of every issue. These standard abbreviations do not need to be spelled out within paper. However, non-standard and undefined abbreviations used five or more times should be listed in the footnote. Abbreviations should be defined where first mentioned in the text. Do not use abbreviations in the title or in the Abstract. However, they can be used in Figures and Tables with explanation in the Figure legend or in a footnote to the Table.

Abstract. In second page, abstract should follow the title (no authors' name) in structured format of not more than 250 words and must be able to stand independently and should state the Background, Methods, Results and Conclusion. Write the abstract in third person. References should not be cited and abbreviations should be avoided.

Keywords. A list of three to five keywords for indexing should be included at bottom of the abstract. Introduction should contain a description of the problem under investigation and a brief survey of the existing literature on the subject.

Materials and Methods. Sufficient details must be provided to allow the work to be repeated. Correct chemical names should be given and strains of organisms should be specified. Suppliers of materials need only be mentioned if this may affect the results. Use System International (SI) units and symbols.

Results. This section should describe concisely the rationale of the investigation and its outcomes. Data should not be repeated in both a Table and a Figure. Tables and Figures should be selected to illustrate specific points. Do not tabulate or illustrate points that can be adequately and concisely described in the text.

Discussion. This should not simply recapitulate the Results. It should relate results to previous work and interpret them. Combined Results and Discussion sections are encouraged when appropriate.

Acknowledgments. This optional part should include a statement thanking those who assisted substantially with work relevant to the study. Grant support should be included in this section.

References. References should be numbered and written in alphabetical order. Only published, "in press" papers, and books may be cited in the reference list (see the examples below). References to work "in press" must be accompanied by a copy of acceptance letter from the journal. References should not be given to personal communications, unpublished data, manuscripts in preparation, letters, company publications, patents pending, and URLs for websites. Abstracts of papers presented at meetings are not permissible. These references should appear as parenthetical expressions in the text, e.g. (unpublished data). Few example of referencing patterns are given as follows:

Bongso A., Lee E. H. and Brenner S. (2005) Stem cells from bench to bed side. World Scientific Publishing Co. Singapore, 38-55 pp.

Haddad F., Gholami V. and Pirayesh Shirazi Nejad M. (2009) Ozone inhalation can induce chromosomal abnormalities in bone marrow cells of Wistar rats. Ferdowsi University International Journal of Biological Sciences 1: 41-46.

Tables and Figures. Tables and Figures should be numbered (1, 2, 3, etc.) as they appear in the text. Figures should preferably be the size intended for publication. Tables and Figures should be carefully marked. Legends should be typed single-spaced separately from the figures. Photographs must be originals of high quality. Photocopies are not acceptable. Those wishing to submit colour photographs should contact the Editor regarding charges.

Page charges. There is no page charge for publication in the Journal of Cell and Molecular Research.

Table of Contents

Journal of Cell and Molecular Research

Volume 4, Number 1, Summer 2012